Ontario Geological Survey
Study 29

Geology, Geotechnique, Mineralogy and Geochemistry of Leda Clay from Deep Boreholes

Hawkesbury Area, Prescott County

by
Robert M. Quigley, Janet E. Haynes, Anne Bohdanowicz, and Q.H.J. Gwyn

1985

Ontario
Ministry of Natural Resources

Copyright 1985 Government of Ontario
Printed in Ontario, Canada

ISSN 0704-2590
ISBN 0-7729-0534-7

Publications of the Ontario Ministry of Natural Resources are available from the following sources. Orders for publications should be accompanied by cheque or money order payable to the *Treasurer of Ontario.*

Reports, maps, and price lists (personal shopping or mail order):
Public Service Centre, Ministry of Natural Resources
Room 1640, Whitney Block, Queen's Park
Toronto, Ontario M7A 1W3

Reports and accompanying maps (personal shopping):
Ontario Government Bookstore
Main Floor, 880 Bay Street
Toronto, Ontario

Reports and accompanying maps (mail order or telephone orders):
Publications Services Section, Ministry of Government Services
5th Floor, 880 Bay Street
Toronto, Ontario M7A 1N8
Telephone (local calls), 965-6015
Toll-free long distance, 1-800-268-7540
Toll-free from area code 807, 0-ZENITH-67200

Every possible effort is made to ensure the accuracy of the information contained in this report, but the Ministry of Natural Resources does not assume any liability for errors that may occur. Source references are included in the report and users may wish to verify critical information.

Parts of this publication may be quoted if credit is given. It is recommended that reference to this report be made in the following form:

Quigley, Robert M., Haynes, Janet E., Bohdanowicz, Anne, and Gwyn, Q.H.J.
1985: Geology, Geotechnique, Mineralogy and Geochemistry of Leda Clay from Deep Boreholes, Hawkesbury Area, Prescott County; Ontario Geological Survey, Study 29, 128p.

1000-85-Deyell

FOREWORD

This report provides a detailed study of the clay deposits found in the Hawkesbury area of Eastern Ontario. These sensitive clays were deposited in the waters of the Champlain Sea which covered much of Eastern Ontario and Quebec during the waning stages of glaciation.

The report not only provides a review of the mineralogy, geochemistry and geotechnique of the deposits known informally as Leda Clay but it both supplements and complements other studies on these deposits by staff of the Ontario Geological Survey and the Ontario Ministry of Natural Resources. We are pleased to publish this report by Professor Quigley and his colleagues.

V.G. Milne
Director
Ontario Geological Survey

PREFACE

This report presents the final results of a three-phase study of the mineralogy, geochemistry and geotechnical characteristics of Leda clay from deep boreholes at Hawkesbury, Ontario. The work has been done under contract to the Ministry of Natural Resources of the Province of Ontario.

The initial work was done over a 12 month period in 1975-1976 and consisted of extensive mineralogical and geochemical investigations of soil samples provided by the Ministry. During this phase close contact was maintained with the late Dr. D.F. Hewitt and Dr. Q.H.J. Gwyn of the then Phanerozoic Geology Section, Division of Mines (now the Engineering and Terrain Geology Section, Ontario Geological Survey). A report written by Janet E. Haynes and Robert M. Quigley entitled "Mineralogy and Physico-Chemistry, Leda Clay from Deep Boreholes, Hawkesbury, Ontario" was submitted on August 16, 1976.

The second phase was carried out between July 1978 and 1979 and consisted of geotechnical engineering studies necessary to interpret the geochemical profiles obtained in phase one. High quality samples were taken for engineering testing and piezometer nests were installed in two boreholes to determine the *in situ* groundwater conditions. Close contact was maintained with Dr. Owen L. White, Chief of the Engineering and Terrain Geology Section of the Ontario Geological Survey during this phase. A report authored by Robert M. Quigley and Anne Bohdanowicz entitled "Supplementary Research, Piezometric Water Conditions, Preconsolidation and Isotope Analyses on Leda Clay from Deep Boreholes, Hawkesbury, Ontario" was submitted on July 24, 1979.

The third and final phase of the work has been carried out since July 1979 and has consisted of preparing an organized final report based on a critical review of the first two reports. Imperfect test results obtained on disturbed samples for phase one have been excluded. Dr. Q.H.J. Gwyn, now at the Université de Sherbrooke, has been involved from the beginning of the project and has prepared the geology section for this final report.

The authors would particularly like to extend a word of appreciation to Dr. Owen L. White for his continued strong support of this project which has enabled us to assemble an extremely interesting interdisciplinary study which we hope will be of value in future research on Champlain Sea clays.

It should be noted that this is essentially a report of work done, not a literature review. The list of references is therefore short and pertains only to material featured in the report.

CONTENTS

Foreword iii
Preface iv
Conversion Factors ix
Definition of Selected Terms x
Abstract 2
Introduction 3
Site Location 4
Quaternary Geology 7
  Marine Deposits 7
  Deltaic and Fluvial Deposits 8
  Fluvial Erosion 8
  Geochronology 9
Field Investigations 10
  Phase 1 10
  Phase 2 10
Laboratory Investigations 11
  Geotechnical Studies 11
  Geochemical Studies 11
  Mineralogical Studies 11
  Oxygen and Hydrogen Isotope Studies 12
  Scanning Electron Microscopy 12
Geotechnique 13
  Soil Classification and Index Testing 13
  Shear Strength 14
    Boreholes 75-1 to 75-9 14
    Boreholes 78-1 and 78-2 14
  Consolidation 27
  Water Conditions 27
  Discussion 27
Mineralogy 34
  Qualitative Mineralogy 34
    Clay Mineralogy, Oxidized Crust 34
    Clay Mineralogy, Deposit Below Crust 34
    Mineralogy of Non-Clay Components 35
    Amorphous Materials 35
  Semi-Quantitative Mineralogy 45
  Scanning Electron Microscopy 45
Geochemistry 56
  Carbonates 56
  pH 56
  Salinity 56
  Porewater Cations 56
  Organic Matter 57
  Discussion 57
Porewater Isotopes 61
  Results 62
  Discussion 62
Summary 71
  Geology 71
  Geotechnique 71
  Mineralogy 72
  Geochemistry 72

Appendix A. Testing Procedures for Geotechnical, Geochemical and Mineral Analysis 75
Geotechnical Testing Methods 75
Geochemical Testing Methods 75
Mineralogical Testing Methods 76
Scanning Electron Microscopy 78
Appendix B. Unconfined Compression Test Results 80
Appendix C. Consolidation Test Results 82
Appendix D. Geotechnical Data 89
Appendix E. Geochemical Data 100
Appendix F. Analyses of Fluid Extracts after Selective Dissolution Treatment . . 103
Appendix G. 1978 Field Investigations 115
References 119
Index 121

TABLES

1. Semi-quantitative mineralogy of clay samples 46
2. Assumptions and limitations of the semi-quantitative mineralogy determinations 48
C-1. Specific gravity measurements of samples from boreholes 78-1 and 78-2 . 82
D-1. Field vane data, borehole 75-1 89
D-2. Field vane data, borehole 75-2 89
D-3. Field vane data, borehole 75-3 90
D-4. Field vane data, borehole 75-4 90
D-5. Field vane data, borehole 75-5 91
D-6. Field vane data, borehole 75-6 91
D-7. Field vane data, borehole 75-7 92
D-8. Field vane data, borehole 75-8 92
D-9. Field vane data, borehole 75-9 93
D-10. Laboratory vane data, borehole 75-3 93
D-11. Laboratory vane data, borehole 75-4 94
D-12. Laboratory vane data, borehole 75-6 94
D-13. Index tests, borehole 75-1 95
D-14. Index tests, borehole 75-2 95
D-15. Index tests, borehole 75-5 96
D-16. Index tests, borehole 75-7 97
D-17. Index tests, borehole 75-8 98
D-18. Index tests, borehole 75-9 99
D-19. Additional grain-size data for boreholes 75-4, 75-5, 75-6, and 75-8 99
E-1. Carbonate contents determined by gasometric analysis 100
E-2. Salinity and porewater cation analyses of samples from boreholes 75-1, 75-2, 75-5, 75-7, and 75-8 101
E-3. Organic matter content in samples from boreholes 78-1 and 78-2 102
F-1. Segalen 'amorphous' contents extrapolated from time-dissolution curves 103
F-2. Dissolution analyses for amorphous material, in order completed 104
G-1. Record of piezometer readings for boreholes 78-1 and 78-2 118

FIGURES

1. Quaternary geology of the Hawkesbury area 5
2. Borehole location map 6
3. Stratigraphic cross-section A-A′ of Hawkesbury area 15
4. Stratigraphic cross-section B-B′ of Hawkesbury area 16
5. Geotechnical profile for borehole 75-1 17
6. Geotechnical profile for borehole 75-2 18
7. Geotechnical profile for borehole 75-3 19
8. Geotechnical profile for borehole 75-4 20
9. Geotechnical profile for borehole 75-5 21
10. Geotechnical profile for borehole 75-6 22
11. Geotechnical profile for borehole 75-7 23
12. Geotechnical profile for borehole 75-8 24
13. Geotechnical profile for borehole 75-9 25
14. Water content, shear strength, salinity and organic matter vs depth, borehole 78-1 26
15. Water content, shear strength, salinity and organic matter vs depth relationships, borehole 78-2 26
16. Preconsolidation pressure, effective stress and undrained shear strength vs depth, borehole 78-1 29
17. Preconsolidation pressure, effective stress and undrained shear strength vs depth, borehole 78-2 29
18. Consolidation test results, borehole 78-1 30
19. Consolidation test results, borehole 78-2 30
20. Piezometric water levels for borehole 78-1 31
21. Piezometric water levels for borehole 78-2 31
22. Piezometric water level readings for boreholes 78-1 and 78-2 taken on May 19, 1979 32
23. Stress-depth relationships and possible post-depositional erosion for lower clay plain 32
24. Stress-depth relationships and possible post-depositional erosion for upper clay plain 33
25. X-ray diffraction pattern of sample 75-2-1 36
26. X-ray diffraction patterns of $< 2\ \mu$m material from samples 75-2-11 and 75-2-13 37
27. X-ray diffraction patterns of $< 2\ \mu$m material from samples 75-7-13 and 75-7-19 38
28. X-ray diffraction pattern of $< 2\ \mu$m material from sample 75-5-7 39
29. Powder patterns for samples from borehole 75-2 40
30. Powder patterns for samples from borehole 75-6 41
31. Dissolution rates of minerals in Hawkesbury clay, samples 75-6-6 and 75-6-10 42
32. X-ray diffraction patterns before and after HCl/NaOH selective dissolution, sample 75-2-17 43
33. Percentage of amorphous material extracted vs depth and elevation 44
34. Scanning electron photomicrograph of horizontal face, sample 75-2-2 49
35. Scanning electron photomicrograph of vertical face, sample 75-2-2 50
36. Scanning electron photomicrograph of horizontal face, sample 75-2-17 . . . 51
37. Scanning electron photomicrograph of vertical face, sample 75-2-17 51
38. Scanning electron photomicrograph of vertical face, sample 75-6-3 52
39. Scanning electron photomicrograph of horizontal face, sample 75-6-16 . . . 52
40. Scanning electron photomicrographs of cemented inclusion 53
41. Scanning electron photomicrographs of cemented layer 54

42. Scanning electron photomicrographs of cemented material 55
43. Geochemical data for borehole 75-1 58
44. Geochemical data for borehole 75-2 58
45. Geochemical data for borehole 75-5 59
46. Geochemical data for borehole 75-7 59
47. Geochemical data for borehole 75-8 60
48. Oxygen, deuterium and tritium analyses for boreholes 78-1 and 78-2 64
49. Map of United States showing approximate contours for δ^2H and $\delta^{18}O$ of present day meteoritic water 65
50. World map showing approximate $\delta^{18}O$ contours in ‰ SMOW of annual present-day precipitation 65
51. Relationship between $\delta^{18}O$ and salinity for ocean water diluted with fresh melt water 66
52. Oxygen-18 vs depth for Champlain Sea 67
53. Relationship between salinity and oxygen-18 of present-day arctic waters and predicted relationship for Champlain Sea water 68
54. Relationship of δ^2H to $\delta^{18}O$ from Hawkesbury Leda clay 69
55. $\delta^{18}O$ and organic matter vs elevation, Hawkesbury area Leda clays from upper and lower clay plains 70
56. Sensitivity, salinity, carbonate, 'amorphous' matter and liquidity index vs depth relationships for lower level clay plain 74
57. Sensitivity, salinity, carbonate, 'amorphous' matter and liquidity index vs depth relationships for upper level clay plain 74
A-1. Determination of abundance of quartz by method of additions 79
B-1. Stress-strain curves for piston samples, borehole 78-1 80
B-2. Stress-strain curves for piston samples, borehole 78-2 81
C-1. Consolidation curves for borehole 78-1, 4.75 m and 9.65 m depth 83
C-2. Consolidation curves for borehole 78-1, 13.9 m and 18.5 m depth 84
C-3. Consolidation curves for borehole 78-1, 23.1 m and 27.6 m depth 85
C-4. Consolidation curves for borehole 78-2, 3.2 m and 6.3 m depth. 86
C-5. Consolidation curves for borehole 78-2, 9.3 m and 12.4 m depth 87
C-6. Consolidation curves for borehole 78-2, 18.4 m and 24.6 m depth 88
F-1. Time-rate of dissolution curves for amorphous determinations 106
F-2. Time-rate of dissolution curves for amorphous determinations 107
F-3. Time-rate of dissolution curves for amorphous determinations 108
F-4. Time-rate of dissolution curves for amorphous determinations 109
F-5. Time-rate of dissolution curves for amorphous determinations 110
F-6. Time-rate of dissolution curves for amorphous determinations 111
F-7. Time-rate of dissolution curves for amorphous determinations 112
F-8. Time-rate of dissolution curves for amorphous determinations 113
F-9. Time-rate of dissolution curves for amorphous determinations 114
G-1. Detailed site plans, borehole 78-1 and borehole 78-2 115
G-2. Sample locations, boreholes 78-1 and 78-2 116
G-3. Piezometer layout in boreholes 78-1 and 78-2 117

CONVERSION FACTORS

LENGTH

1 foot = 0.3048 m
1 inch = 2.540 cm
1 mile = 1.609 km
1 μm = 1 micron = 10^{-6} m
1 angstrom = 1 Å = 0.1 nm (nanometre)

AREA

1 square mile = 2.590 km^2
1 square foot = 0.093 m^2

WEIGHT

1 pound force = 4.448 N (Newton)

UNIT WEIGHT

1 pound/cubic foot = 0.157 kN/m^3
100 pound/cubic foot = 15.71 kN/m^3

MASS

1 pound $\equiv$ 0.4536 kg
1 pound/cubic foot $\equiv$ 16.02 kg/m^3
100 pound/cubic foot $\equiv$ 1602 kg/m^3 = 1.602 Mg/m^3

STRESS

1 psf (pound/square foot) = 0.048 kN/m^2 (kPa)
1 psi (pound/square inch) = 6.895 kPa
1 tsf (ton/square foot) = 95.76 kPa

DEFINITION OF SELECTED TERMS

Water content, ω_n, (percent)

Defined as $\frac{\text{(weight of water)}}{\text{(weight of solid)}} \times 100$

Liquid limit, ω_l, (percent)

That water content at which a soil behaves essentially like a fluid.

Plastic limit, ω_p, (percent)

That water content at which a soil behaves essentially like a solid.

Activity, A_c

Defined as $\frac{(\omega_l - \omega_p)}{(\text{percentage} < 2\ \mu\text{m})}$

Liquidity Index, L_i

Defined as $\frac{(\omega_n - \omega_p)}{(\omega_l - \omega_p)} = L_i$

Soils with a natural water content greater than the liquid limit become extremely soft when disturbed. A high liquidity index generally signifies a high sensitivity.

Sensitivity, S_t

Defined as the ratio $\frac{\text{(Undisturbed strength)}}{\text{(Remoulded strength)}}$

Consistency

Descriptive terms for strength designation for clays:

Consistency	*Undrained shear strength, kPa*
Very soft	0-12
Soft	12-25
Medium (firm)	25-50
Stiff	50-100
Very stiff	100-200

Salinity

Normally expressed as grams/1000 grams (‰) but approximated as g/L NaCl equivalent for this report.

Preconsolidation pressure, p_c

Maximum stress to which a soil can be stressed before consolidation commences in a consolidation test. Normally caused by previous consolidation but may be caused by cementation.

In situ effective stress, $\bar{\sigma}_v$

Total stress less the porewater pressure.

Overconsolidation ratio, O.C.R.

Ratio of p_c to $\bar{\sigma}_v$. A value of unity indicates the present vertical stresses are the maximum ever experienced by the clay soil. (P_o is frequently used in place of $\bar{\sigma}_v$).

Framboid

Agglomeration of tiny pyrite crystals into a raspberry-like cluster. Probably of bacterial origin.

***del* oxygen-18, $\delta^{18}O$**

An expression of the deviation of ^{18}O relative to its normal abundance in standard seawater (defined in text under "Porewater Isotopes").

SMOW

Standard mean ocean water (reference water for standard $^{18}O/^{16}O$ ratio).

PDB

Pee Dee Limestone (reference rock for standard $^{18}O/^{16}O$ ratio on mineral matter).

GEOLOGY, GEOTECHNIQUE, MINERALOGY AND GEOCHEMISTRY OF LEDA CLAY
FROM DEEP BOREHOLES, HAWKESBURY AREA, PRESCOTT COUNTY

ROBERT M. QUIGLEY[1], JANET E. HAYNES[1], ANNE BOHDANOWICZ[1], AND Q.H.J. GWYN[2]

1. Faculty of Engineering Science, The University of Western Ontario, London, Ontario.
2. Université de Sherbrooke, Sherbrooke, Québec.

Manuscript approved for publication October 5, 1981, by the Director, Ontario Geological Survey.
Published with the permission of V.G. Milne, Director, Ontario Geological Survey.

ABSTRACT

Field mapping and geotechnical studies have shown that the 30 m thick deposits of Champlain Sea clay at Hawkesbury, Ontario, were unloaded by rapid erosion of surface sands prior to complete consolidation of the clays. An ancestral meander of the Ottawa River is shown to have been responsible for erosion of the lower clay plain where about 21 m of sands were removed. A stratigraphic scheme suggests that about 11 m of sand was removed from the upper clay plain at the location studied.

Quantitative mineralogical studies show a constant suite of minerals consisting of quartz, feldspar, amphibole, illite/mica, chlorite, vermiculite, carbonate, and small amounts of smectite. Increases in smectite at surface reflect weathering, and pyritic framboids in black mottled areas at depth reflect bacterial reduction.

Porewater analyses, including salinity, soluble cations and isotopic composition, suggest different sedimentation salinities for the upper and lower level clays. Chemical profiles which seem incompatible with the geotechnical profiles suggest leaching by diffusion.

Geology, Geotechnique, Mineralogy, and Geochemistry of Leda Clay from Deep Boreholes, Hawkesbury Area, Prescott County, by Robert M. Quigley, Janet E. Haynes, Anne Bohdanowicz, and Q.H.J. Gwyn. Ontario Geological Survey, Study 29, 128p. Published 1985. ISBN 0-7729-0534-7.

INTRODUCTION

Over the past twenty years, the geotechnical, geochemical and mineralogical characteristics of the sensitive clays in eastern Canada have been frequently examined. Most of the previous work, however, has concentrated on landslide and building sites and usually focused on only one of the above three areas of research. The main aim of this project has been to obtain a fairly comprehensive assessment of the geotechnical, geochemical and mineralogical aspects of deep deposits of Leda clay, which were deposited in the Champlain Sea near Hawkesbury, Ontario. Furthermore, the work is intended to supplement field mapping studies by the Ontario Geological Survey in the Hawkesbury area carried out by one of the authors (Q.H.J. Gwyn).

A total of eleven boreholes were put down in an area just south and west of Hawkesbury; nine in 1975 followed by two in 1978. Samples from the 1975 holes served to define the geochemistry, soil mineralogy and index characteristics. Samples from the 1978 holes have been used to determine the preconsolidation state of the clays and have provided water samples for oxygen isotope analyses. Piezometers installed in the 1978 holes have served to define the present-day groundwater conditions.

SITE LOCATION

The study area is located south of the Ottawa River and extends from Hawkesbury in the east to Plantagenet in the west. Figures 1 and 2 are maps of the area showing the surficial geology and the borehole locations, respectively.

The topography of the region consists of a central, low-level plain at an elevation of approximately 50 m, rising irregularly to the east to an upper plain at an elevation about 75 m. Much of the low-level plain is believed to represent an erosional surface created by an ancestral meander of the Ottawa River following isostatic uplift of the region. An east-west profile showing the main topographic features is given in Figure 3.

The majority of creeks in the study area drain northwards to the Ottawa River although a few of the more southerly areas such as Alfred Bog also drain in the opposite direction towards South Nation River.

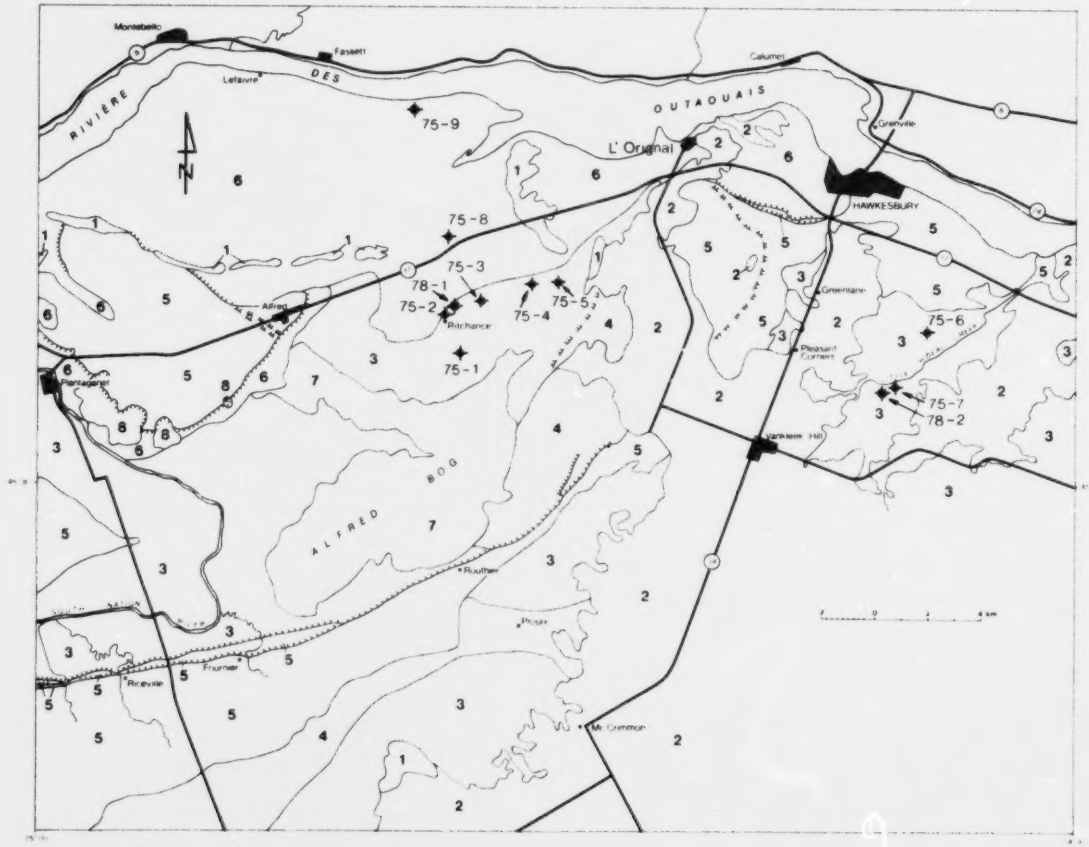

LEGEND

QUATERNARY

8 Landslide debris: highly disturbed medium to fine sand silt and clay

7 Bog deposits: peat, organic silt and marl

6 Older alluvium: mainly silt and sandy silt, some medium to fine sand

5 Deltaic deposits: medium to fine sand

4 Rhythmites: rhythmically interbedded clay and sandy clayey silt or silty sand and very sandy clayey silt

3 Marine deep-water deposits: clay with rare fossils

2 Fort Covington Till: cobbly to bouldery sandy silt till

LOWER AND MIDDLE ORDOVICIAN

1 Limestone, dolostones, shale and sandstone

SYMBOLS

Geological boundaries

River-cut terrace scarp and earth flow escarpment

Borehole site and number

Figure 1. Quaternary geology of the Hawkesbury area. Modified after Gwyn and Lohse (1973) and Gwyn and Thibault (1975).

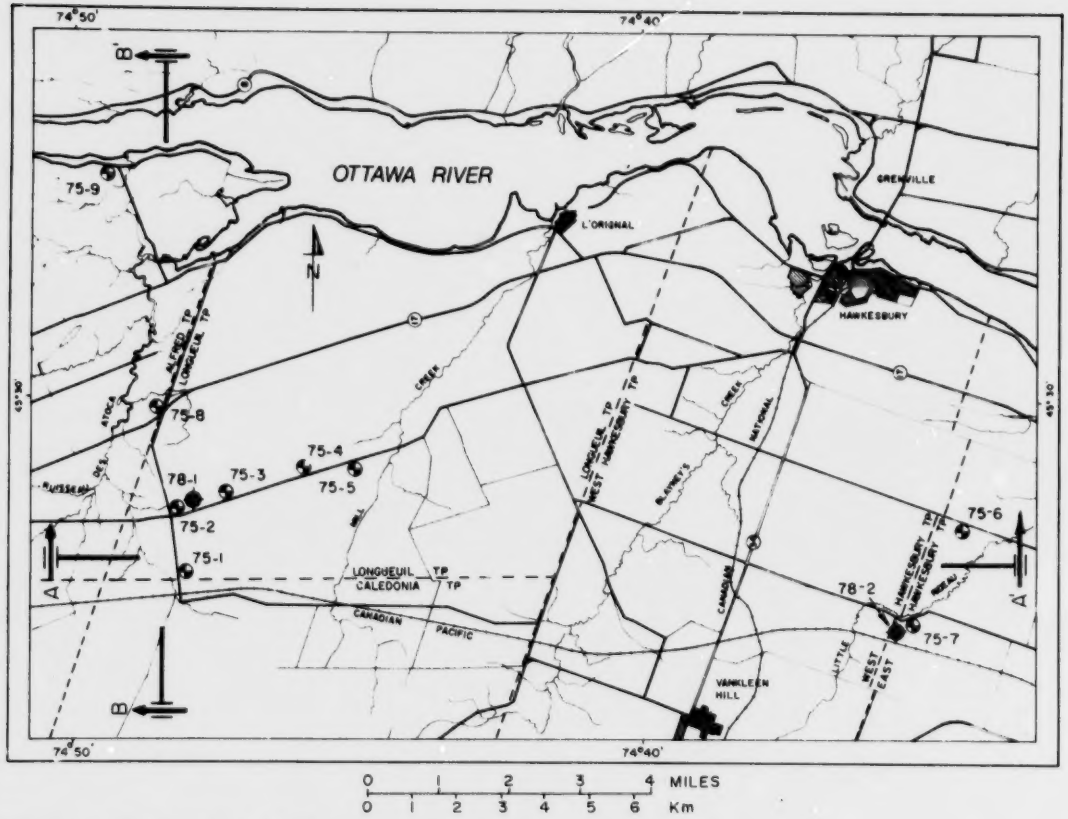

Figure 2. Borehole location map. Boreholes 75-1 to 75-9 were drilled in summer 1975; boreholes 78-1 and 78-2 were drilled in July 1978. Basemap is NTS 31G/10, "Hawkesbury Sheet".

QUATERNARY GEOLOGY

In summarizing the Quaternary geology in the Hawkesbury area, four aspects in particular are discussed:

1. the definition and distribution of marine sediments;
2. the definition and distribution of fluvial sediments;
3. the subsequent erosion of the fluvial and marine deposits; and
4. the chronology of the post-glacial evolution.

Following the retreat of ice from the Ottawa-St. Lawrence Lowland, the Hawkesbury area was inundated by marine waters of the Champlain Sea. Based on landforms and deposits on the Canadian Shield north of the Ottawa River, the maximum elevation of the Champlain Sea itself was 180 to 190 m relative to present sea level, or approximately 60 m above the highest point in the study area (122 m) at Vankleek Hill (see Figure 1). Thus the primary process active immediately after deglaciation was deep-water marine sedimentation.

MARINE DEPOSITS

Two types of fine-grained marine and transitional sediments were identified and mapped. These include deep-water deposits and shallower-water rhythmites. Coarse-grained fossiliferous marine and beach gravels, also mapped, do not concern us directly in this study.

The marine sediments were identified primarily on the basis of their texture, fossil content and their primary structures. The sediments typically consist of massive, grey coloured clay containing infrequent specimens of *Portlandia arctica*. They are easily penetrated with a hand soil-auger since they rarely have a resistant crust more than 1 m thick.

The clays are widely distributed across the area but are most extensive in the low lying flat area defined by the villages of L'Orignal, McCrimmon and Plantagenet (see Figure 1). In the zone mapped as till, fine-grained deposits are found as a patchy cover of variable thickness (up to 10 m).

The clays vary in thickness from a feather edge along their eastern and southern limits to a maximum of about 60 m at the Ottawa River east of Lefaivre (see Figure 1). Typically, they are in the order of 30 to 35 m thick. In the less extensive area of clays to the east and west of Little Rideau Creek they have a maximum thickness of about 30 m (see Figure 1).

The second type of fine-grained deposits consists of rhythmically interbedded sandy clay and slightly sandy clayey silt in the lower part of the unit, and silty very fine sand and very sandy clayey silt in the upper part of the unit. They contain very few fossils. In section, the rhythmites are less than 7 m thick and grade down into the massive marine clays. The rhythmic banding is the most easily mapped characteristic.

The rhythmites are exposed in a band, 2 km wide, extending southwestwards from Proulx. They underlie the surface deposits to the northwest and extend as far as the terrace scarps trending through the hamlets of Riceville, Fournier and Routhier (see Figure 1). They also underlie the large area of deltaic sediments between Plantagenet and Alfred where they are exposed in several sections. The rhythmites are easily traced in the field because of their distinctive structure and their association with the marine clays.

It is suggested that these sediments were formerly more extensive and may have covered much of the zone between the Alfred-Plantagenet area and the Riceville-Fournier-Routhier area (see Figure 1).

Though discussed here with the marine sediments, the rhythmite unit is clearly a transitional sequence (possibly a distal deltaic facies) between the marine clays and the overlying freshwater sediments.

DELTAIC AND FLUVIAL DEPOSITS

Following the marine transgression, the land surface gradually emerged isostatically, though perhaps at a slower rate than other areas that were never submerged. An island first appeared at Vankleek Hill (elevation 122 m) between 10,500 and 10,800 radiocarbon years B.P. (ref. QU-283,285)*. From that time until the land had risen sufficiently to form the lowest beaches at 91 m, the water continued to support marine fauna. However, some time following this, the transition from marine to fluvial sedimentation occurred. During this transition, the main process active in the area was the sedimentation of the upper units of the rhythmite deposits and the deposition of an extensive delta by the emerging ancestral Ottawa River.

The deltaic sediments consist of medium to fine sand and silty sand contained in massive bedded units, plain bedded and ripple-drift laminations. The sands range between 8 and 10 m in thickness and have a maximum elevation of about 85 m. Their characteristic textures and structures make them easy to trace over large areas. They are presently distributed as large remnants in the Plantagenet-Alfred area and in the Riceville-Fournier-Routhier area as well as in smaller remnants east and south of L'Orignal (see Figure 1). The lateral limits of the deltaic deposits are for the most part defined by erosional terrace scarps (see Figure 1).

Subsequent to the formation of the delta, the predominantly depositional processes were replaced by dominantly erosional processes but including some fluvial sedimentation. Two types of fluvial sediments have been found. The most widespread consists of grey and red-brown banded, stiff silts and sandy silts, that are restricted to an area bordering the Ottawa River and which were probably deposited during overbank flooding. The second and very patchy unit includes massive, plain laminated and cross laminated fine to medium sand and silty sand. The sand both overlies and underlies the silts.

FLUVIAL EROSION

With continued emergence of the area, the Ottawa River both maintained and eroded large channels in the surficial deltaic sediments. Alfred Bog is located in one of these channels (see Figure 1). The primary evidence for an erosional origin of these channels includes the presence of several persistent terrace-scarp systems, the general absence of fluvial sediments in the larger channels and the presence of curvilinear flutings cut into the marine clays in the channels.

The flutings, which in general parallel the main channels, are a maximum of 2 to 3 km long, 10 m wide and 2 m deep. They are irregularly spaced a few tens of metres apart and are subparallel to one another. First recognized on air photographs because of their darker tone, they are usually infilled with bog deposits. The flutings were clearly cut or gouged into the soft marine clays because the banding in the clay has been both contorted and truncated in the flutes.

The terrace scarps have a maximum elevation of 85 m and range progressively down to between 60 and 55 m. The highest terrace is at the northwest end of the large deltaic deposit between Plantagenet and Alfred (see Figure 1). The scarp is on the northeast side of a small (0.5 km wide) channel which had begun to dissect this section of the delta. It was abandoned, as were all the channels of the ancestral Ottawa River, because of a bedrock sill encountered in the channel during the down-cutting. An intermediate-level set of scarps occurs between 75 and 68 m elevation in the

*These numbers are test identification numbers and refer to a series of radiocarbon dates (of shell material) provided by the Ministère de l'énergie et des ressources du Québec (QU) and by the Department of Geological Sciences, Brock University, Ontario (BGS).

Alfred-Plantagenet area as well as in the area between L'Orignal and Hawkesbury (see Figure 1). A third, even lower set of terrace scarps were mapped at 65 m down to 55 m between L'Orignal and Hawkesbury and in the Riceville-Fournier-Routhier area (see Figure 1).

Based on the elevation of these terrace scarps and the correlation of the marine and deltaic sediments into which they were cut, it is calculated that erosion has removed a maximum of 33 m and a minimum of 18 m of sediments in the large channel in the study area.

GEOCHRONOLOGY

A series of radiocarbon dates on shells from marine beaches and two dates on wood from a channel fill deposit permit the quantitative estimation of the date and rate of emergence of the study area. A beach built on the highest point of land at elevation 122 m was dated at 10,500 years B.P. (Ref. QU-282,283). The lowest level beaches (four sites at elevation 91 m) have an approximate age of 10,000 years B.P. (Ref. QU-292,293,294). These data yield an approximate rate of emergence of 30 m in 500 years.

Two dates on wood from a channel-fill deposit of sandy gravel (elevation 53 to 61 m) at Hawkesbury, give an average age of 9,200 years B.P. (Ref. QU-297,BGS-257). This corresponds to an approximate rate of emergence of 30 m in the 800 years between the formation of the lowest marine beaches (elevation 91 m) and channel infilling.

Two areas where the clays were drilled and sampled are below the lowest marine beaches, therefore, an approximation can be made of the time of emergence of these two areas using the later rate of emergence. The Little Rideau Creek sites at approximately 75 m elevation may have emerged about 9,600 years B.P. whereas the Ritchance sites at elevations of approximately 52 m may have emerged about 9,000 years B.P.

FIELD INVESTIGATIONS

The field investigations pertinent to this report consisted of two phases of drilling which included vane testing, soil sampling and piezometer installations.

PHASE 1

The first phase of drilling was carried out by the Ministry of Natural Resources under the direction of Q.H.J. Gwyn and consisted of nine soil borings put down during the early summer of 1975. The locations of these boreholes (No. 75-1 to 75-9) are shown on Figure 2. *In situ* strength testing using a standard 2-inch diameter vane was carried out at each hole location. Soil samples were obtained from boreholes 75-1 to 75-8 using 2-inch diameter Shelby tubes which provided good samples for mineralogical, geochemical, and engineering index or classification testing.

PHASE 2

The phase 2 drilling was carried out in July 1978 by Golder Associates (Ottawa) and consisted of two auger borings (78-1 and 78-2) at the locations shown on Figure 2. Three-inch (76 mm) diameter piston samples were taken in each hole and these provided high quality samples for consolidation testing.

Nests of four piezometers were installed in each hole at depths of 3, 9, 18 and 28 m to accurately assess the *in situ* piezometric groundwater conditions. Five sets of piezometer readings were taken between July 1978 and May 1979 by Golder Associates; the first author was present for the November 1978 readings. The holes were spotted by Q.H.J. Gwyn to ensure their location near 1975 borehole sites.

In view of the importance of these two holes to the overall success of this project, details of the borehole locations, piezometer layout, etc. are presented in Appendix G from data supplied by Golder Associates.

LABORATORY INVESTIGATIONS

The laboratory testing program may be divided into four main areas of concentration:

1. geotechnical index testing on the 1975 samples and consolidation testing on the 1978 samples;
2. geochemical analyses of the 1975 and 1978 samples;
3. mineralogical analyses of the 1975 samples; and
4. oxygen, deuterium and tritium analyses on pore water squeezed from the 1978 samples.

In addition, a minor amount of scanning electron microscopy was done to assess soil fabric and framboid agglomeration of some samples.

In order to keep the number of analyses to a manageable size, only five of the nine original boreholes (75-1, 75-2, 75-5, 75-7 and 75-8) were selected for detailed analysis. However, samples from boreholes 75-3, 75-4 and 75-6 were analyzed at depths where anomalous values appeared in the field vane strength data. Check tests were also run on samples from boreholes 78-1 and 78-2.

GEOTECHNICAL STUDIES

Classification tests included Atterberg limits, grain size analyses, specific gravity tests and wet and dry unit weights and moisture contents. These data provide a good engineering description of the deposits in this part of the Champlain Sea.

Unconfined compression tests and laboratory vane tests were run on many samples as a check on the field vane results. Consolidation tests were run on samples from boreholes 75-2, 78-1 and 78-2. The samples from borehole 75-2 were only 2 inches in diameter and hence were somewhat disturbed. Therefore, only the consolidation data obtained on the 3-inch diameter samples from the latter two holes are included in this final report.

GEOCHEMICAL STUDIES

In order to investigate any relationships between engineering and geochemical properties, boreholes 75-1, 75-2, 75-5, 75-7 and 75-8 were selected for porewater salinity and cation analysis, carbonate determination and pH measurement. The porewater specimens were obtained by pressure squeezing of samples selected from regular intervals in the boreholes, and samples selected at zones where sudden changes in geotechnical properties occurred. The total porewater salinity and the concentrations of Ca, Na, Mg, K and Fe were measured by conductivity and atomic absorption spectrophotometry, respectively. The percentage of carbonate was determined by the gasometric method using a Chittick apparatus. Check testing of porewater salinity was also done on samples from boreholes 78-1 and 78-2.

The percentage of organic matter was determined on all samples from boreholes 78-1 and 78-2 using the modified Walkley Black method. More details concerning the testing procedures may be found in Appendix A.

MINERALOGICAL STUDIES

Initially, qualitative analyses were performed on a large number of samples to identify any gross mineralogical trends in the deposit. On the basis of this preliminary work, and after examining the geotechnical and geochemical data, 39 samples from boreholes 75-1, 75-2, 75-4, 75-5, 75-6, 75-7 and 75-8 were selected for semi-quantitative analysis. The main tool in all of the mineral analyses was X-ray diffraction, but chemical analysis was used in the semi-quantitative mineral determinations.

A final stage of the mineral analyses was the measurement of the amorphous constituent commonly reported for Champlain Sea clays (Yong *et al.* 1979). Eighteen samples were chosen from four boreholes, at different depths and elevations, and from samples of medium and stiff strength, in order to provide specimens representing all soil conditions in the deposits.

OXYGEN AND HYDROGEN ISOTOPE STUDIES

In an attempt to unravel the depositional history of the Hawkesbury clays, oxygen-18, deuterium and tritium determinations were made on the porewater squeezed from samples taken from boreholes 78-1 and 78-2, drilled in July 1978. In particular, it was anticipated that these determinations would aid in explaining the bow-shaped salinity profiles encountered in the geochemical analyses.

The analyses were performed by Peter Fritz at the University of Waterloo. Bulk samples of the soil were submitted to Fritz who used contamination-free porewater squeezing techniques necessary to obtain reliable mass spectrometer results.

SCANNING ELECTRON MICROSCOPY

Four soil samples were selected for scanning electron microscope (SEM) examination. The purpose of this testing was to visually characterize the soil fabric and to examine any differences in fabric with depth. One of the samples (75-6-3) was selected because of the excessively low remoulded shear strength recorded immediately above it. In addition, some brassy coloured cemented materials discovered in various samples were prepared for SEM examination.

GEOTECHNIQUE

The important features of both the field and laboratory engineering testing programs are described in this section. More detailed information including selected stress-strain curves and consolidation test results may be found in Appendices B and C.

A geotechnical profile for each borehole is presented in Figures 5 to 15 inclusive. These individual profiles were used to prepare the stratigraphic cross-sections shown in Figures 3 and 4. The position of the bedrock surface on the E-W profile was estimated from the overburden thickness map for the area (Gwyn and Thibault 1973b).

The Champlain Sea clays are located in two rock-basins, at different elevations, separated by a north-trending bedrock ridge as shown in Figure 3. Significant differences in the physical and chemical characteristics of the clays in these two basins are discussed throughout the text.

The clay deposits within each basin have been separated into four main components based on shear strength (soft to very stiff) and appearance as shown on Figures 3 and 4. At the surface, there is a thin (1 to 3 m thick) crust of medium to stiff, desiccated, oxidized and fissured, brown to grey clay derived by weathering from underlying soft to medium grey clay and silty clay with brown layers. The strength increases with depth so that the "soft zone" is normally about 4 to 6 m thick in the low elevation holes. In boreholes 75-6 and 75-7, located at approximately 20 m higher elevation, the "soft zone" appears thicker (approximately 11 m). This is significant since it suggests either less preconsolidation of the higher elevation clays or significant erosion of sediments from the area of the lower elevation boreholes.

The main stratum shown in Figure 4 for the low elevation holes consists of medium to stiff grey, brown and brown grey clay and silty clay about 14 m thick. This is underlain by stiff to very stiff, grey and brownish grey clay and silty clay deposits. In Figure 3, the soft clays in boreholes 75-6 and 75-7 are underlain by stiff grey clay and silty clay with grey brown layers.

SOIL CLASSIFICATION AND INDEX TESTING

The percentage of clay size ($< 2\,\mu$m) material in the soils varies from 43 to 93 percent and averages 83 percent. The soils may be classified, therefore, as slightly silty to silty clays with occasional silty layers. Most of the low clay contents occur near the base of the boreholes as shown on the profiles, however, scattered silt layers do occur in the sequence as may be observed in borehole 75-5 at 4 m depth.

The Atterberg limit tests yielded liquid limits in the range of 60 to 84 percent with an average of about 70 percent for most of the samples. Occasional values as low as 34 percent were obtained in silty layers. The plastic limits varied from 19 to 32 and averaged 28.

The activity (A_c) of the soil varies from 0.4 to 0.6 which is low and typical for Leda clays which are composed primarily of inactive clay minerals and rock flour.

The water content (ω_n) profiles generally follow the same trends as the liquid limit (ω_l) profiles; ω_n values are quite close to the ω_l values yielding an average liquidity index of 0.97 for the whole deposit. For the low elevation holes (Figures 5 to 9 and 14), the moisture contents of the samples at depth tend to be less than the liquid limit. For the high elevation holes (Figures 11 and 15) the moisture contents at depth are consistently above the liquid limit. Within the crust, desiccation has normally reduced ω_n to values well below ω_l resulting in higher crustal strengths except where excessively fissured.

Wet unit weights for the deposits ranged from about 15.5 kN/m^3 at surface to about 16.2 kN/m^3 at depth (99 to 103 pounds per cubic foot). Higher values (16.8 kN/m^3) at extreme depth on the logs generally reflect the presence of siltier soils.

SHEAR STRENGTH

BOREHOLES 75-1 TO 75-9

Most of the strength data shown on the logs for boreholes 75-1 to 75-9 represent *in situ* undisturbed and remoulded field vane values obtained with a standard 2-inch diameter by 4 inch long (5.1 cm by 10.2 cm) vane, slowly torqued by hand. Ten to twenty revolutions were used to remould the clay. Where strength values were missing and 2-inch tube samples were available, unconfined compression and laboratory vane tests were run to complete the strength profiles.

In Figures 6 and 11 for boreholes 75-2 and 75-7, the unconfined compression shear strength values are much lower than the field vane values indicating sample disturbance. The laboratory vane strengths recorded in Figure 7 and 8 for boreholes 75-3 and 75-4 show similar disturbance although not so great. In spite of these problems, the crustal zone could in some cases be clearly defined by the strength profiles as in boreholes 75-3, 75-6 and 75-7.

Below the thin crust, the undisturbed field vane strength generally shows a gradual increase with depth, from 40 kPa to approximately 130 kPa. Field vane tests have been found reliable for measuring *in situ* strength where the deposit is not heavily over-consolidated (Eden 1966). Since the material in the Hawkesbury area is generally of medium to stiff consistency (S_u = 25 to 100 kPa), the undisturbed strengths are probably close to the true field strengths, however, anisotropy effects have not been considered.

The remoulded vane strength also increases with depth, with the lowest values (2 to 5 kPa) observed just below the crust and highest values (12 to 25 kPa) at the base. The increase in remoulded shear strength concurrent with undisturbed shear strength keeps the sensitivity comparatively constant and relatively low (5 to 25) throughout the deposit.

The highest values of sensitivity generally occur in the soft zone just beneath the crust where values range from 20 to infinity and correlate with the lowest salinities measured.

In low elevation boreholes 75-1 to 75-5, the sensitivity (by field vane) decreases from about 15 to 30 in the near surface soft zone to values of about 5 to 10 at depth. In boreholes 75-6 and 75-7 on the upper clay plain, the sensitivity shows a definite increase with depth, a phenomenon compatible with the increasing liquidity index values also shown by these clays.

It is important to note that some of the tube samples occasionally yielded siltier clays in which the water content was far in excess of the liquid limit (e.g. borehole 75-7 at 13 m depth). This individual soil had a liquidity index of 2.7 and should have been very sensitive indeed, had it been encountered by the field vane.

BOREHOLES 78-1 AND 78-2

Twelve unconfined compression tests were run on the 3-inch piston samples from the 1978 boreholes with the results shown in Figures 14 and 15.

Several of the stress-strain curves presented in Appendix B are rather flat indicating some sample disturbance, usually, but not always, for the deeper samples. The laboratory vane test values, also plotted on Figures 14 and 15, are similar to the unconfined shear strength results.

The bow-shaped strength profile shown on Figure 15 is very significant and will be discussed later in relation to the preconsolidation history of the deposit.

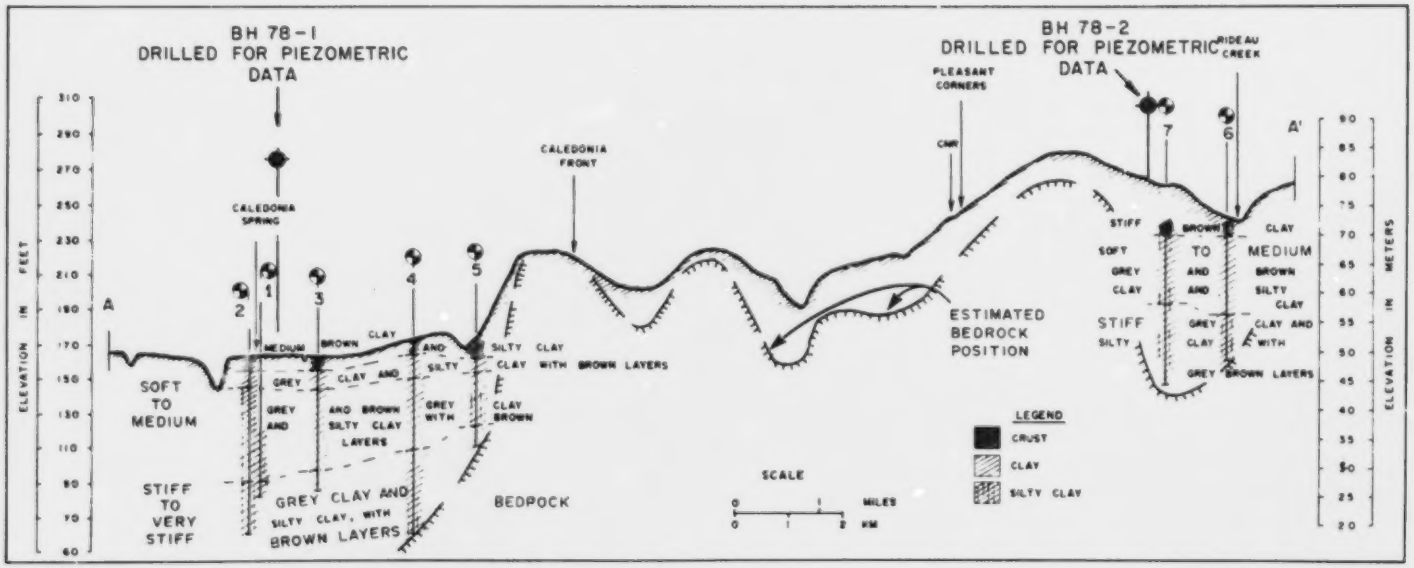

Figure 3. Stratigraphic cross-section A-A'; see Figure 2 for location. (Boreholes 1 to 7 represent holes 75-1 to 75-7).

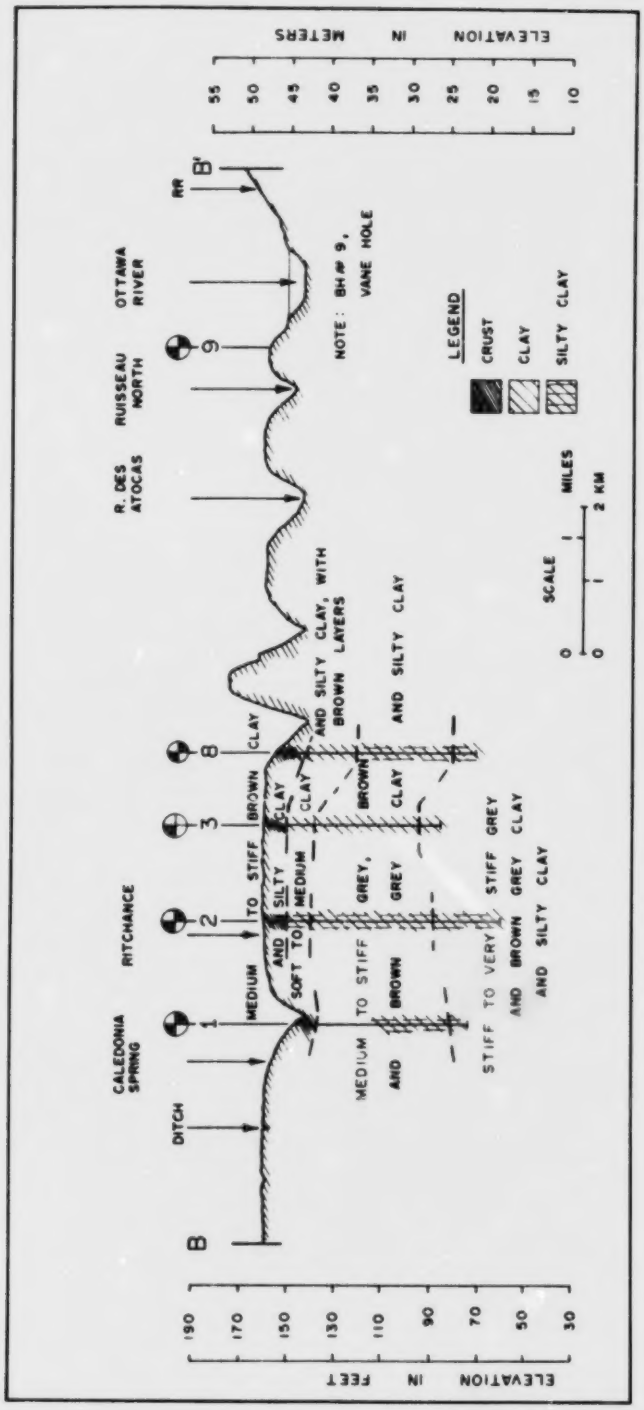

Figure 4. Stratigraphic cross-section B-B'; see Figure 2 for location. (Boreholes 1,2,3,8 and 9 drilled in 1975).

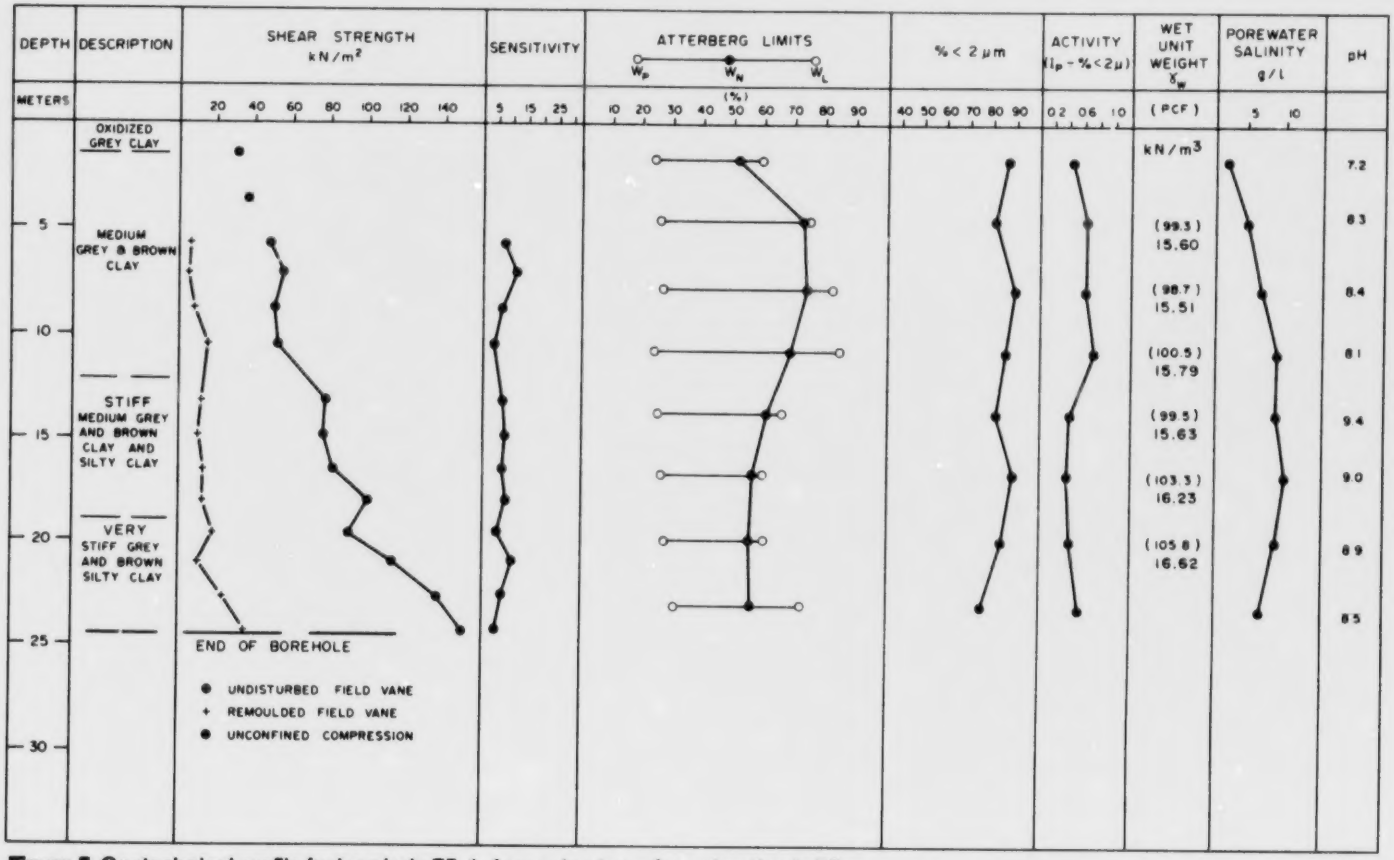

Figure 5. Geotechnical profile for borehole 75-1. Approximate surface elevation is 53 m.

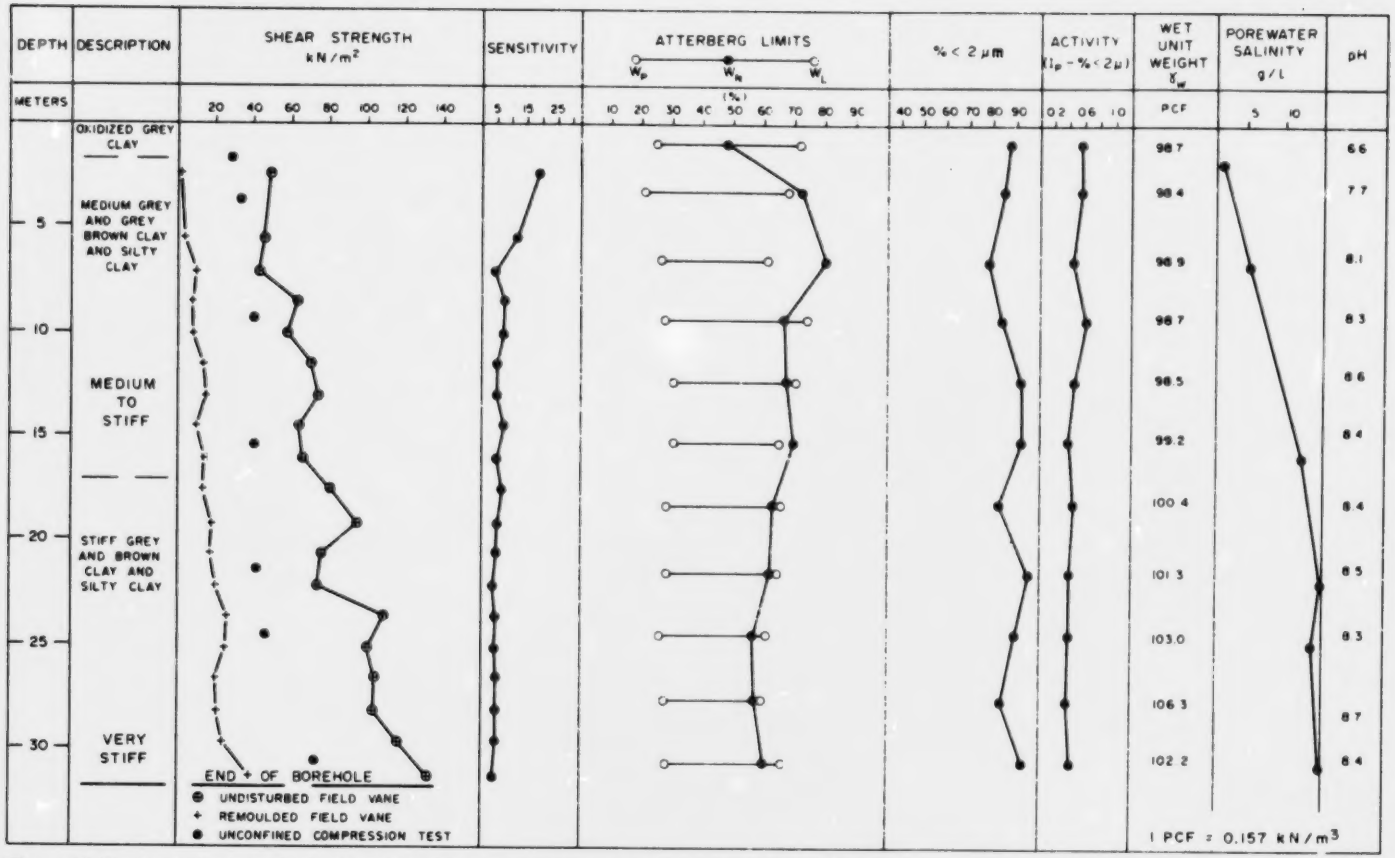

Figure 6. Geotechnical profile for borehole 75-2. Approximate surface elevation is 53 m.

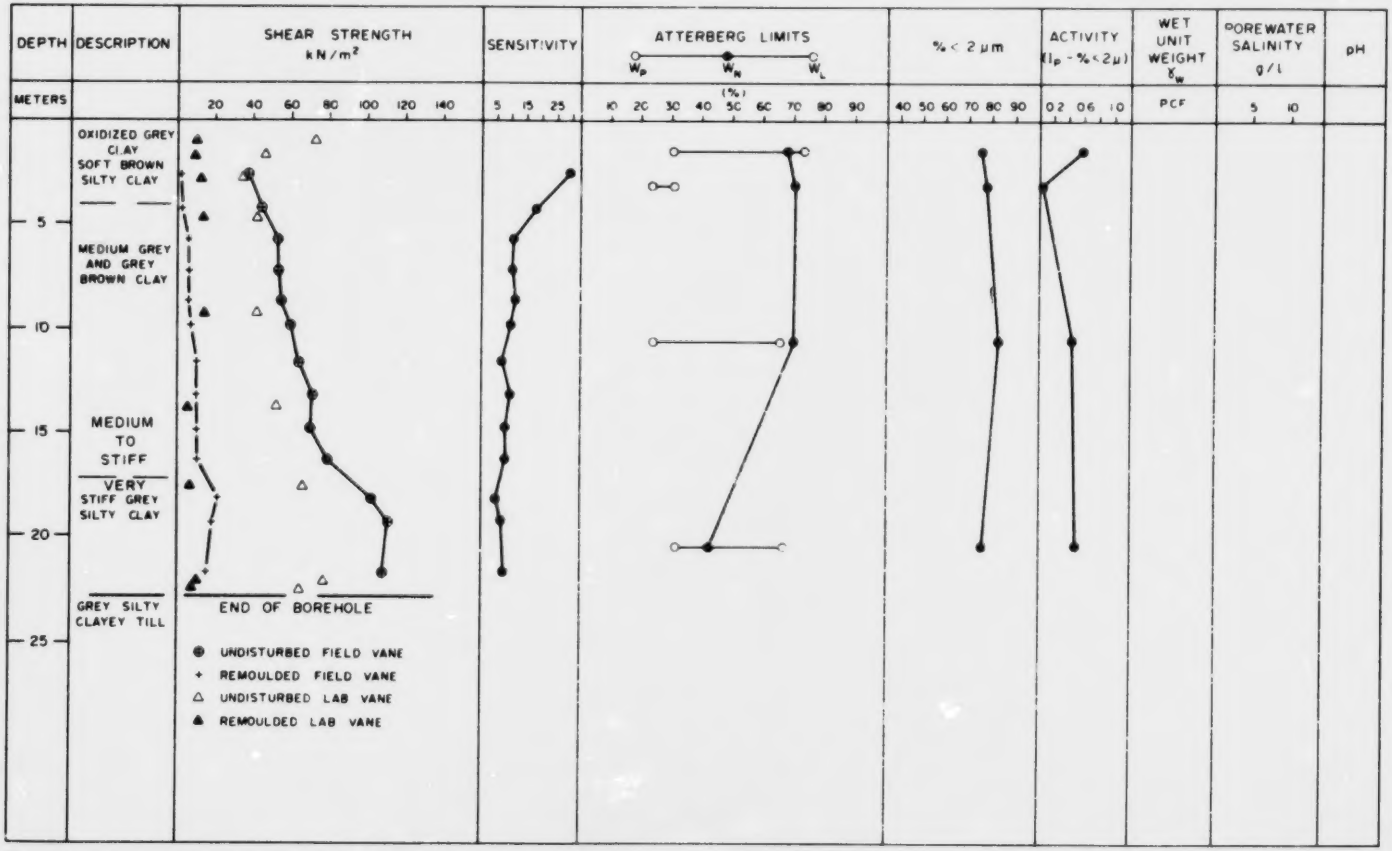

Figure 7. Geotechnical profile for borehole 75-3. Approximate surface elevation is 53 m.

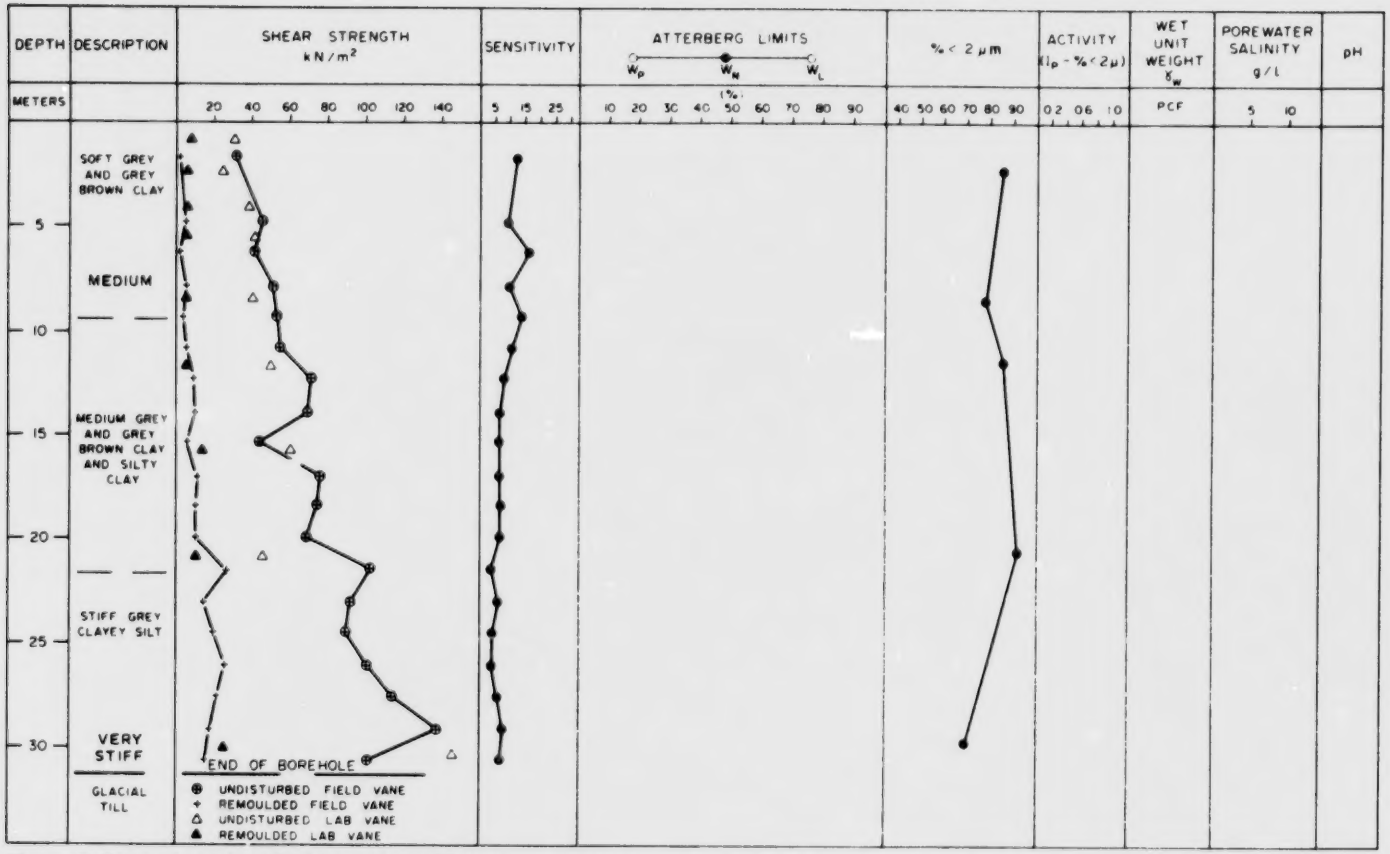

Figure 8. Geotechnical profile for borehole 75-4. Approximate surface elevation is 53 m.

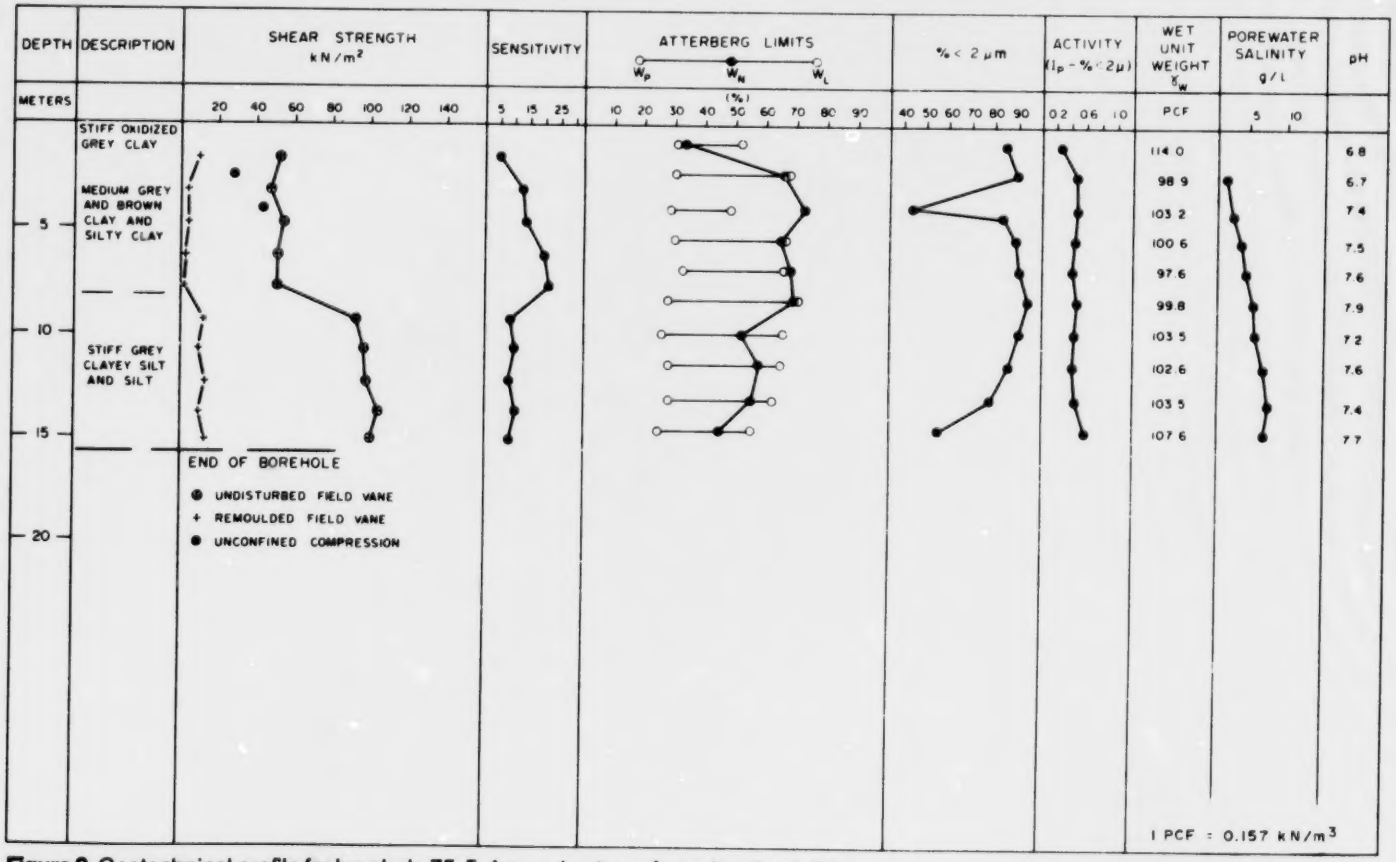

Figure 9. Geotechnical profile for borehole 75-5. Approximate surface elevation is 53 m.

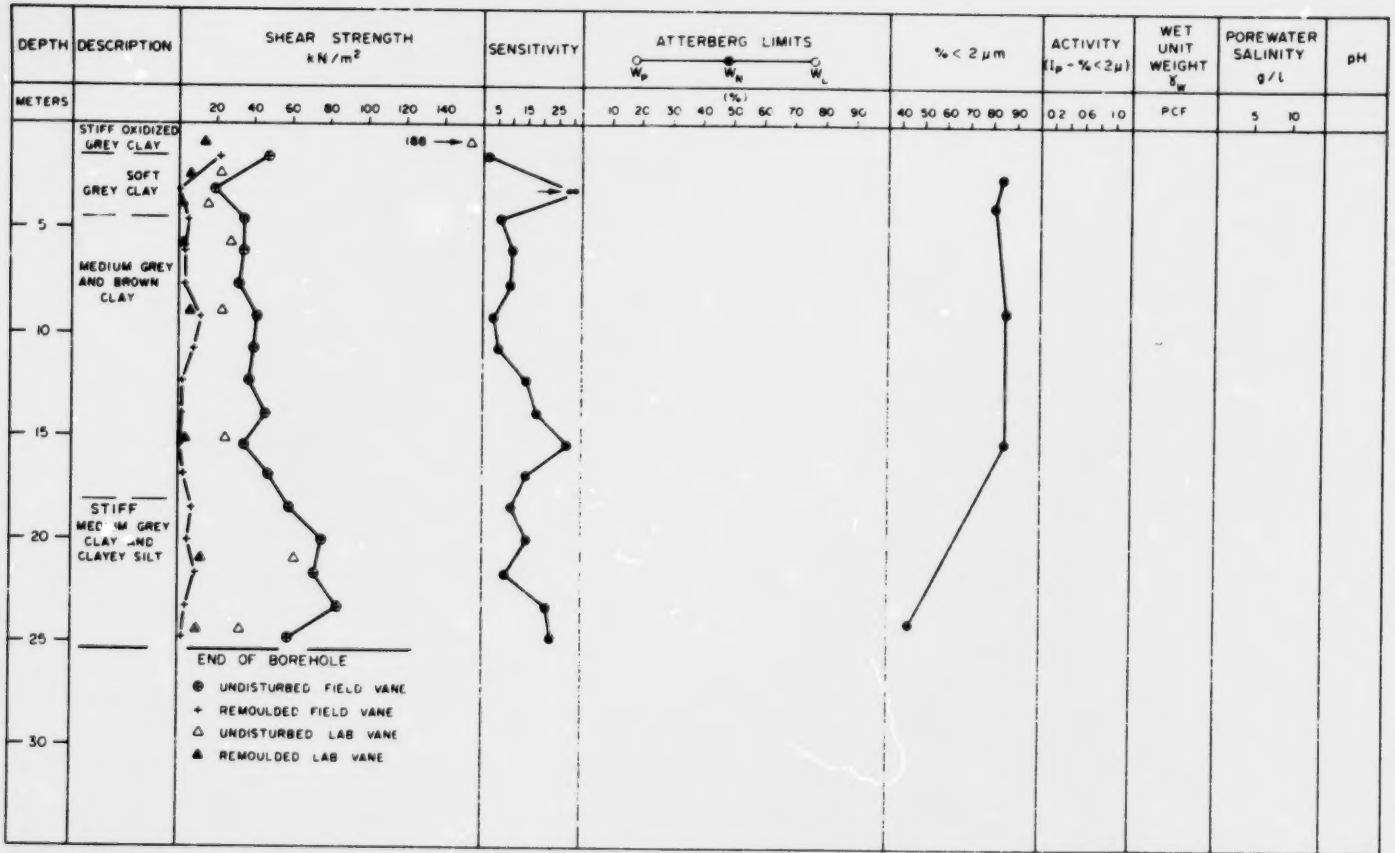

Figure 10. Geotechnical profile for borehole 75-6. Approximate surface elevation is 71 m.

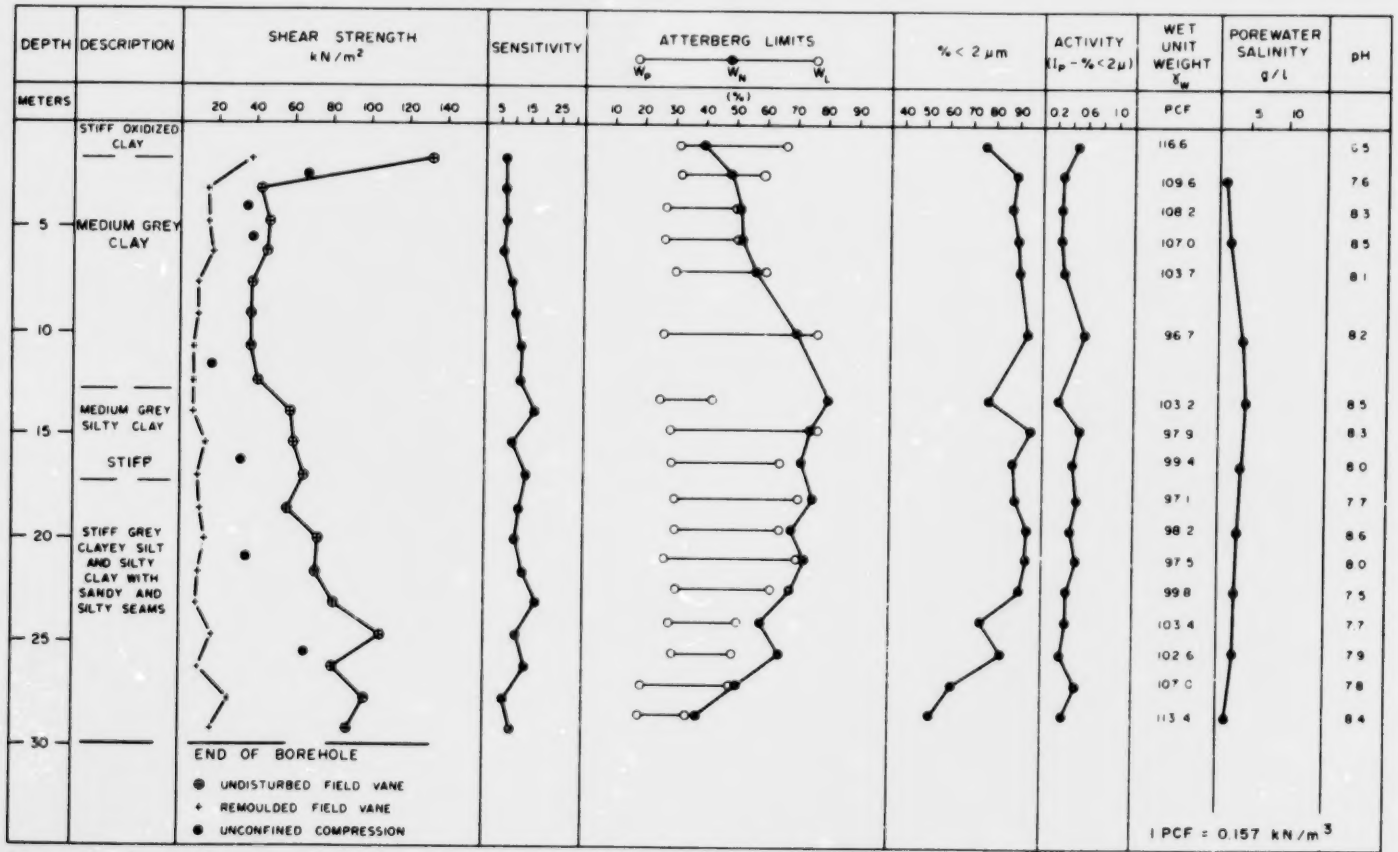

Figure 11. Geotechnical profile for borehole 75-7. Approximate surface elevation is 71 m.

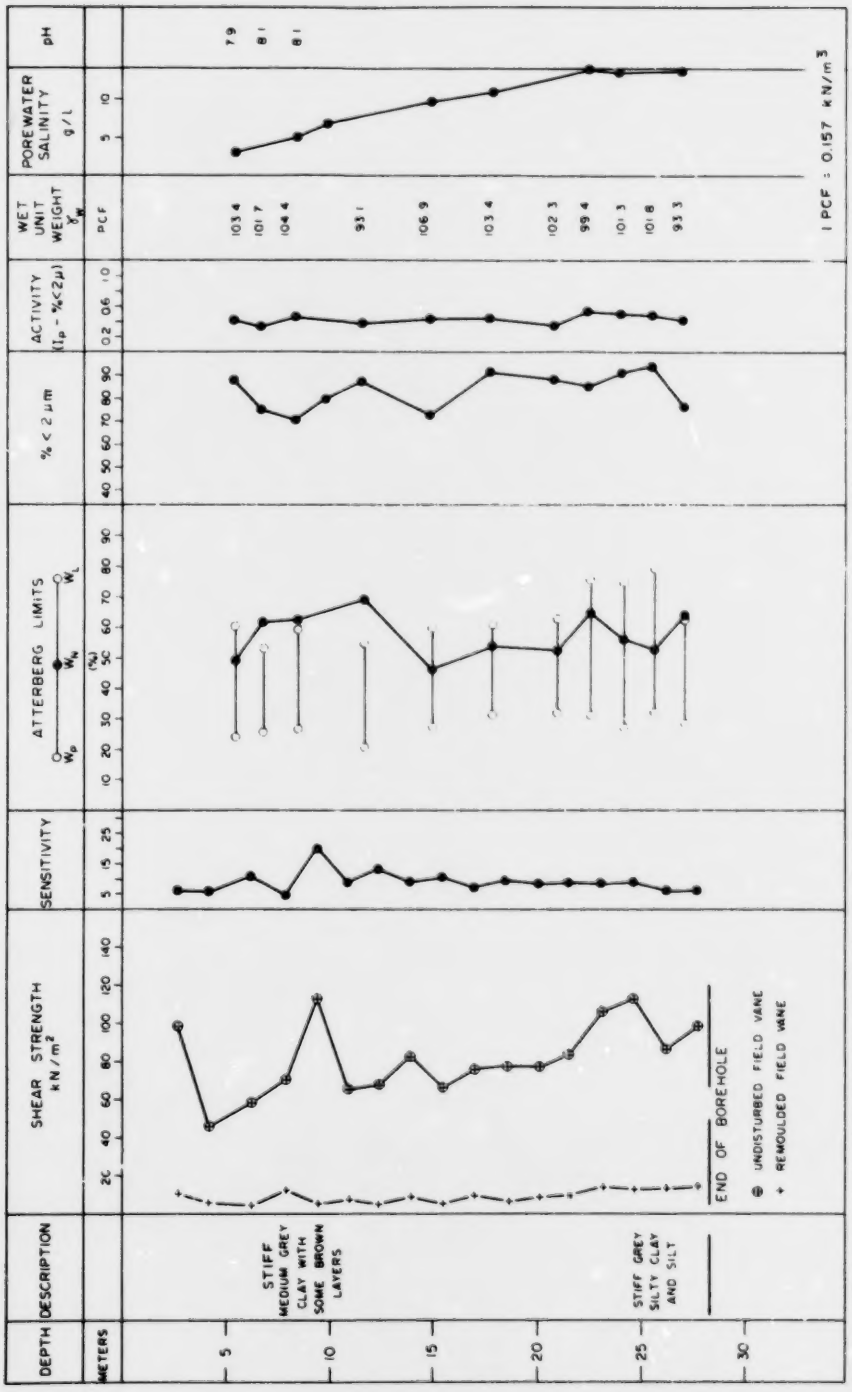

Figure 12. Geotechnical profile for borehole 75-8. Approximate surface elevation is 53 m.

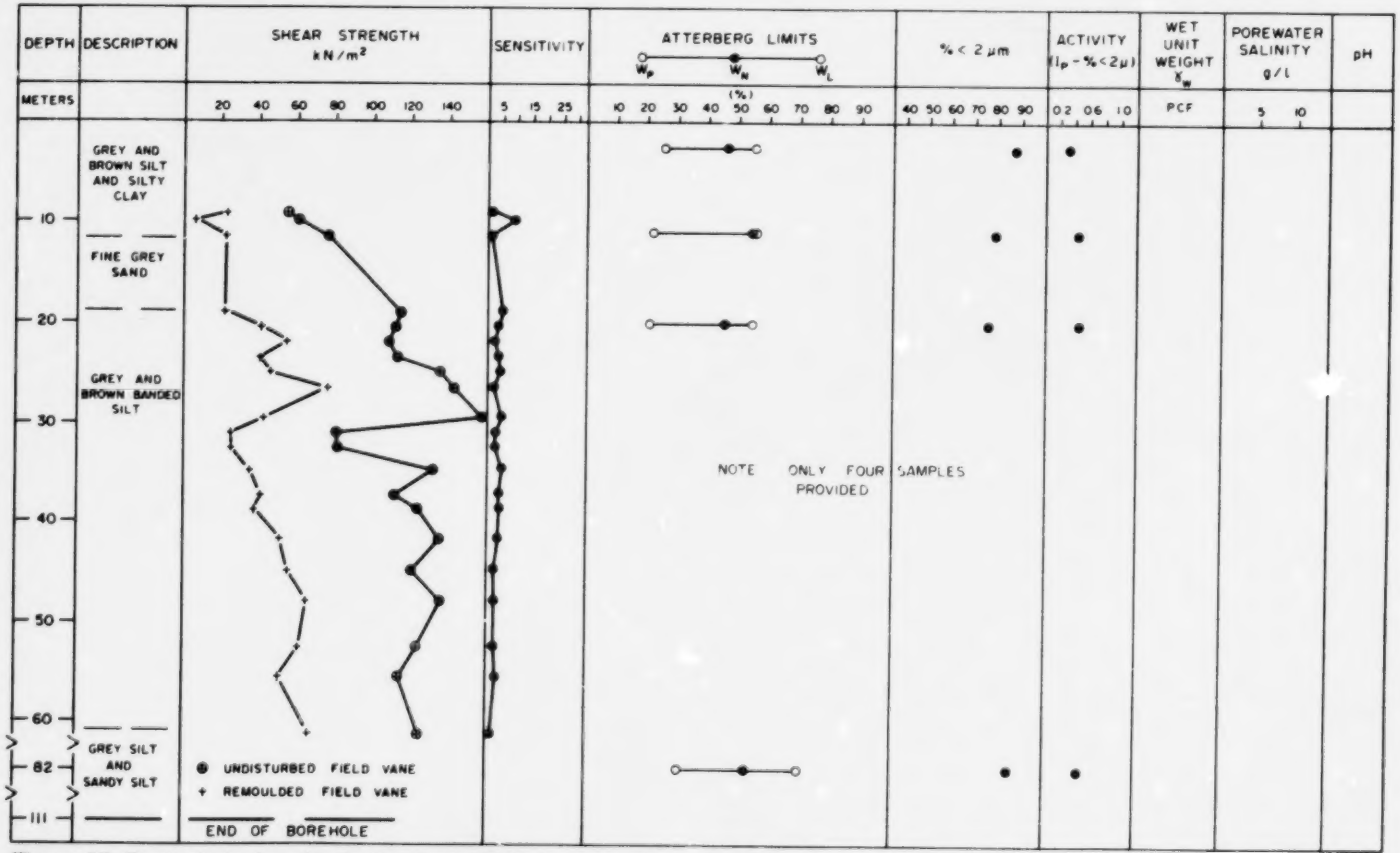

Figure 13. Geotechnical profile for borehole 75-9. Approximate surface elevation is 45 m.

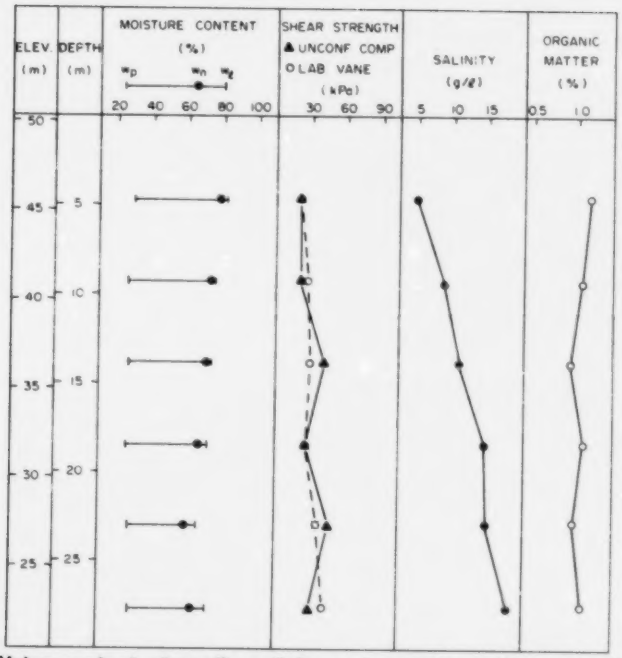

Figure 14. Water content, strength, salinity and organic matter vs depth, borehole 78-1. Approximate surface elevation is 50 m.

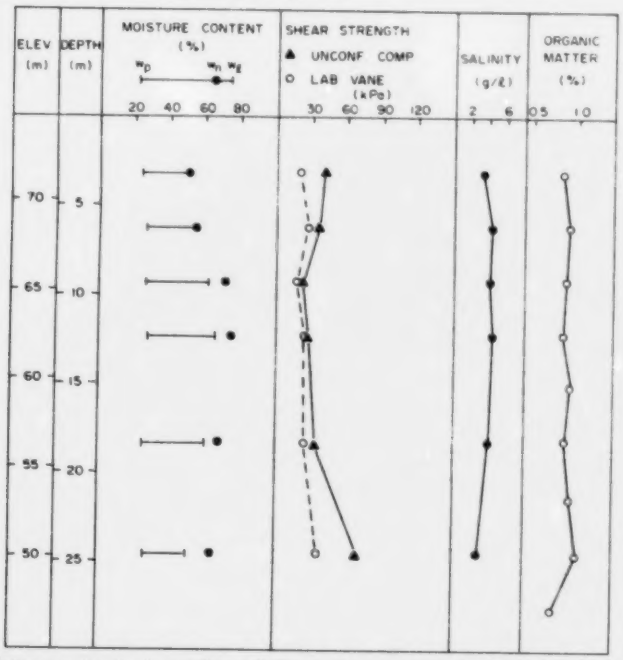

Figure 15. Water content, strength, salinity and organic matter vs depth relationships, borehole 78-2. Approximate surface elevation is 75 m.

CONSOLIDATION

Consolidation curves for the twelve samples tested are presented in Appendix C along with estimated values of *in situ* effective stress, p_o, and preconsolidation pressures, p_c, determined by a Casagrande construction. Values of over-consolidation ratio (O.C.R.) defined as p_c/p_o are noted next to each curve.

Summary plots of preconsolidation pressure versus depth are given on Figures 16 and 17 for the two 1978 boreholes in comparison to the corresponding *in situ* effective stress values. If the central p_c value on borehole 78-1 is ignored, then both figures indicate that the Hawkesbury Leda clay is preconsolidated at the top and bottom and essentially normally consolidated at the centre relative to the *in situ* effective stress values. The curves strongly suggest that the entire area was unloaded prior to complete consolidation of the clay stratum at some time in the past. Since the piezometers indicate close to hydrostatic conditions at the site (see next section), then a central, under-consolidated zone is not an alternative explanation.

Figure 19 for borehole 78-2 shows a strong inverse correlation between over-consolidation ratio and natural or initial moisture content. This correlation strongly suggests that, at borehole 78-2, a volume decrease due to consolidation by a previous load is indeed responsible for the preconsolidation, and that unloading, possibly by erosion, prevented preconsolidation in the central portion of the clay layer.

Figure 18 for borehole 78-1 is more difficult to interpret since the preconsolidation at surface is accompanied by an increase in moisture content. Such a phenomenon is suggestive of significant cementation bonding that would create a preconsolidation state without volumetric compression.

WATER CONDITIONS

The five sets of piezometer readings for boreholes 78-1 and 78-2 are plotted on Figures 20 and 21, respectively. The lower three piezometers in each hole had stabilized by August 1978 and remained essentially constant to May 1979. The shallow piezometer (3 m) in each hole recorded a fairly low water level until November when both rose to an equilibrium depth of 0.8 or 0.9 m. The lower summer readings probably reflect surface drying as expressed by the brown crust at both sites.

The groundwater flow regime on May 19, 1979 is illustrated by the summary plot on Figure 22. At boring 78-1 on the lower clay plain, there is a small downward flow under a gradient of 0.047. At borehole 78-2 on the higher clay plain there is a slight upward flow under a gradient of 0.021. The plots of effective stress versus depth shown on Figures 16 and 17 have been calculated using measured unit weights and *in situ* pore pressures for May 1979.

DISCUSSION

Using the piezometric data given on Figure 22, a series of seepage calculations have been carried out to establish a possible travel distance of leachate waters. The assumptions used for the calculations are as follows:

1. Permeability, $k = 10^{-8}$ cm/sec $\sim$ 0.315 cm/yr.

This value corresponds to an average of those calculated from the consolidation test results which ranged from 10^{-7} to 10^{-9} cm/sec. For simplicity, k is assumed to be constant with depth.

2. Porosity, n = 64 percent = 0.64

The *in situ* porosity values vary from about 67 percent at surface to 62 percent at depth. For simplicity, n is assumed to be constant at 64 percent for seepage velocity calculations.

3. Time for flow = 9000 years.

As discussed in the Quaternary geology section, the upper and lower clay plains, respectively, are believed to have emerged some 9600 and 9000 years before present. Initial pore pressures must have been positive followed by some negative pore pressures during unloading by erosion, so that an estimate of flow time is strictly for purposes of illustration.

4. Present gradients: borehole 78-1, i = 0.0467 downwards; borehole 78-2, i = 0.021 upwards.

For purposes of illustration, the present-day gradients are assumed to have applied over the past 9000 years. This, of course, is very unlikely.

5. Darcy flow equation applies.

Average linearized seepage velocity, $v_s = ki/n$. This is a highly simplified assumption if applied to chemical migration since 9000 years of diffusion is very significant for low gradient situations.

Using these figures, it is calculated that pore water would have moved a distance downwards of 2.1 m in borehole 78-1 and upwards a distance of 0.9 m in borehole 78-2. These flow distances are minimal compared to the clay thickness at each site and suggest little advective leaching. Much more work could be done on these calculations, however, it seems inappropriate for this report.

The preconsolidation profiles shown in Figures 16 and 17 indicate that consolidation took place under conditions of top and bottom drainage. In other words, water from the clay mass drained towards both the top and bottom. The resultant salinity, therefore, should have been fairly constant throughout the clay deposit and typical of the salinity of the central portion. Interpretation of the geochemical profiles in the next section must consider the combined effects of consolidation-drainage during loading, rebound swelling during erosion, and subsequent transport of fluids by both advection and long term diffusion.

The lower drainage boundary below the clay deposits was only approximately located by the exploration program carried out. Nevertheless, the preconsolidation profiles may be used to illustrate the approximate load removed by erosion. One can then speculate as to the original soil conditions that first created the load and then were removed by erosion. The results of such an interpretation are shown on Figures 23 and 24 for the lower and upper clay plains, respectively. The lower and upper drainage boundaries shown on the figures are assumed to be 100 percent consolidated and are located to fit the shape of the preconsolidation versus depth profiles for boreholes 78-1 and 78-2. Since both sets of p_c values indicate upward drainage and marked near-surface preconsolidation, it is inferred that surface sands existed at both sites.

The scheme shown on Figure 23 indicates removal by erosion of 21 m of submerged sand. For this case it is assumed that the surface sands were deltaic deposits and hence submerged most of the time prior to erosion. This amount of erosion compares reasonably well with the possible range of 18 to 33 m of erosion based on residual deposits of sands on the lower clay plain as discussed under "Fluvial Erosion".

The speculative scheme shown on Figure 24 indicates erosion of soil having a total potential effective stress at the present surface of some 145 kPa. This would be satisfied by erosion of 11 m of sand with a water table 3.5 m below original surface as shown. Although other schemes could be suggested, the shape of the present p_c profile strongly suggests that considerable sand has been eroded off the upper clay plain. For more details, see Quigley *et al.* (1983).

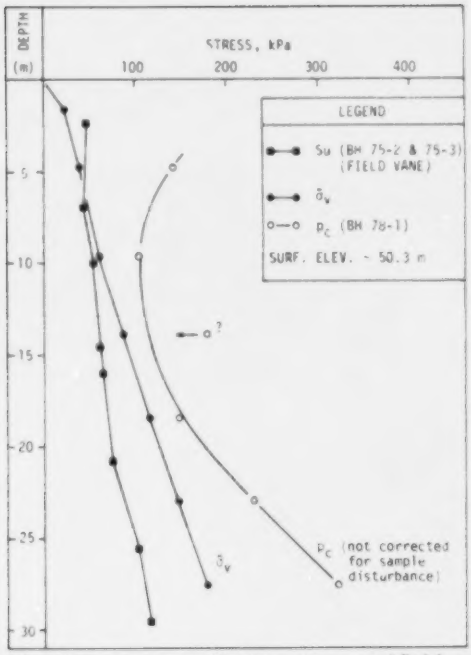

Figure 16. Preconsolidation pressure, effective stress and field vane shear strength vs depth, borehole 78-1.

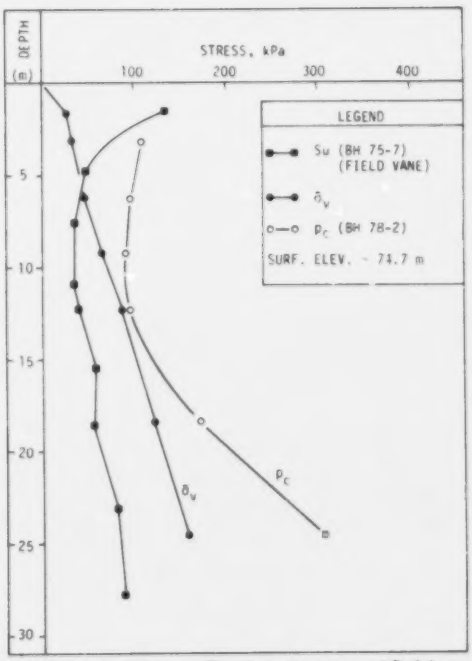

Figure 17. Preconsolidation pressure, effective stress and field vane shear strength vs depth, borehole 78-2.

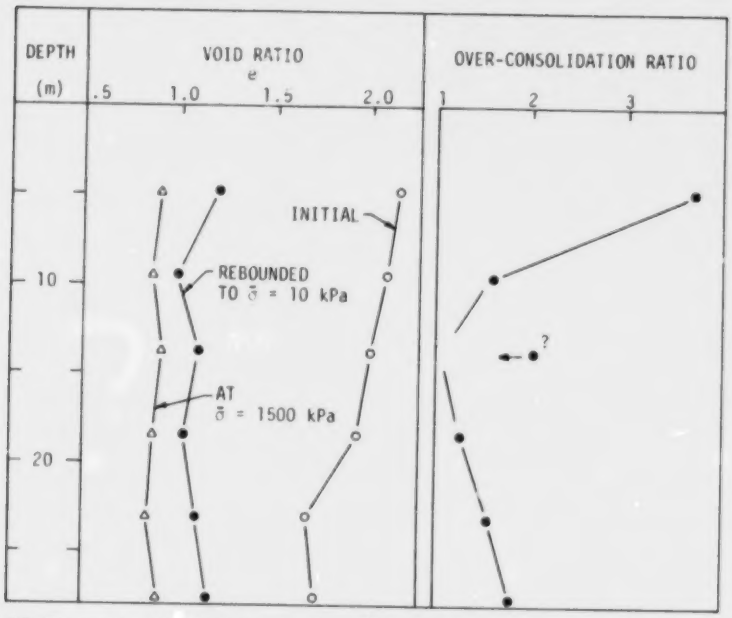

Figure 18. Consolidation test results, borehole 78-1.

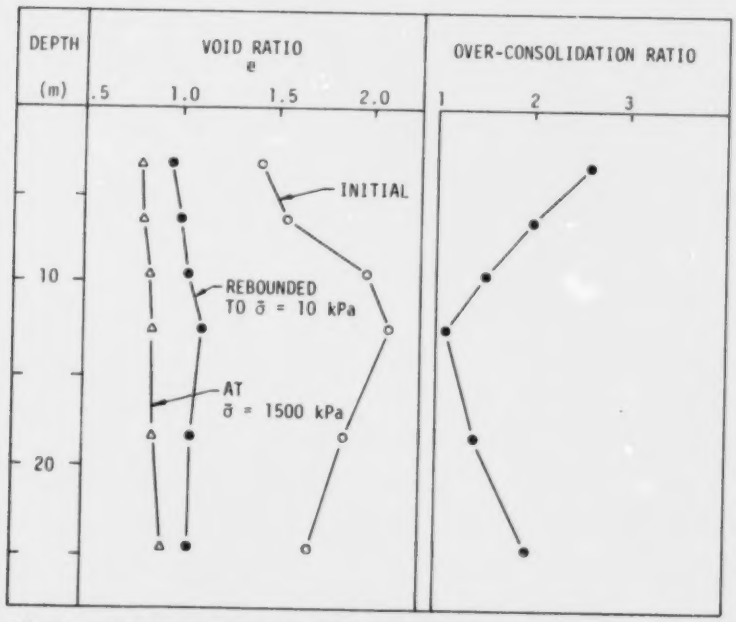

Figure 19. Consolidation test results, borehole 78-2.

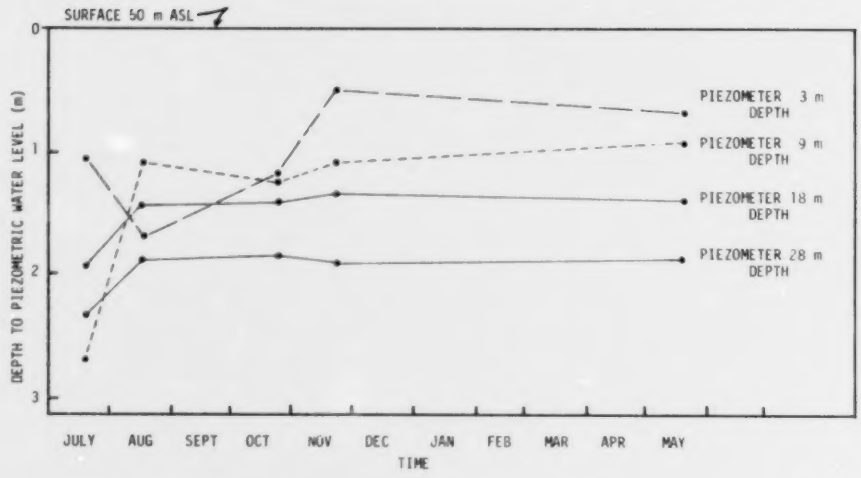

Figure 20. Piezometric water levels for borehole 78-1 (July 1978 to May 1979).

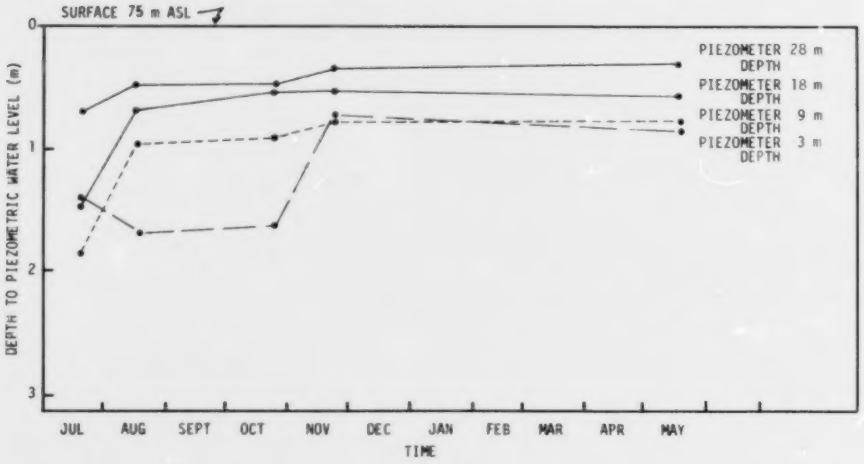

Figure 21. Piezometric water levels for borehole 78-2 (July 1978 to May 1979).

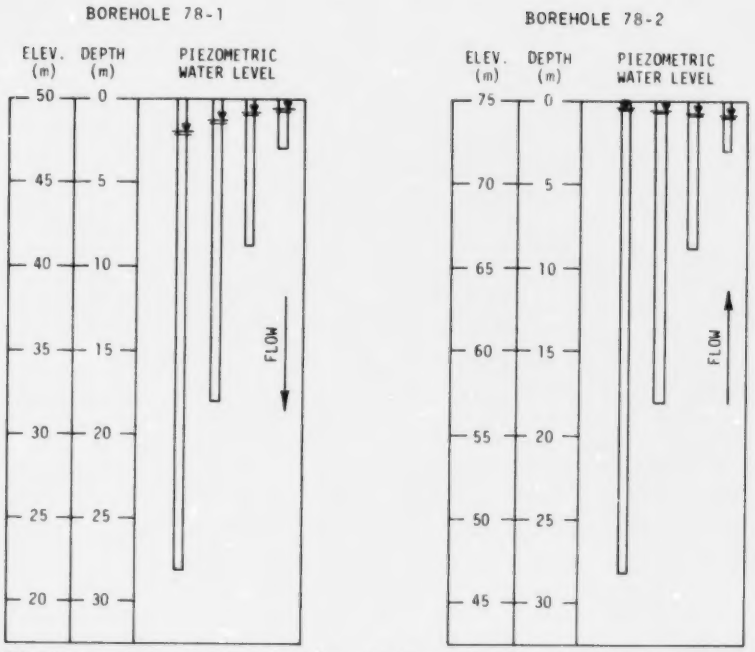

Figure 22. Piezometric water level readings for boreholes 78-1 and 78-2 taken on May 19, 1979.

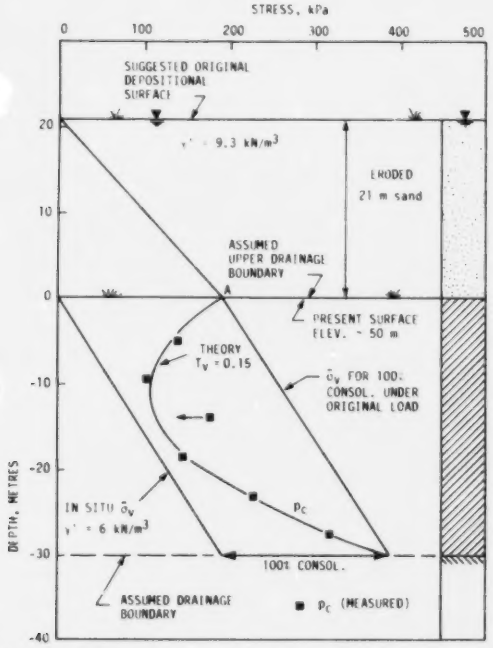

Figure 23. Stress-depth relationships and possible post-depositional erosion (borehole 78-1). Lower clay plain.

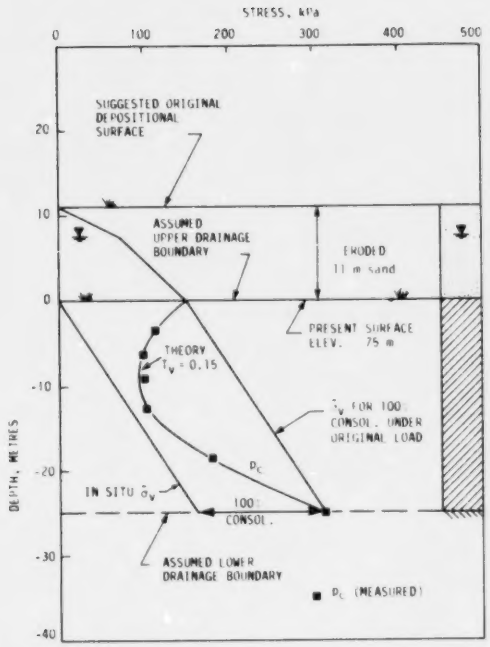

Figure 24. Stress-depth relationships and possible post-depositional erosion (borehole 78-2). Upper clay plain.

MINERALOGY

QUALITATIVE MINERALOGY

Analysis of the X-ray diffraction data indicates that all samples studied in the Hawkesbury Leda clay deposits contain quartz, plagioclase feldspar, potassium feldspar, amphibole, illite/mica, chlorite, vermiculite and small amounts of smectite. Trace amounts of heavy minerals are also present.

CLAY MINERALOGY, OXIDIZED CRUST

As mentioned previously, the top metre of clay has been weathered, and this has caused significant changes in the clay mineralogy. Figure 25 shows a typical X-ray diffraction trace of $<2\ \mu$m material from the oxidized crust. It is apparent that, in addition to illite/mica, chlorite and amphibole, there is a significant percentage of vermiculite and an expandable or swelling clay. In the 'natural' trace, a strong 15.2 Å (1.52 nm) peak that expands to 16.7 Å upon glycolation is produced by this smectite. The expandable material appears to be a low charge vermiculite or a vermiculite/smectite. It does not expand with glycolation after K-saturation, yet does expand to 17 Å with glycolation after Mg-saturation. Vermiculite comprises 13 to 20 percent of the $<2\ \mu$m fraction in samples taken from the crust based on glycol retention analyses. This percentage probably includes some of the expandable vermiculite/smectite.

Only small amounts of the vermiculite and vermiculite/smectite are present in the bulk of the deposit at depth. Their increased proportion in the crust is due to weathering, probably the oxidation of Fe-chlorite. Edge weathering of the illite/mica component could also be a minor source of vermiculite.

CLAY MINERALOGY, DEPOSIT BELOW CRUST

Five representative X-ray diffraction traces of oriented $<2\ \mu$m material are provided in Figures 26, 27 and 28. These figures and the hundreds of other X-ray traces run indicate that the same mineral suite occurs in all samples.

The illite/mica component produces a strong, slightly asymmetrical 10 Å peak. The origin of the micaceous minerals forming this peak would include both illites from the underlying Ordovician sedimentary rocks and micas from the Precambrian rocks of the Canadian Shield to the north. No distinction is made between the illites and micas. Magnesium saturation generally decreases the intensity of the 10 Å peak and enhances the 14 Å peak. It is possible that the Mg is homoionizing frayed edges and weathered mica/illite particles, expanding their interlayer spacings to a uniform 14 Å. This would decrease the 10 Å reflection and intensify the 14 Å peak. Mg^{++} homoionization of the vermiculite itself would also contribute to a better defined 14 Å peak.

Fe-chlorite is frequently the second most abundant clay mineral in these clay deposits. It produces weak 14 Å peaks and strong 7 Å peaks that remain unaltered after K-saturation, and X-ray using CuKα radiation.

Vermiculite, present in varying amounts, produces a 14 Å peak and a weaker 7 Å peak. Since vermiculite will collapse to 10 Å after K-saturation, a decrease in the relative intensity of the 14 Å peak in the K-saturated trace as compared to the Mg-saturated trace is used to establish the presence of vermiculite.

In most samples there is an expandable clay mineral, previously identified as a low charge vermiculite or vermiculite/smectite. This material produces a peak or increase in background at 17 to 15 Å in the natural and Mg-saturated glycolated traces. Its presence is clear on all traces in Figures 26 to 28. Some samples, such as 75-7-19 (Figure 27), appear to contain a trace of montmorillonite. However, these expandable minerals are present in very small amounts and are of minor importance to the engineering properties, except perhaps the permeability. It should be noted that the apparent proportion of swelling clay tends to be exaggerated because (1) the reflected intensity

becomes much greater at low values of 2θ; (2) the centrifugal sedimentation method of sample preparation enhances the reflections of the very fine clays, the fraction in which the expandable minerals are concentrated; and (3) glycolation will also slightly increase the reflected intensity at low 2θ. Of the non-clay components in the clay-size fraction — quartz, feldspars and amphibole — only amphibole produces a peak between 14° and 2° 2θ. It is apparent on all traces at 8.58 Å.

Figure 26 provides a comparison of grey (75-2-11) and brown (75-2-13) clay samples. No greater differences were observed between the brown and grey clays than were observed between all grey clay samples. Examination of the four X-ray traces of $< 2\,\mu$m grey clay provided in Figures 26 to 28 will confirm this.

MINERALOGY OF NON-CLAY COMPONENTS

Figures 29 and 30 illustrate four representative powder pattern diffraction traces. The main peaks for quartz (3.35 and 4.26 Å), plagioclase feldspar (3.17 to 3.21 Å), potassium feldspar (3.26 Å), amphibole (8.58 Å) and the clay minerals illite/mica and chlorite are apparent on all traces. Some traces show calcite (3.03 Å) and dolomite (2.88 Å) peaks, although generally these minerals are not abundant enough or present in large enough crystals to produce clear diffraction peaks.

The relative intensity of an X-ray peak is related to the abundance and crystallinity of that particular mineral. However, it is also markedly affected by the grain size distribution, the composition of the mineral itself, and especially the presence of amorphous coatings acting as shields to the X-rays. Bearing these restraints in mind, it is still clear from the variations in peak heights from trace to trace that the relative percentages of the non-clay minerals do vary between samples as calculated later.

'AMORPHOUS' MATERIALS

The Segalen selective dissolution technique, used to determine the amount of amorphous constituents, is based on the assumption that amorphous material dissolves at a faster rate than crystalline minerals of similar composition. Once a constant dissolution rate is achieved, extraction is stopped. The concentrations of extracted Si, Al and Fe are plotted as shown in Figure 31 and the percentage of amorphous material determined by extrapolation. The data for the other 17 samples are provided in Appendix F. An average of 12 percent amorphous material was extracted from the Hawkesbury samples. The Segalen technique is now believed to be too severe for these soils (Quigley 1980), and the measured amounts probably include dissolved clay minerals.

The exact form of the amorphous material is unknown. It could exist as a precipitate at particle contacts, as a general coating around the soil particles and/or as an outer phase of the mineral particles. 'Extraction' of the soils by this method certainly produces clearer X-ray diffraction traces, with lower background noise, suggesting a general 'cleaning up' of the soil particles as illustrated for oriented traces of sample 75-2-17 on Figure 32. After treatment, the feldspar peaks are generally much more distinct and the clay mineral peaks are sharper and more symmetrical. Some of the increased intensity of the clay peaks may be attributable to the better disaggregation, and hence better subsequent orientation, following this technique. Removal of frayed edges, which could have resulted from glacial grinding or previous weathering, would also contribute to the greater symmetry of the clay peaks.

Originally, it was suspected that the stiff layers in some boreholes (e.g., borehole 75-8, Figure 12) may have contained higher concentrations of 'amorphous' material acting as a cementing agent. No such correlation was found.

Figure 33 illustrates that there is no clear relationship between the percentage of 'amorphous' material and either sample depth or elevation, although there does appear to be a slight increase at lower elevations. The 12 percent 'amorphous' material recorded

for the Hawkesbury samples is comparable to values obtained using the same technique for other locations in the Champlain Sea (McKyes *et al.* 1974; Haynes 1975). It is possible that the percentages of 'amorphous' material may result as much from the testing procedures and stripping of 'amorphous' rinds from glacially ground rock flour as they do from removal of a potential cementing agent. It could be of interest to compare the results of these extraction procedures on Canadian and Scandinavian sensitive marine clays since the Scandinavian clays have a similar geological origin but generally lack a highly cemented structure.

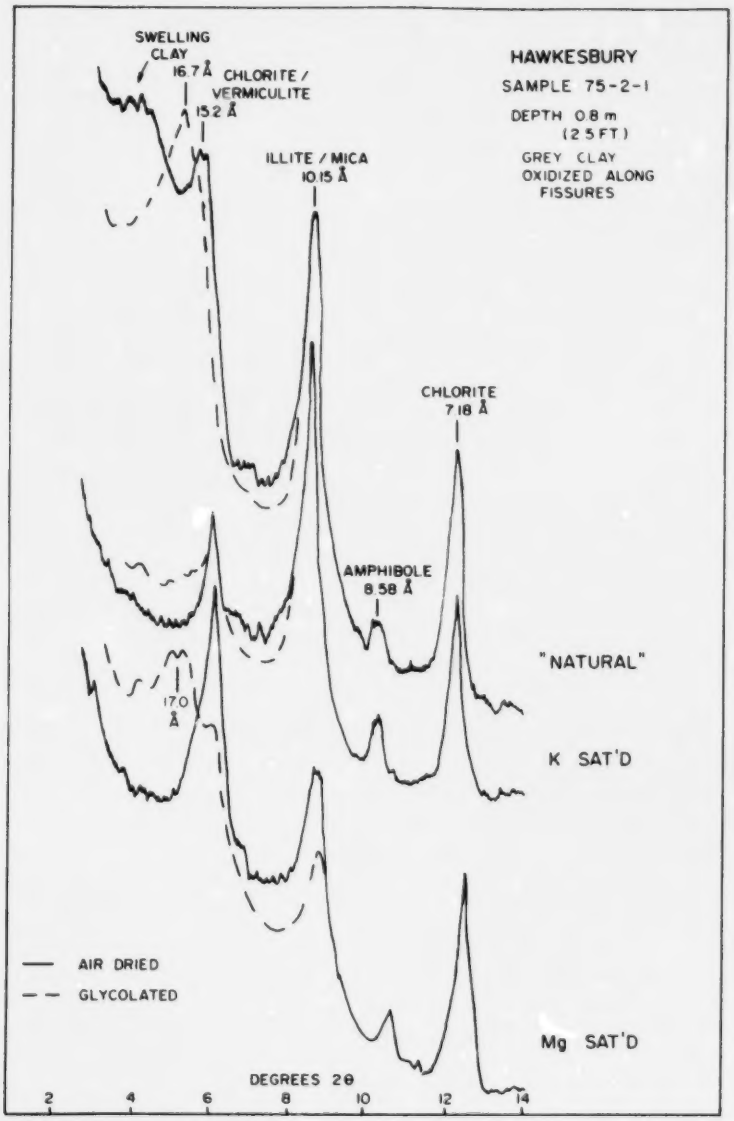

Figure 25. X-ray diffraction pattern of sample 75-2-1. Centrifuge-oriented, < 2 μm material.

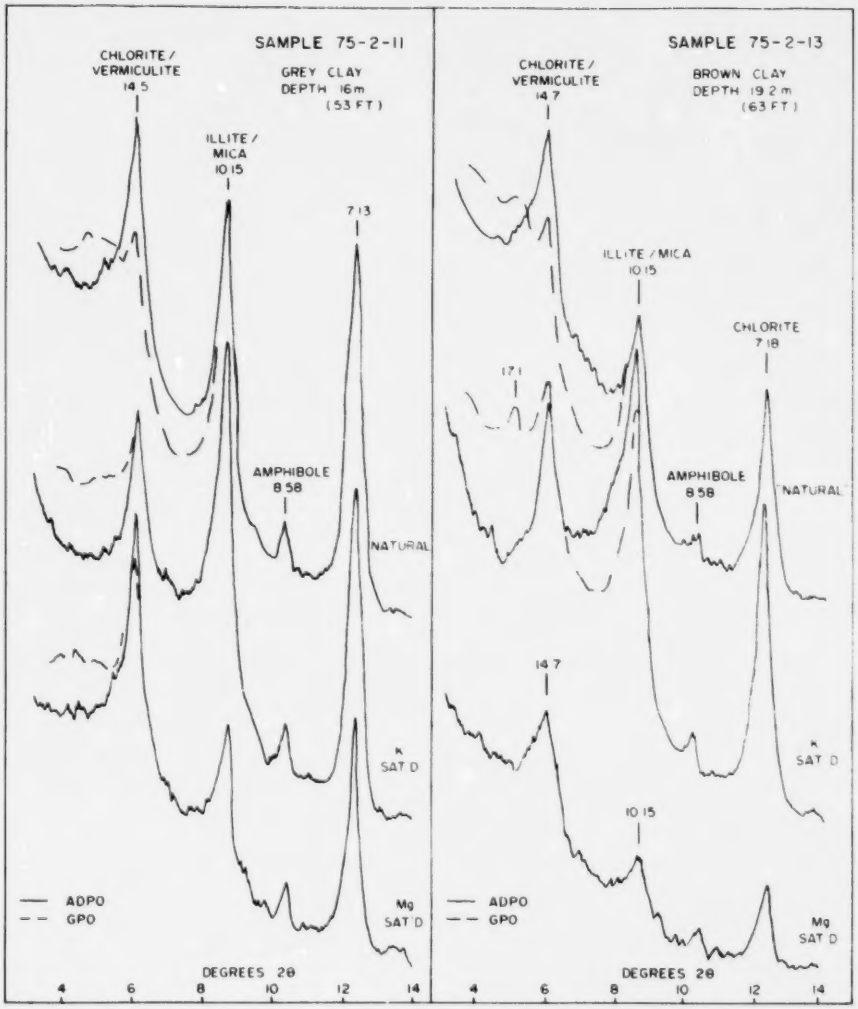

Figure 26. X-ray diffraction patterns of $< 2\ \mu m$ material from samples 75-2-11 and 75-2-13. Centrifuge-oriented, air-dried (ADPO) and glycolated (GPO).

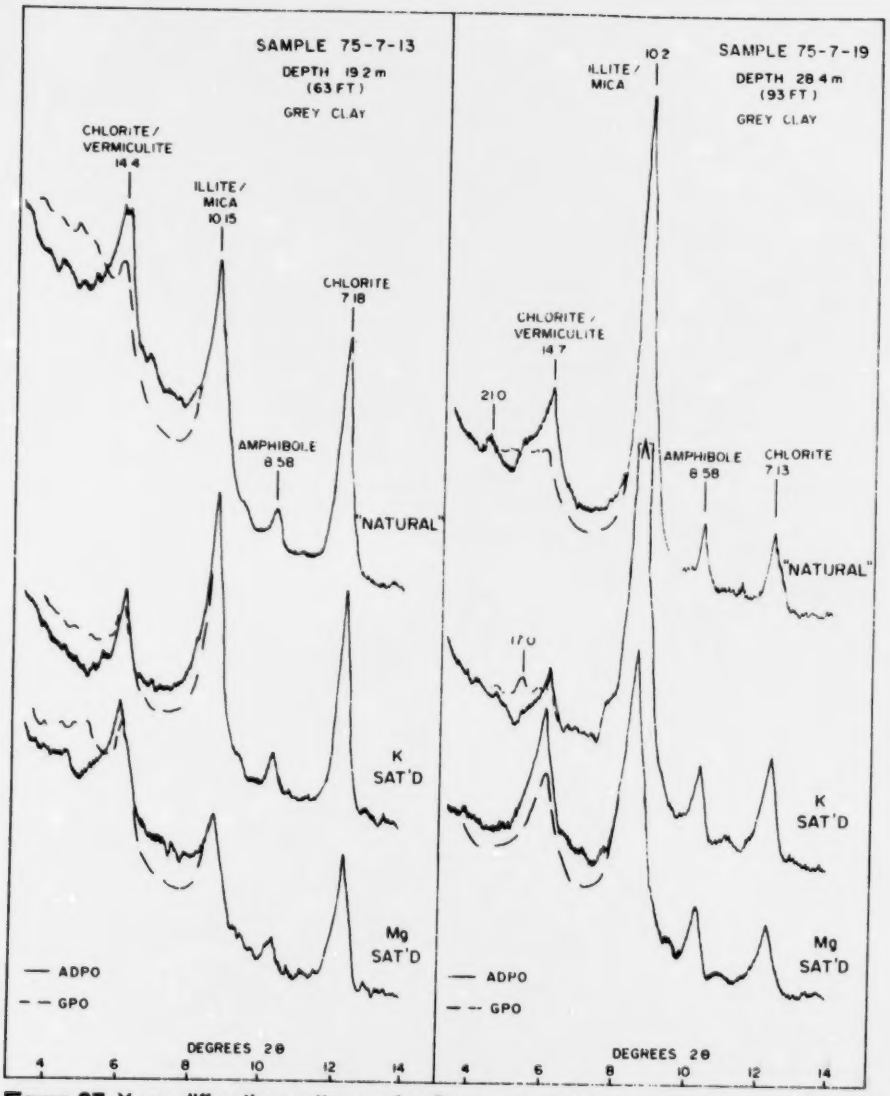

Figure 27. X-ray diffraction patterns of $< 2\ \mu m$ material from samples 75-7-13 and 75-7-19. Centrifuge-oriented, air-dried (ADPO) and glycolated (GPO).

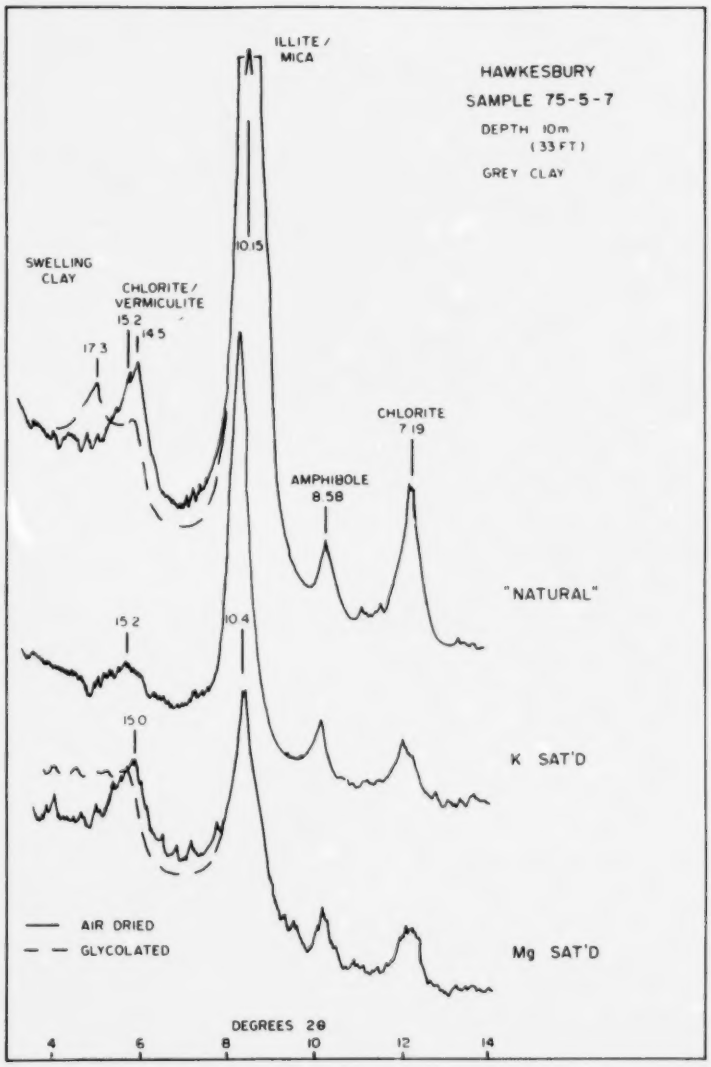

Figure 28. X-ray diffraction pattern of $< 2\ \mu m$ material from sample 75-5-7. Centrifuge-oriented.

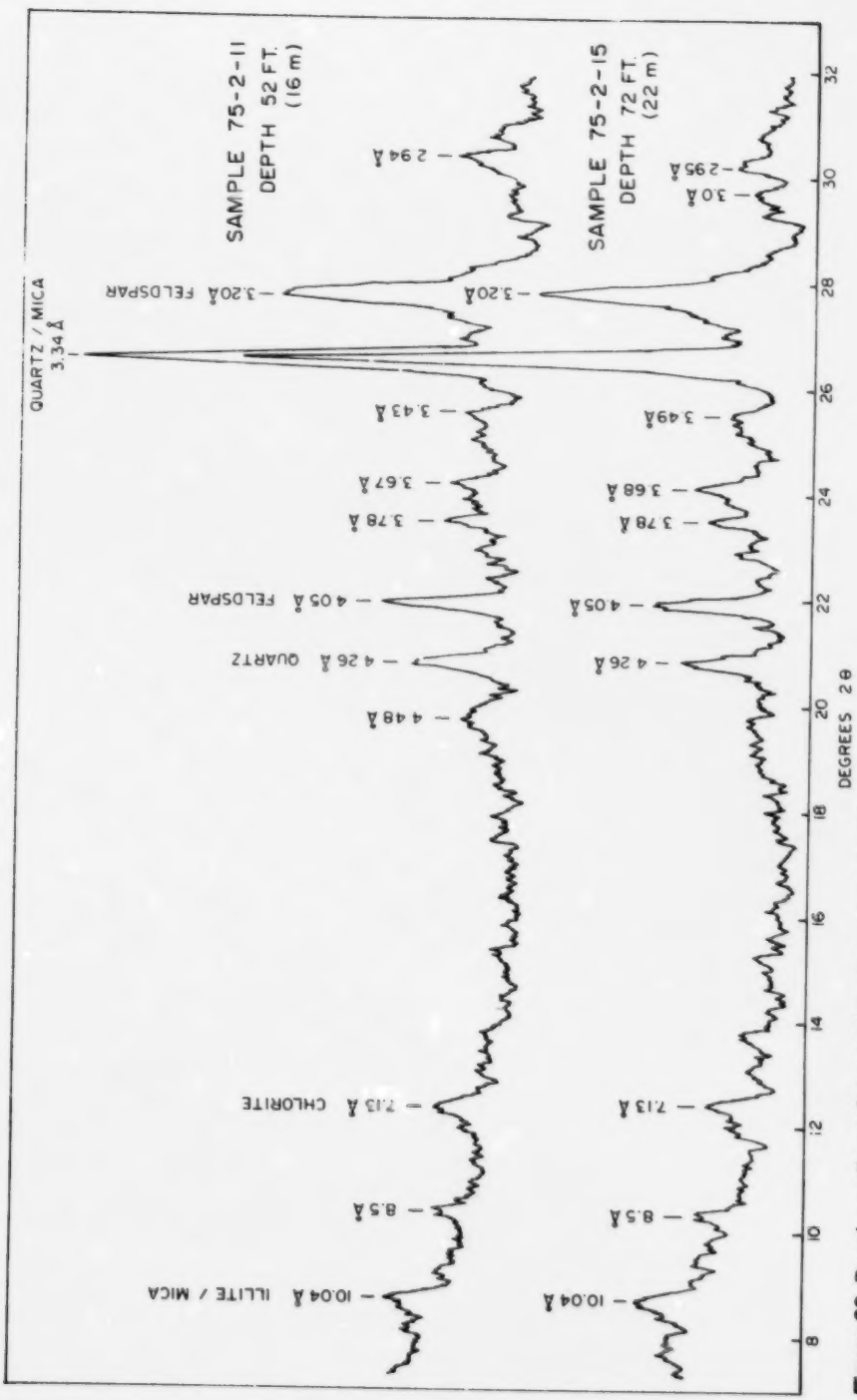

Figure 29. Powder patterns for samples from borehole 75-2.

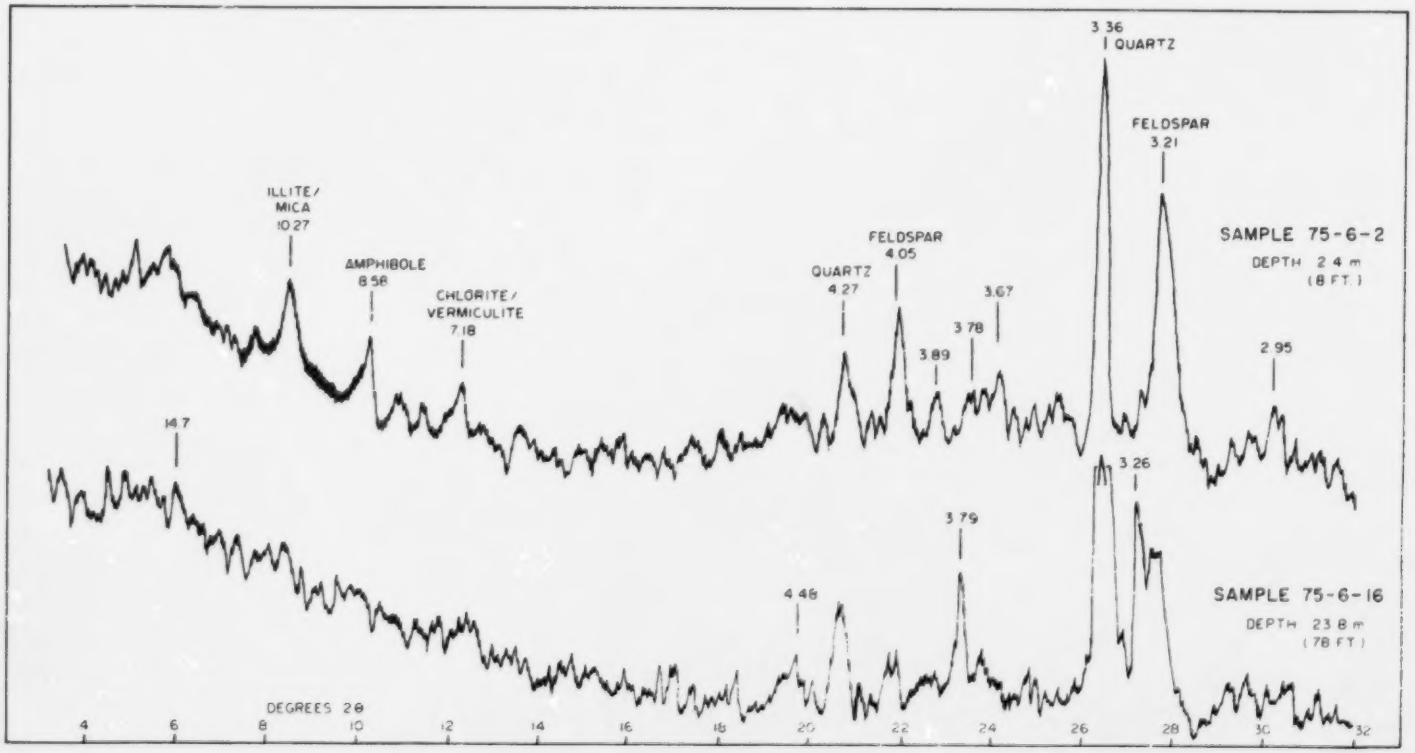

Figure 30. Powder patterns for samples from borehole 75-6.

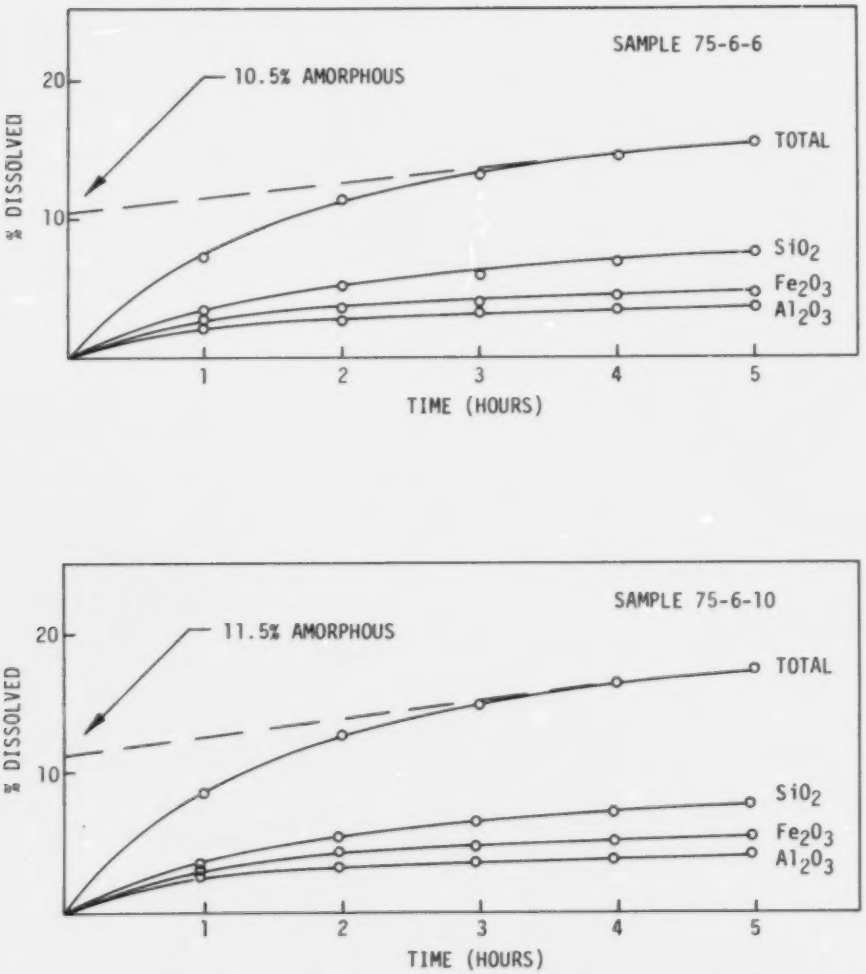

Figure 31. Dissolution rates of minerals in Hawkesbury clay, samples 75-6-6 and 75-6-10.

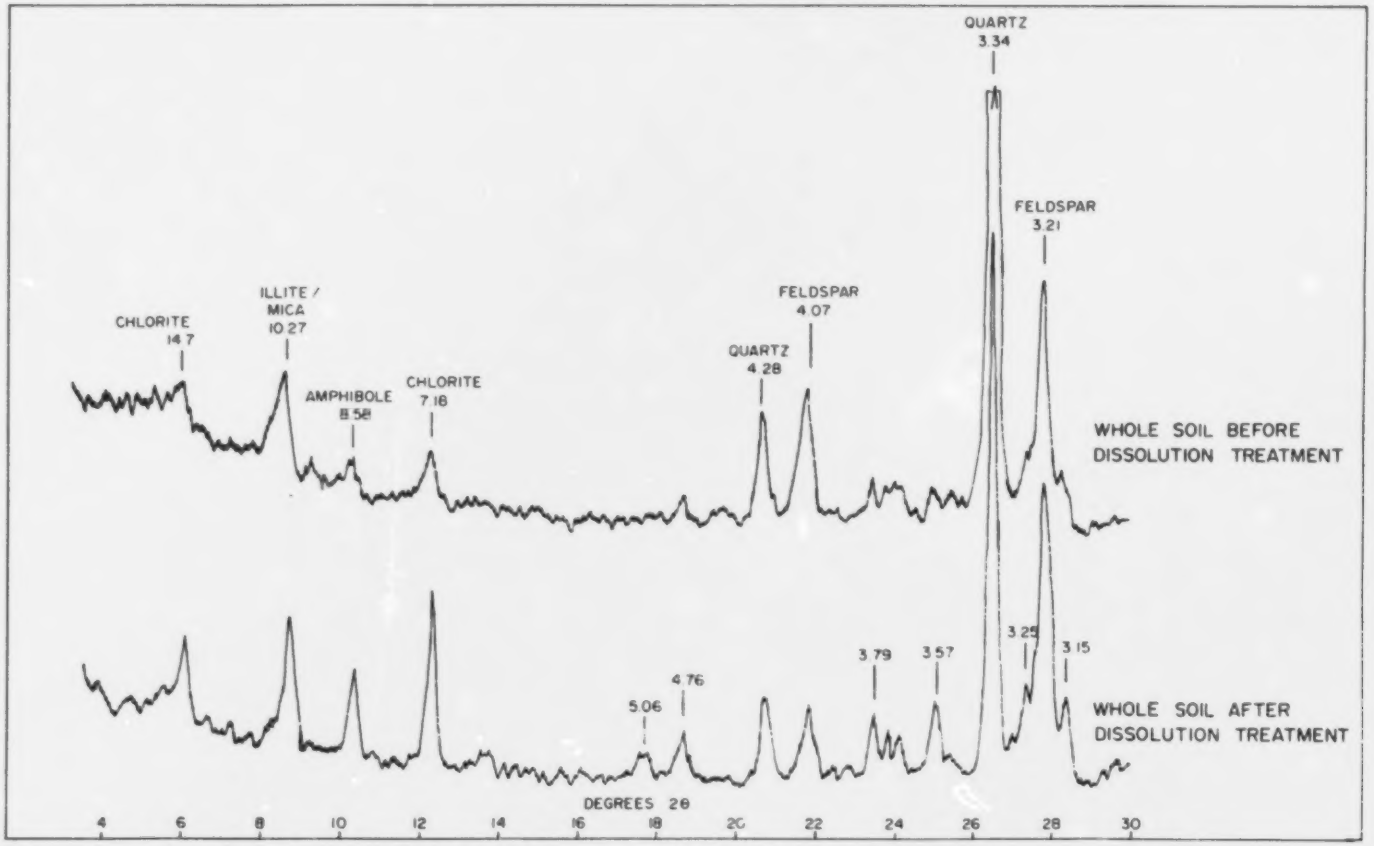

Figure 32. Powder patterns for sample 75-2-17, before and after HCl/NaOH selective dissolution.

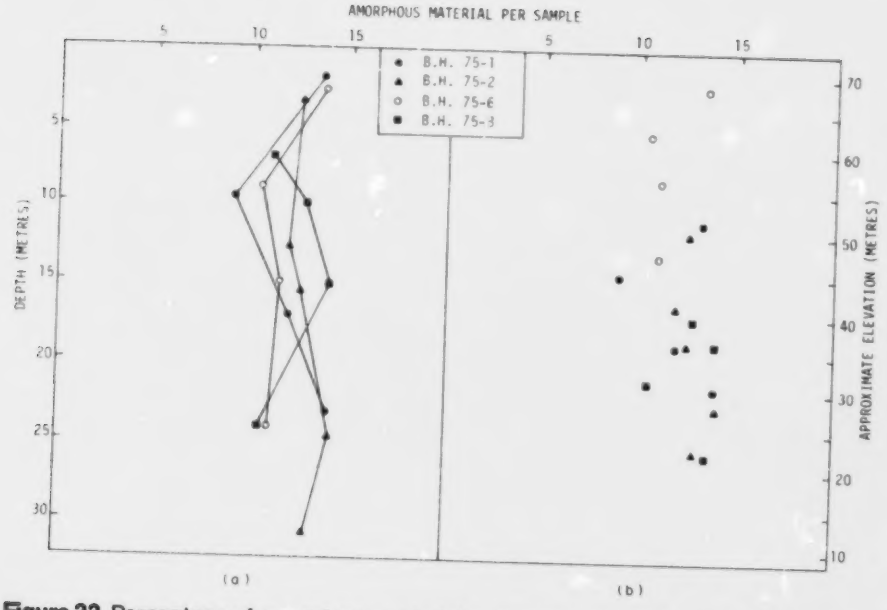

Figure 33. Percentage of amorphous material extracted vs depth (a) and elevation (b).

SEMI-QUANTITTATIVE MINERALOGY

Semi-quantitative mineral abundances for the Hawkesbury clays are provided in Table 1 along with a list of assumptions used in determining the percentages in Table 2. The normal range in abundance for each mineral species throughout unweathered portions of the deposit is summarized below.

Illite/mica	10-46 percent
Chlorite (estimated)	2-22 percent
Vermiculite (including vermiculite/smectite)	3-13 percent
Quartz	10-28 percent
K-feldspar (estimated)	6-38 percent
Plagioclase feldspar (estimated)	4-23 percent
Amphibole (estimated)	2-10 percent
Carbonate	2-13 percent

These percentages do not include the 'amorphous' materials which generally comprise an average of 12 percent of the soil solids.

The amount of chlorite and vermiculite tends to decrease with depth, while the percentage of feldspars, and, to a lesser degree, quartz, increases in relative abundance. The illite/mica and amphibole contents exhibit no distribution trends. None of the above trends is particularly distinct nor apparent in all boreholes, and any pattern or distribution appears to be largely the result of increasing grain size with depth in some boreholes.

Further discussion of the carbonate distribution may be found under "Geochemistry".

Finally, it should be noted that, in multi-minerallic systems, there are many problems in determining the amounts of the individual minerals present. In Champlain Sea clays, the standard problems of variation in chemical composition, grain size factors, selection of the correct internal standard, etc. are compounded by the presence of amorphous material. This material will affect the reflected X-ray intensity, and since it is not known where it is distributed, it has to be assumed that it will affect all intensities equally. Fluctuations in composition, particularly in iron content, between samples will greatly affect comparative peak heights. Furthermore, the amorphous constituents will produce a higher and more irregular background, making accurate measurements of peak heights, used in estimating relative mineral percentages, even more difficult.

SCANNING ELECTRON MICROSCOPY

Figures 34 to 39 photographically illustrate the fabric of vertical and horizontal fracture surfaces of four samples. The photographs generally show numerous voids and no strongly developed particle orientation. In other words, a random fabric typical of Champlain Sea clays is observed. The greatest orientation of particles is seen in sample 75-2-2 in Figures 34 and 35. No significant differences are discernible between the fabrics observed in the surface samples (75-2-2 and 75-6-3 in Figures 34, 35 and 38) and samples near the base of the boreholes (Samples 75-2-17 and 75-6-16 in Figures 36, 37 and 39).

Figures 40 to 42 are photomicrographs of dark grey cemented layers and irregular 'inclusions' discovered in various samples. These materials are believed to result from the cementing of sand and silt grains by pyrite precipitated after deposition. Some may consist only of precipitated pyrite crystals. As is apparent from the micrographs, the particles exhibit pyrite crystal shapes and framboid-like structures, possibly of bacterial origin (Haynes and Quigley 1978).

TABLE 1 SEMI-QUANTITATIVE MINERALOGY (AMORPHOUS COMPONENT EXCLUDED) OF LEDA CLAY SAMPLES FROM BOREHOLES 75-1 TO 75-8

SAMPLE NO.	DEPTH (m)	ILLITE/MICA % (Measured)	CHLORITE % (Estimated)	VERMICULITE % (Measured)	QUARTZ % (Measured)	POTASSIUM FELDSPAR % (Estimated)	PLAGIOCLASE FELDSPAR % (Estimated)	CARBONATES % (Measured)	AMPHIBOLE % (Estimated)	NON-CLAY MINERALS Average Percentage
75 – 1-2	1.8	25-30	20-26	14-18	9-11	5-9	4-8	5-7	3-5	33
7	9.6	27-31	16-22	9-13	11-13	6-10	6-10	7-9	4-6	41
12	17.2	27-31	10-20	8-10	12-18	8-14	8-12	6-8	3-5	47
14	20.2	21-25	6-10	9-11	20-26	12-20	9-13	4-6	3-5	59
16	23.3	17-21	~2	6-10	20-28	20-28	15-23	~2	~2	71
75 – 2-1	1.0	21-25	10-20	15-19	14-20	8-14	10-14	~2	2-4	45
3	3.4	20-24	9-17	11-15	14-18	10-20	9-13	3-5	5-7	52
5	6.4	22-26	20-30	6-10	10-14	6-12	6-10	7-9	5-7	43
9	12.5	25-30	6-10	9-13	16-20	7-15	11-15	4-6	5-7	53
11	15.5	24-28	11-21	6-10	14-18	10-14	12-14	2-4	5-7	50
13	18.6	24-28	10-20	5-9	14-18	10-14	10-14	5-7	5-7	52
17	24.7	25-29	11-21	5-9	14-18	11-17	10-12	3-5	4-6	50
21	30.8	28-32	9-17	7-11	13-17	7-15	6-10	6-8	6-8	48
75 – 4-2	2.6	20-28	8-14	11-15	15-23	12-18	7-15	4-6	~2	52
6	9.5	20-30	4-10	10-12	15-21	12-20	7-15	7-9	3-5	57
8	11.7	16-26	10-16	8-12	15-23	12-18	10-18	5-7	~2	56
14	20.9	20-31	10-14	8-12	15-21	10-16	7-15	7-9	~2	52
20	30.0	25-35	2-6	5-9	20-24	12-18	10-16	4-6	~2	59
75 – 5-3	4.1	25-31	15-20	8-12	14-18	10-14	6-12	3-5	3-5	45
4	5.6	20-30	4-8	8-12	14-20	12-18	10-16	8-10	3-5	59
5	7.2	25-33	10-20	10-14	10-16	9-13	8-16	3-5	3-5	44
6	8.7	25-35	4-10	10-12	18-24	10-14	6-14	4-6	3-5	52
7	10.2	25-33	2-4	12-16	12-18	15-20	7-15	~3	6-10	54
10	14.8	25-31	4-6	3	20-26	15-23	7-15	~3	6-10	64
75 – 6-2	2.4	25-33	16-25	8-12	10-14	6-8	8-12	4-6	5-7	40
3	4.1	25-33	15-21	8-10	10-12	6-10	7-11	8-12	5-7	44
6	8.7	28-34	10-14	8-12	10-14	10-14	4-8	9-13	5-7	47
10	14.8	38-46	5-9	8-10	12-16	8-10	6-10	~4	5-7	42
16	23.9	10-20	2	10-14	12-18	26-38	10-14	5-7	5-7	71

SAMPLE NO.	DEPTH (m)	ILLITE/MICA % (Measured)	CHLORITE % (Estimated)	VERMICULITE % (Measured)	QUARTZ % (Measured)	POTASSIUM FELDSPAR % (Estimated)	PLAGIOCLASE FELDSPAR % (Estimated)	CARBONATES % (Measured)	AMPHIBOLE % (Estimated)	NON-CLAY MINERALS Average Percentage
75 – 7-2	2.6	20-30	10-18	10-14	12-16	10-16	12-16	4-6	~3	49
5	7.2	20-30	5-13	10-12	14-18	12-16	10-20	5-7	2-6	55
9	13.3	20-26	10-14	8-12	14-18	10-16	12-20	5-7	2-6	55
13	19.4	23-31	6-14	8-12	12-18	10-14	12-20	5-7	2-6	53
16	23.9	25-35	5-9	6-8	18-22	12-20	12-20	~2	~2	56
19	28.5	15-23	3	4-6	23-28	16-20	12-20	8-12	~3	72
75 – 8-2	7.2	18-26	6-14	4-6	20-24	12-18	16-20	3-5	3-5	63
4	10.2	25-35	10-20	4-6	14-18	10-18	6-14	4-6	4-6	50
7	14.8	20-30	15-20	6-8	10-16	10-14	6-14	7-9	6-10	51
8	23.9	21-31	8-12	8-10	15-23	10-16	12-18	3-5	3-5	55

TABLE 2 ASSUMPTIONS AND LIMITATIONS OF THE SEMI-QUANTITATIVE MINERALOGY

Item No.	Assumption
1.	Variations in grain size and their effect on the X-ray peak intensity have been ignored.
2.	The presence of amorphous material equally affects all mineral peak intensities.
3.	The illite/mica component of this soil contains 10% K_2O. This percentage can vary from 6 to 10% depending on the soil.
4.	In order to provide a rough correction for the contribution of clay sized potassium feldspar to the measured percentage K_2O, approximately one quarter of the estimated percentage of K feldspar was assumed to be of clay size.
5.	The decrease in glycol retention following K saturation is completely attributable to the collapse of vermiculite, therefore, the recorded percentage of vermiculite includes some of the expandable clays identified on the oriented X-ray diffraction traces.
6.	Estimation of the amounts of feldspar and chlorite was determined from the powder patterns using the following peak intensity ratios for equal amounts of mineral (Kenney 1967).

Quartz	(4.26 Å)	1
K feldspar	(3.25 Å)	1
Na-Ca feldspar	(3.19 Å)	3
Calcite	(3.03 Å)	2
Illite	(10 Å)	2
Chlorite	(14 Å)	1

7.	For oriented X-ray traces, all clay mineral components were assumed to have the same degree of orientation so that the above ratios for powder samples apply.

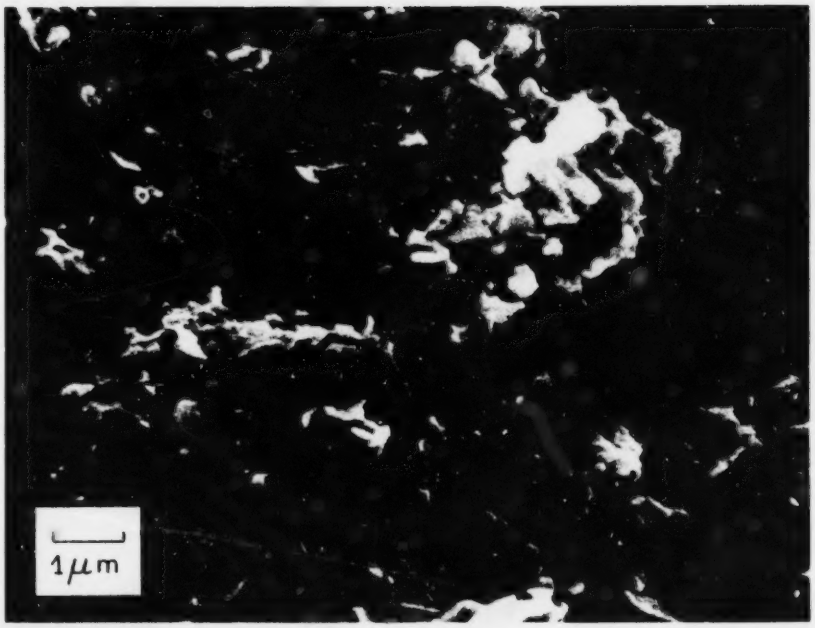

Figure 34. Scanning electron photomicrograph of horizontal face, sample 75-2-2 (X 10000).

Figure 35. Scanning electron photomicrograph of vertical face, sample 75-2-2 (X 10000).

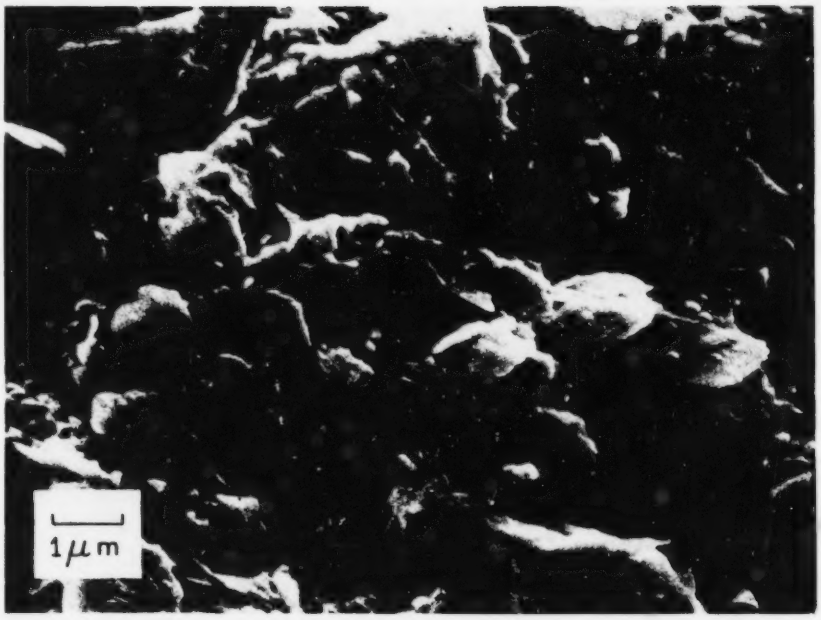

Figure 36. Scanning electron photomicrograph of horizontal face, sample 75-2-17 (X 10000).

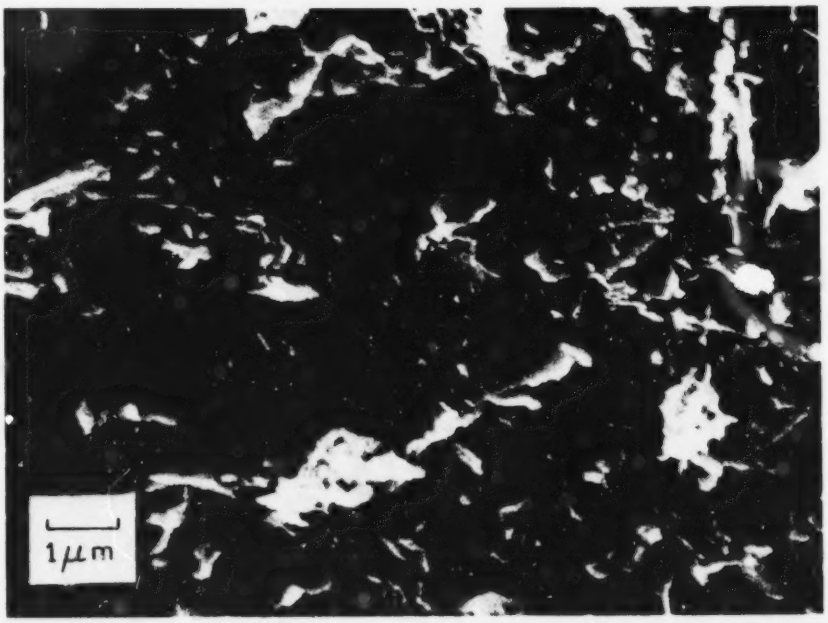

Figure 37. Scanning electron photomicrograph of vertical face, sample 75-2-17 (X 10000).

Figure 38. Scanning electron photomicrograph of vertical face, sample 75-6-3 (X 10000).

Figure 39. Scanning electron photomicrograph of horizontal face, sample 75-6-16 (X 10000).

400X 25μ

2000X 5μ

10000X 1μ

Figure 40. Scanning electron photomicrographs of cemented inclusion, sample 75-7-7, Hawkesbury, showing framboid-like structures.

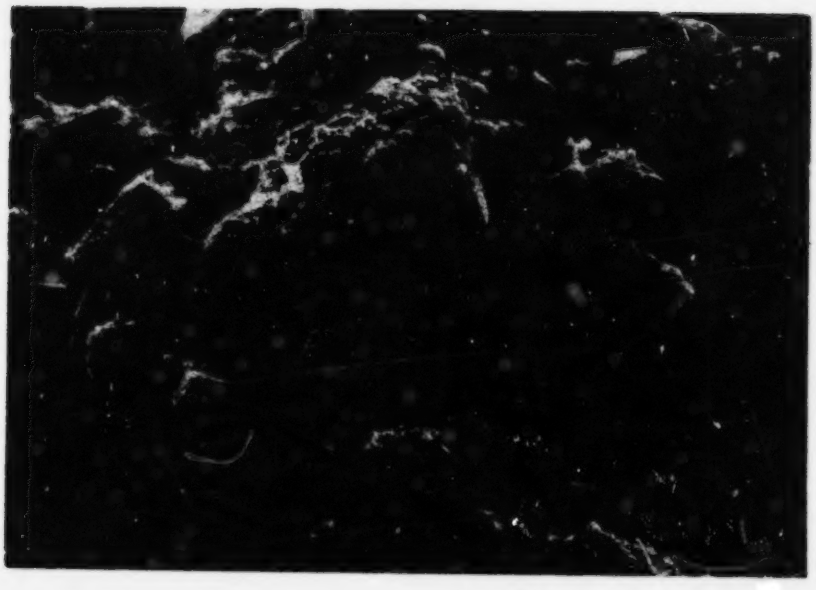

1000X 10μ

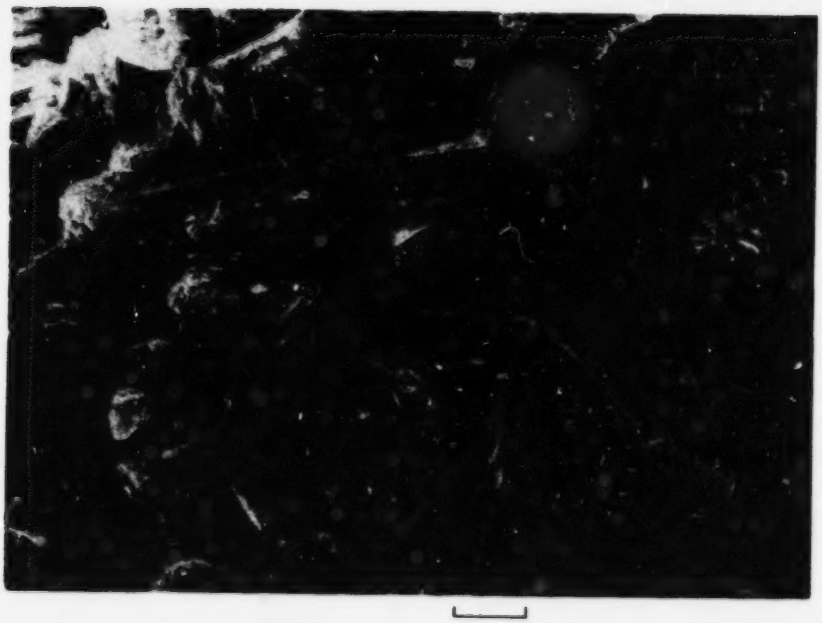

4000X 2.5μ

Figure 41. Scanning electron photomicrographs of cemented layer, sample 75-2-9. Note pyrite crystals.

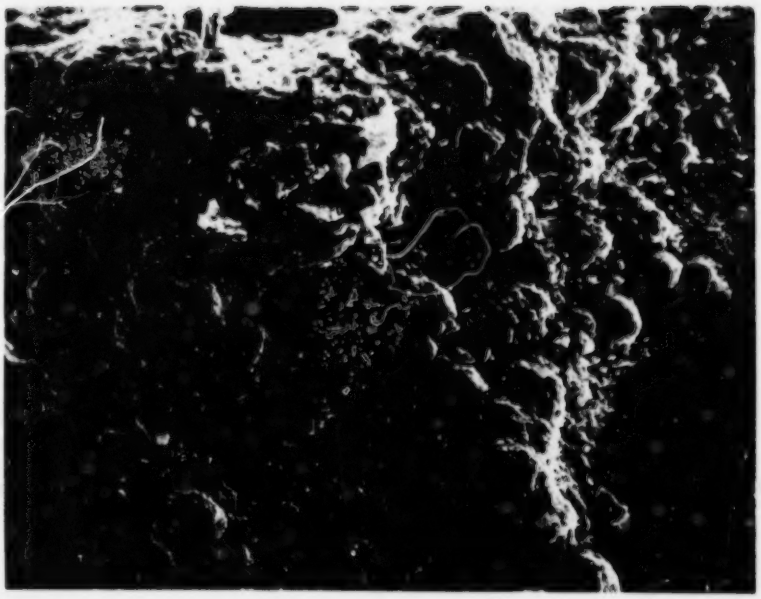

40X 2.5 mm

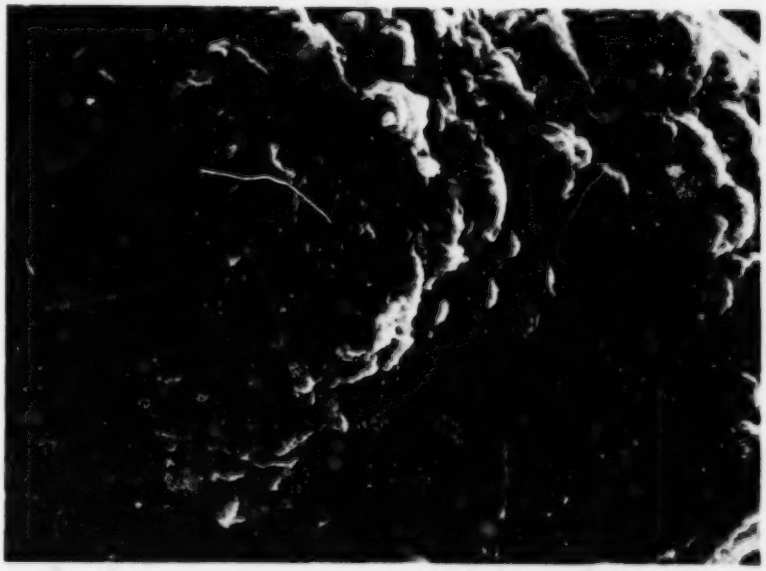

1000X 10μ

Figure 42. Scanning electron photomicrographs of cemented material, sample 75-1-16.

GEOCHEMISTRY

The results of the chemical testing are presented in Figures 43 to 47 inclusive. The pH measurements are given in the borehole logs (see Figures 5-13).

CARBONATES

The carbonate content of the deposits varies from about 2 to 10 percent with most values between 4 and 6 percent. The values are somewhat erratic although there seems to be a general tendency to decrease with depth in most of the five holes tested.

There seems to be no particular correlation of carbonate content with the other chemical test results. No attempt has been made to separate foreign clastic carbonate from carbonate which was formed by plankton living in the saline Champlain Sea.

pH

The pH values tabulated on the borehole logs vary from about 7.5 to 8.6 through the bulk of the deposit with scattered values slightly higher and lower. These values seem typical of Leda clay deposits.

Near surface, the pH decreases to values as low as 6.5, probably reflecting H^+ adsorbed on some of the exchange sites of the clay minerals within the weathered crust.

SALINITY

The values of total salinity expressed in grams/litre, NaCl equivalent, were obtained by conductivity measurements. In the lower-elevation boreholes 75-1, 75-2, 75-5, 75-8 and 78-1 the salinity generally increases with depth from about 1 or 2 g/L at surface to maximum values of 7 to 15 g/L at 15 to 20 m depth depending on the hole.

The salinities in boreholes 75-7 and 78-2 (Figures 46 and 15) on the upper clay plain are significantly lower, a maximum value of about 4 g/L being reached at 10 m depth.

POREWATER CATIONS

The porewater cation analyses identify Na^+ as the predominant cation throughout the deposit, with Mg^{++} generally second in abundance. K^+ and Ca^{++} are present in approximately equal amounts at a lower concentration. Iron was not present in detectable amounts.

In the lower level boreholes 75-1, 75-2,75-5 and 75-8, Na^+ values vary from 1500 to 9600 ppm and form profiles with depth very similar in shape to the salinity profiles. The corresponding Mg^{++} profiles also follow the salinity profile trends at concentrations of 75 to greater than 600 ppm. Some Mg^{++} scatter is apparent in Figure 43 for borehole 75-1. The K^+ and Ca^{++} values vary from about 25 to nearly 200 ppm and likewise follow the trends of the salinity curves.

In borehole 75-7, the cation profiles continue to follow the trend of the salinity profile, however, all values are significantly lower as is the total salinity. The Mg^{++} concentrations, however, are much lower relative to the K^+ and Ca^{++} observed in the lower elevation boreholes. In fact, Mg^{++} was measured at a concentration of only 8 ppm at the base of the hole, well below values for K^+ and Ca^{++} (Figure 46). This was the only hole in which this relationship occurred.

ORGANIC MATTER

Measured values of organic carbon are plotted versus depth on Figures 14 and 15 for boreholes 78-1 and 78-2, respectively, and are tabulated in Table E-3 (Appendix E). The values vary from about 0.82 percent to 1.1 percent of the soil solids, and thus seem typical of Leda clay (Quigley 1980). A comparison of the two holes, however, shows clearly that the upper elevation clays contain an average of 0.88 percent organics compared to 1.04 percent for the lower elevation clays.

DISCUSSION

In all boreholes, the porewater salinity is high enough to maintain a fairly high remoulded shear strength. Torrance (1975) reported a significant increase in remoulded shear strength when the porewater salinity of test samples was increased to values of 1 to 3 g/L from 0.34 g/L, and further less significant increases when the salinity was increased up to 20 g/L. The measured vane sensitivities of 5 to 25 seem compatible with the relatively high salinities of 1 to 15 g/L measured in the bulk of the clay specimens.

A further discussion of sensitivity as a function of soil composition, fabric and porewater chemistry is presented in the Summary.

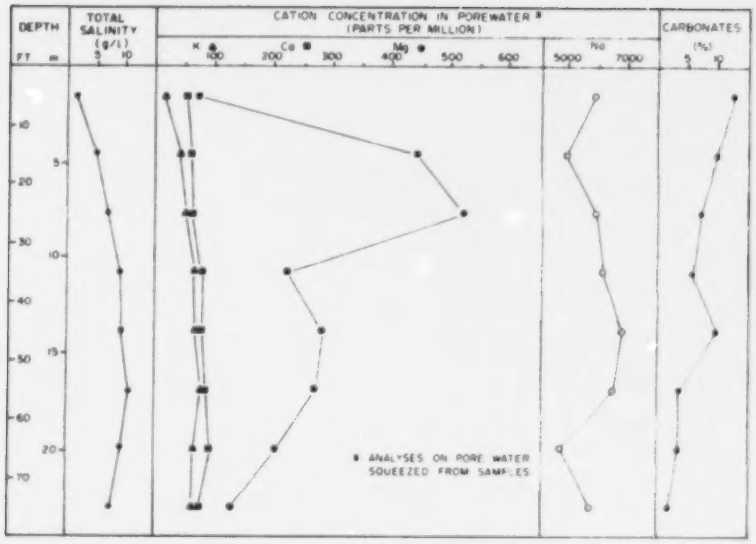

Figure 43. Geochemical data for borehole 75-1.

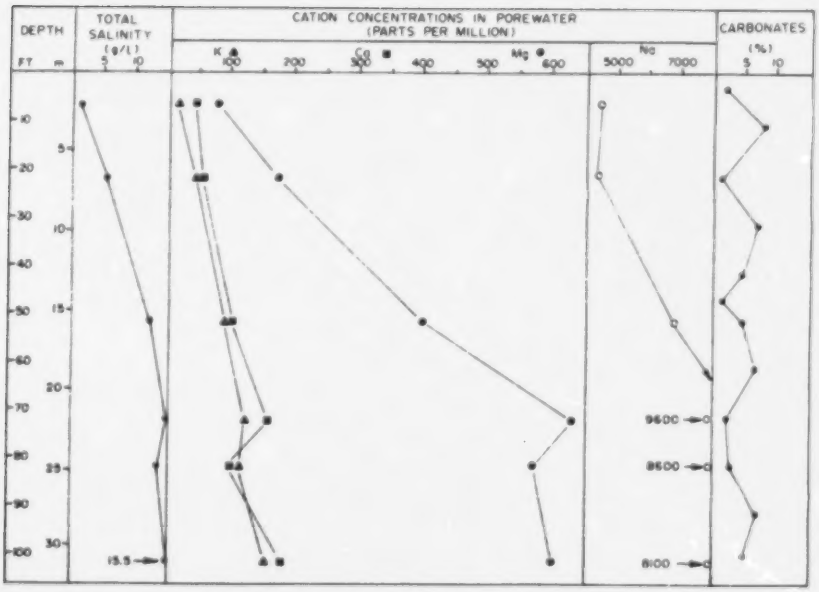

Figure 44. Geochemical data for borehole 75-2.

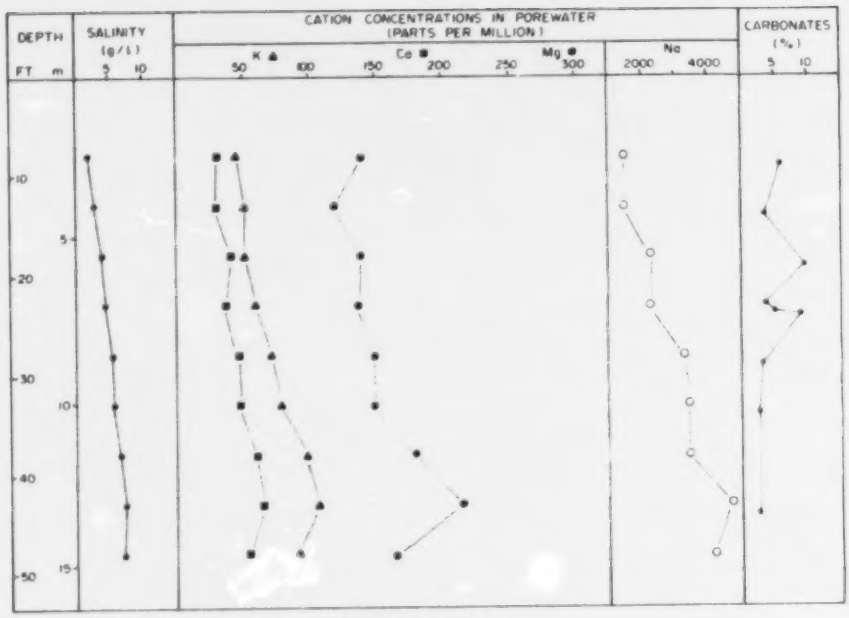

Figure 45. Geochemical data for borehole 75-5.

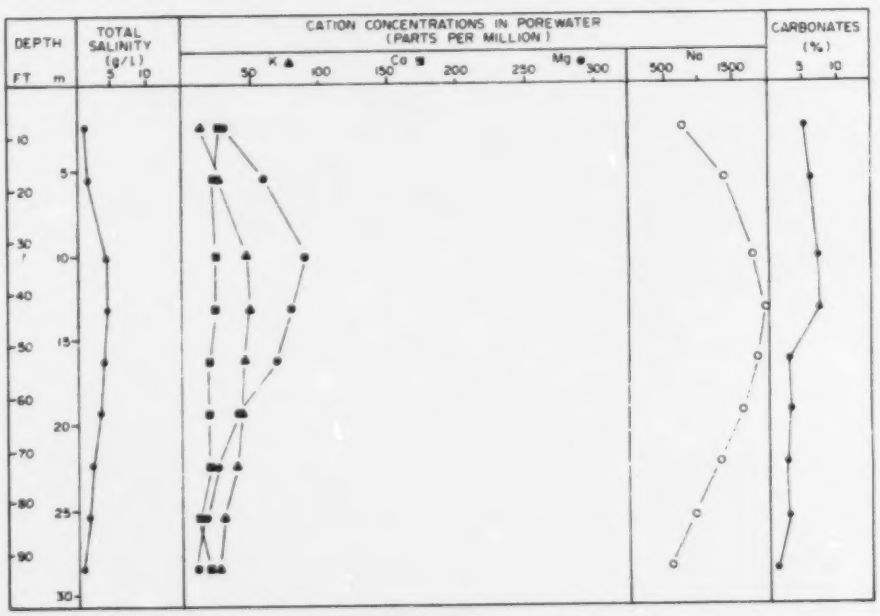

Figure 46. Geochemical data for borehole 75-7.

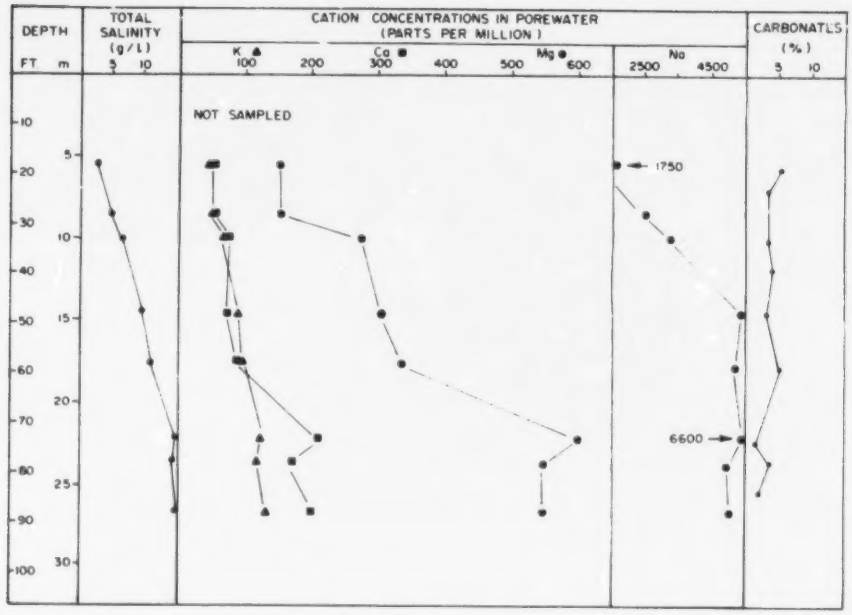

Figure 47. Geochemical data for borehole 75-8.

POREWATER ISOTOPES

Differences in the mass of atoms composing molecules influence some of their thermodynamic properties. Since hydrogen (^1H) and oxygen-16 (^{16}O) are lighter than deuterium ($D=^2H$) and oxygen-18 (^{18}O), the water molecule $^1H_2{}^{16}O$ will behave slightly differently than $^2H_2{}^{18}O$ in terms of evaporation, condensation, melting, crystallization and ion diffusion (Faure 1977). The $^1H_2{}^{16}O$ molecule has a higher vapour pressure than $^2H_2{}^{18}O$ and therefore during evaporation it is preferentially removed from a water surface. Consequently, the vapour over the oceans is enriched in ^{16}O and ^1H relative to ^{18}O and ^2H while the remaining ocean is enriched in ^{18}O and ^2H relative to ^{16}O and ^1H.

The isotopic compositions of oxygen and hydrogen are reported as per mil differences in the $^{18}O/^{16}O$ and $^2H/^1H$ ratios of a test sample relative to the ratio defined by analysis of Standard Mean Ocean Water (SMOW). The *del* equation is as follows:

$$\delta^{18}O = \left[\frac{(^{18}O/^{16}O)_{sample} - (^{18}O/^{16}O)_{SMOW}}{(^{18}O/^{16}O)_{SMOW}} \right] \times 1000$$

or

$$\delta^{18}O = \left[\frac{(^{18}O/^{16}O)_{sample}}{(^{18}O/^{16}O)_{SMOW}} - 1 \right] \times 1000$$

If the sample was standard mean ocean water, then the δ value would reduce to zero.

Negative values of $\delta^{18}O$ indicate water containing a relative excess of light oxygen and positive values indicate water containing an excess of heavy oxygen. δ^2H values are interpreted in a similar way.

Generally, fresh water has more negative $\delta^{18}O$ and δ^2H values than salt water since temperature and vapour pressure differences cause isotopic fractionation during evaporation (Faure 1977). Colder water, including water found in higher latitudes, is also more negative than warmer water. In addition to this, $\delta^{18}O$ and δ^2H also appear to be positively correlated with salinity so that ^{18}O and ^2H analyses may provide insights into depositional salinity and temperature of Leda clay deposits.

The amount of tritium (^3H) in ground water increased dramatically following atmospheric, atomic bomb testing between 1954 and 1963. The presence of tritium in ground water may therefore be used as a tracer to follow recent (25 year) subsurface flow regimes (Faure 1977). Before nuclear bomb contamination, the ratio of $^3H:^1H$ was about $1:10^{18}$ from which the tritium unit (T.U.) was defined as follows:

$$T.U. = {}^3H/{}^1H \times 10^{18}$$

Pre-bomb values are actually 5 to 20 and measured values of T.U. should not fall below zero, although they occasionally appear to do so because of statistical errors in the counting techniques.

RESULTS

The oxygen, deuterium and tritium analyses reported herein were carried out for the Ontario Ministry of Natural Resources by Peter Fritz of the University of Waterloo, specifically for the Hawkesbury project. Interpretation has been done by the authors of this report assisted generously by a review by Fritz and Desaulniers, University of Waterloo.

The $\delta^{18}O$, $\delta^{2}H$ and tritium values, as they vary with depth, are shown in Figure 48. Pore water $\delta^{18}O$ ranges from −9 to −9.4‰ in borehole 78-1 compared to a range of −10 to −11‰ in borehole 78-2. The $\delta^{2}H$ ranges from −64 to −73.5‰ in borehole 78-1 and −73.5 to −78‰ in borehole 78-2. The tritium plot shows more tritium near surface than at depth with similar values for both the upper and lower elevation clays.

DISCUSSION

Interpretation of the $\delta^{18}O$ and $\delta^{2}H$ values was more difficult than expected, since, at first glance these values appear representative of present-day meteoritic water. A map of the United States (Figure 49) gives approximate contours of $\delta^{2}H$ for present day meteoritic water (Lawrence and Taylor 1972). If these contours are extrapolated into Canada, $\delta^{2}H$ values of between −70 and −80‰ would be found in the Ottawa area, and these closely resemble values measured on the Hawkesbury samples. Using these same contours Lawrence and Taylor (1972) have calculated $\delta^{18}O$ values using Craig's (1961) equation:

$$\delta^{2}H = 8\,\delta^{18}O + 10.$$

This gives an approximate value of −10‰ $\delta^{18}O$ for the − 70‰ $\delta^{2}H$ contour, and −11‰ $\delta^{18}O$ for the −80‰ $\delta^{2}H$ contour. These values are similar to those obtained for the Hawkesbury samples, especially for borehole 78-2. Dansgaard and Tauber (1969) also found that $\delta^{18}O$ of present day rain water (averaged over a 2 to 10 year period) was −10‰ for a latitude of 50°N (Figure 50).

Based on these findings, it appears that the porewater in the Hawkesbury samples is in equilibrium with, and is representative of, present day meteoritic water. This, however, does not seem feasible in light of the high salinities found in the porewater samples. Furthermore, the low tritium levels found at depth (Figure 48) seem to indicate little influence of present day water below about 15 m. Therefore, although the $\delta^{18}O$ values at shallower depths which are subject to water movement may represent present day meteoritic water, the values at depth probably do not.

In search of another explanation, the possibility that the porewater is actually glacial meltwater was examined since the area is believed to have been a meltwater channel after the draining of the Champlain Sea. This explanation is improbable since the $\delta^{18}O$ values are too high to solely reflect glacial water. Glacier ice from Greenland has been found to have a $\delta^{18}O$ value of between −20 and −30‰, and −17‰ has been estimated as the mean $\delta^{18}O$ estimate for the Laurentide ice sheet (Dansgaard and Tauber 1969). Emiliani (1966) also estimated the $\delta^{18}O$ of glacial meltwater at about −15‰. None of the $\delta^{18}O$ values in the Hawkesbury samples are within the −15 to −30 range, and again the salinity profiles indicate significant amounts of NaCl remaining in the porewater.

Since the clays were deposited under marine conditions, it seems that the porewater at depth could still represent the depositional marine environment. Present day ocean water has a $\delta^{18}O$ of zero and during glacial times the $\delta^{18}O$ of the oceans was about one (Dansgaard and Tauber 1969; Shackleton and Opdyke 1973). Since the

Hawkesbury samples are far below the Pleistocene ocean value of +1 and since $\delta^{18}O$ varies positively with salinity and temperature, it is possible that the Hawkesbury porewater reflects clay deposition in a less saline, colder sea than the open ocean. The addition of glacial meltwater to the Champlain Sea would lower the salinity and the $\delta^{18}O$ values of the water.

Epstein and Mayeda (1953) plotted the $\delta^{18}O$ of ocean water samples off the west coast of North America. These samples were taken from currents diluted with fresh meltwater. To these values (Figure 51) a regression line was added which indicates that at salinity = 0, the $\delta^{18}O = -20‰$. This value of −20 corresponds well to values found for glacial ice and also to the value found for present day snow and ice at Trail, B.C. representing the type of contaminant entering the ocean currents (Epstein and Mayeda 1953). Lowering of the salinity by meltwater lowers the $\delta^{18}O$ and if the line in Figure 51 is extrapolated to a $\delta^{18}O$ of between −9 and −11‰, a salinity of between 15‰ and 20‰ is indicated. Clay deposition in the Hawkesbury area may therefore have occurred in moderately saline water (S ~ 15 to 20‰) diluted with glacial meltwater. This is the salinity range actually measured on deeper samples from the lower clay plain (boreholes 75-1 to 75-5 and 78-1).

It should be borne in mind that soft clay consolidation with top and bottom drainage should distribute porewaters characteristic of the central zone throughout the entire clay stratum as discussed under "Geotechnique". A constant $\delta^{18}O$ versus depth is therefore not surprising.

Elson (1969) spoke of an initial cold phase in the Champlain Sea with salinities of over 26‰. Subsequently a reduction in salinity to 6‰ occurred as crustal uplift reduced exchange with the open ocean and meltwater resulted in large additions of fresh water (Elson 1969). Hillaire-Marcel (1979) found $\delta^{18}O$ values in fauna from Champlain Sea sediments from −10‰ PDB near surface to about 0‰ at 35 m depth as shown on Figure 52. The corresponding calculated $\delta^{18}O$ values for the sea water in which the fauna actually lived are also plotted in Figure 52 (lower curve). These $\delta^{18}O$ plots reflect the probable temporal variation in salinity in the Champlain Sea. The constant $\delta^{18}O$ versus depth obtained from this investigation is, therefore, assumed to represent redistribution of pore water as a result of soft clay consolidation.

Figure 53 adapted from Hillaire-Marcel (1979) shows a relationship between $\delta^{18}O$ and salinity for modern day arctic waters and a similar relationship for Champlain Sea waters. The values of $\delta^{18}O$ obtained on the Hawkesbury samples cannot at present be used to infer depositional salinity because of excessive porewater migration. Subsequent $\delta^{18}O$ studies on carbonate shells, however, should enable these salinity estimates to be made. Nevertheless, this discussion of the measured porewater salinities and estimated paleosalinities is essentially consistent with the study results of Wagner (1970) and Cronin (1977a,b).

The small but definite differences in $\delta^{18}O$ and $\delta^{2}H$ that do exist between the upper and lower level clays are illustrated in Figure 54. The lower *del* values in borehole 78-2 may indicate a cooler, less saline environment of deposition. This would seem possible since there are bedrock controls on ice location that could have created an older, extra cold, less saline, high level sea in the area of borehole 78-2 while the lower level area of borehole 78-1 was still ice covered. The salinity values of 5 g/L maximum in borehole 78-2 compared to 20 g/L maximum in borehole 78-1 tend to support this concept, bearing in mind the many complicating water movement factors such as consolidation, rebound, leaching, diffusion, etc.

Alternatively, fresh water overflow currents (Quigley 1980) may have had less effect on deeper basins of the Champlain Sea than shallower basins. At Hawkesbury, the sea would have been 25 m deeper in the area of the westerly, lower level plain, and the significantly greater density of saltier water would have caused it to occupy the deeper basin.

Finally, $\delta^{18}O$ and organic matter are compared in Figure 55 for the upper and lower level clays. It appears significant that the lower organic matter in the upper level clays corresponds to lower $\delta^{18}O$ values that probably reflect less saline conditions.

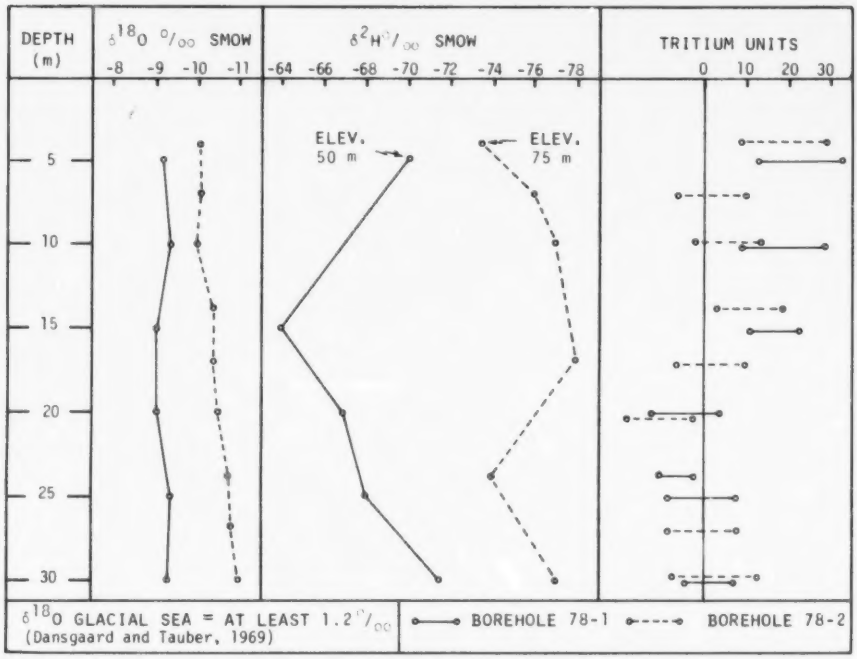

Figure 48. Oxygen, deuterium and tritium analyses, Hawkesbury Leda clay. Analyses by P. Fritz, University of Waterloo.

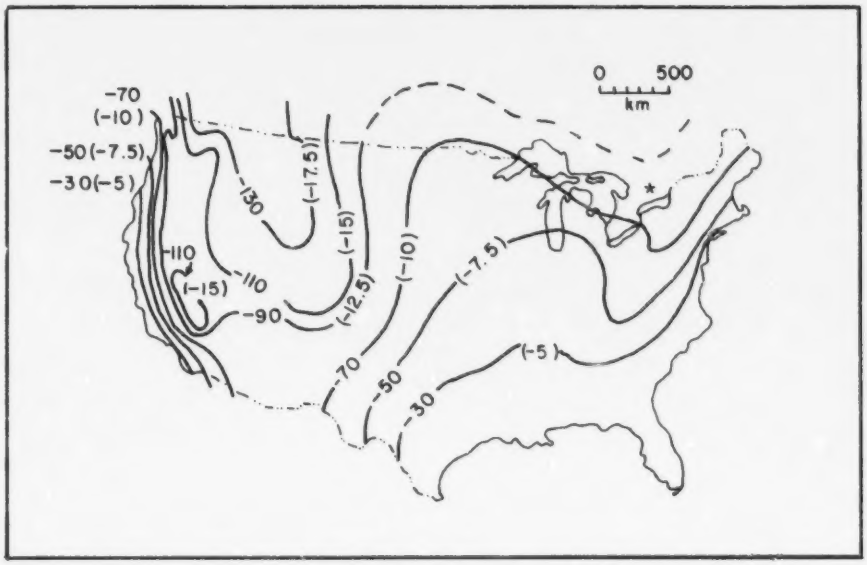

Figure 49. Map of United States showing approximate contours for δ^2H and $\delta^{18}O$ (brackets) of present day meteoritic water (Lawrence and Taylor 1972). Dashed line = extrapolated contour, * = Hawkesbury, Ontario.

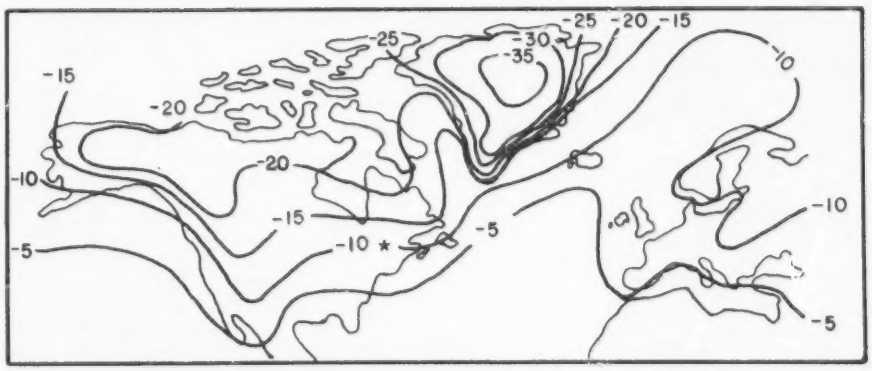

Figure 50. World map showing approximate $\delta^{18}O$ contours in ‰ SMOW of annual present-day precipitation (Dansgaard and Tauber 1969).

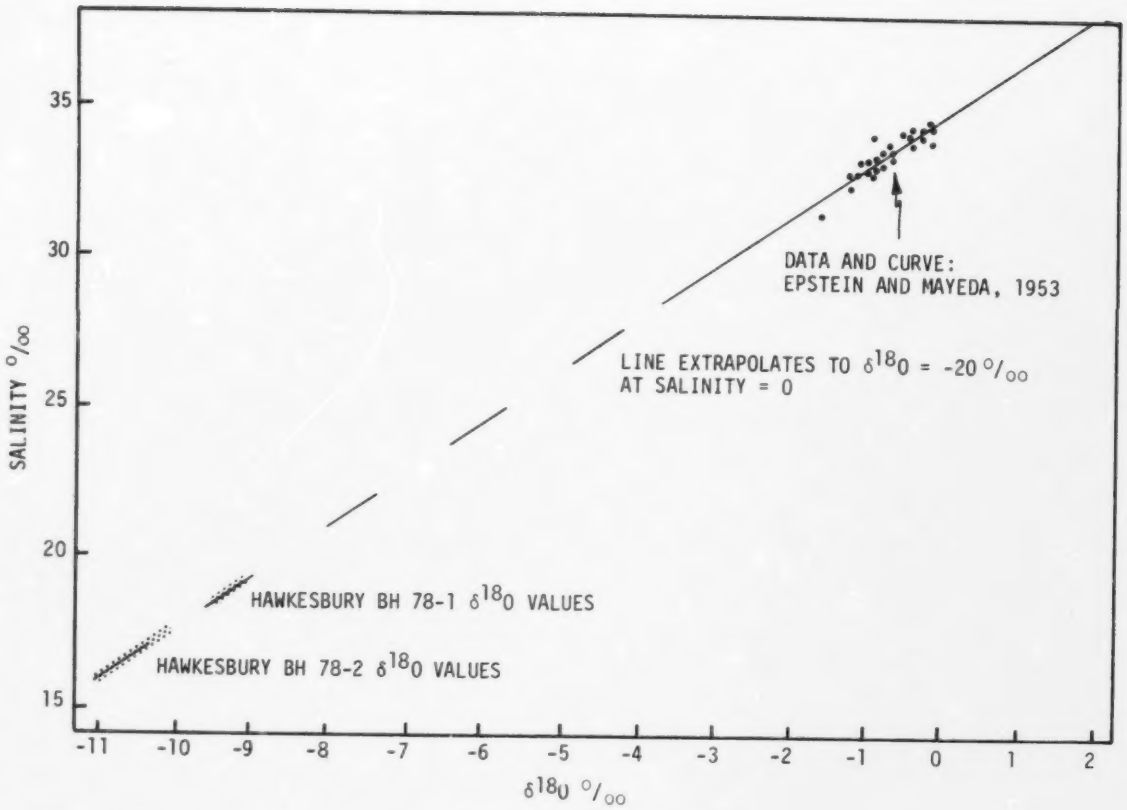

Figure 51. Relationship between $\delta^{18}O$ and salinity for ocean water diluted with fresh melt water (from Epstein and Mayeda 1953).

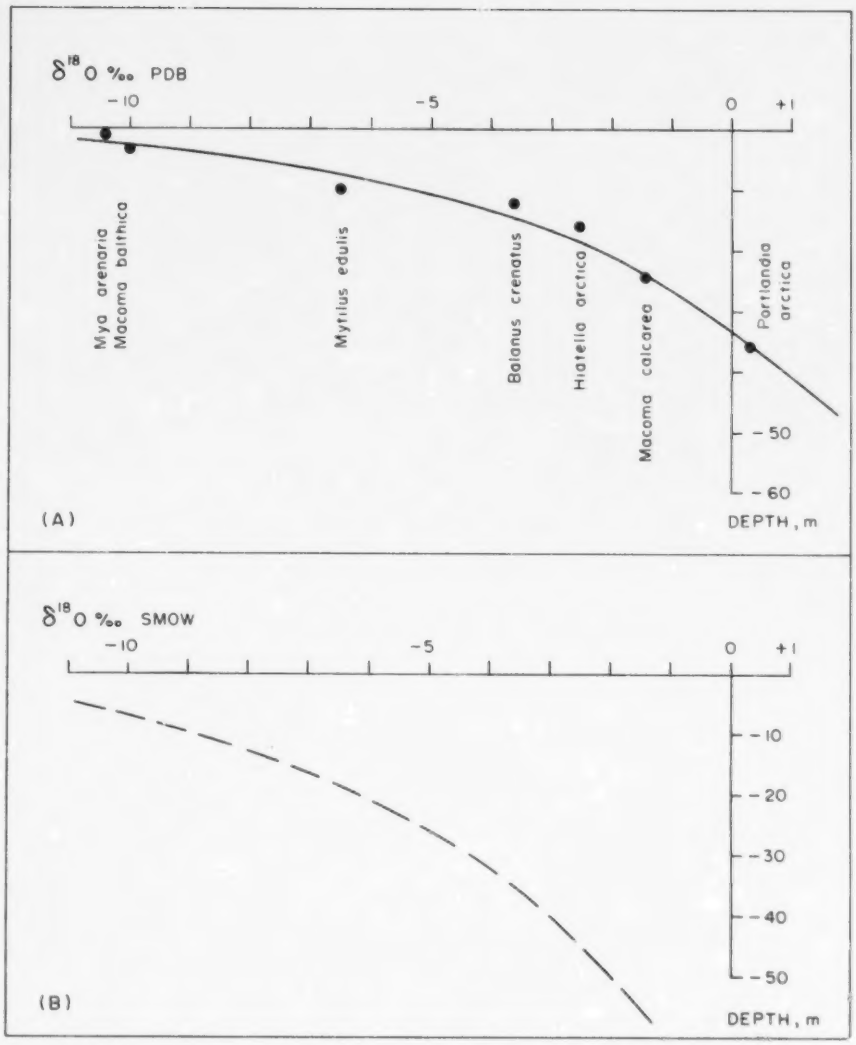

Figure 52. Oxygen-18 vs depth for Champlain Sea. (A) $\delta^{18}O$ vs mean depth for principal fossil groups. (B) Estimated corresponding isotopic composition of seawater (from Hillaire-Marcel 1979, Figure 213).

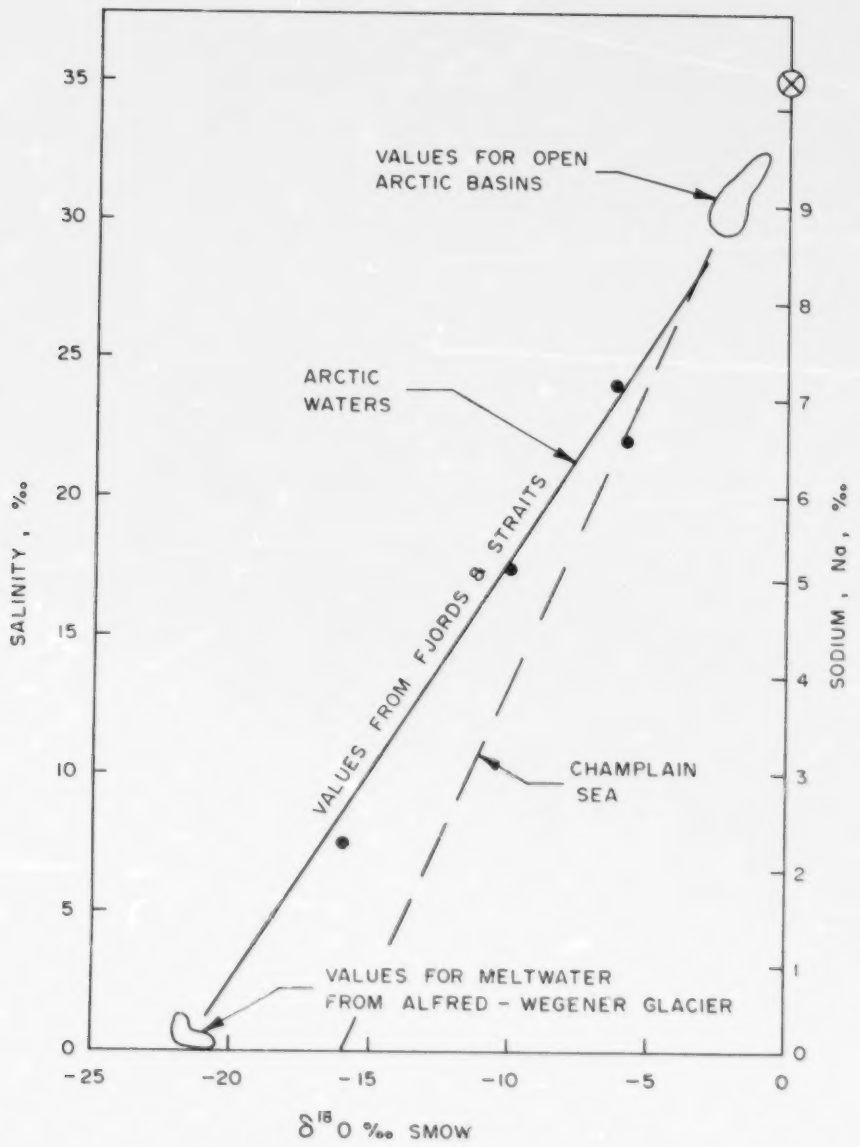

Figure 53. Relationship between salinity and oxygen-18 of present-day arctic waters and predicted relationship for Champlain Sea water (Hillaire-Marcel 1979, Figures 215 and 224).

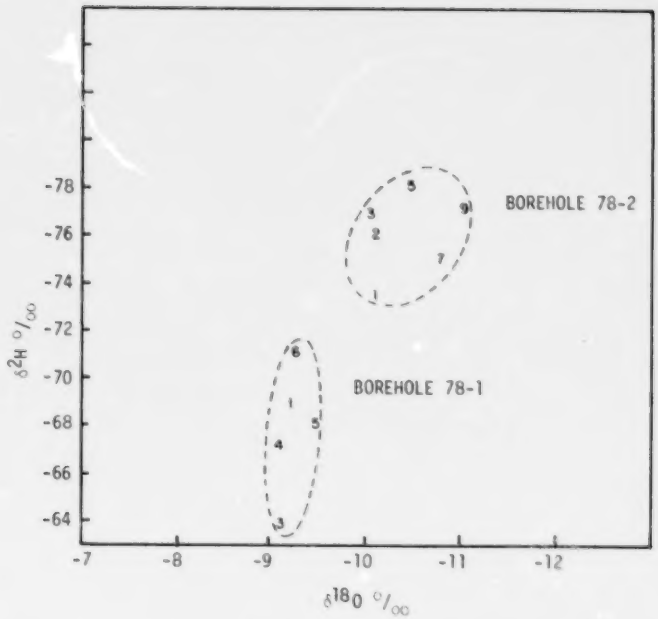

Figure 54. Relationship of δ^2H to $\delta^{18}O$ from Hawkesbury Leda clay (numbers indicate samples tested and depth relative to surface as shown on borehole logs).

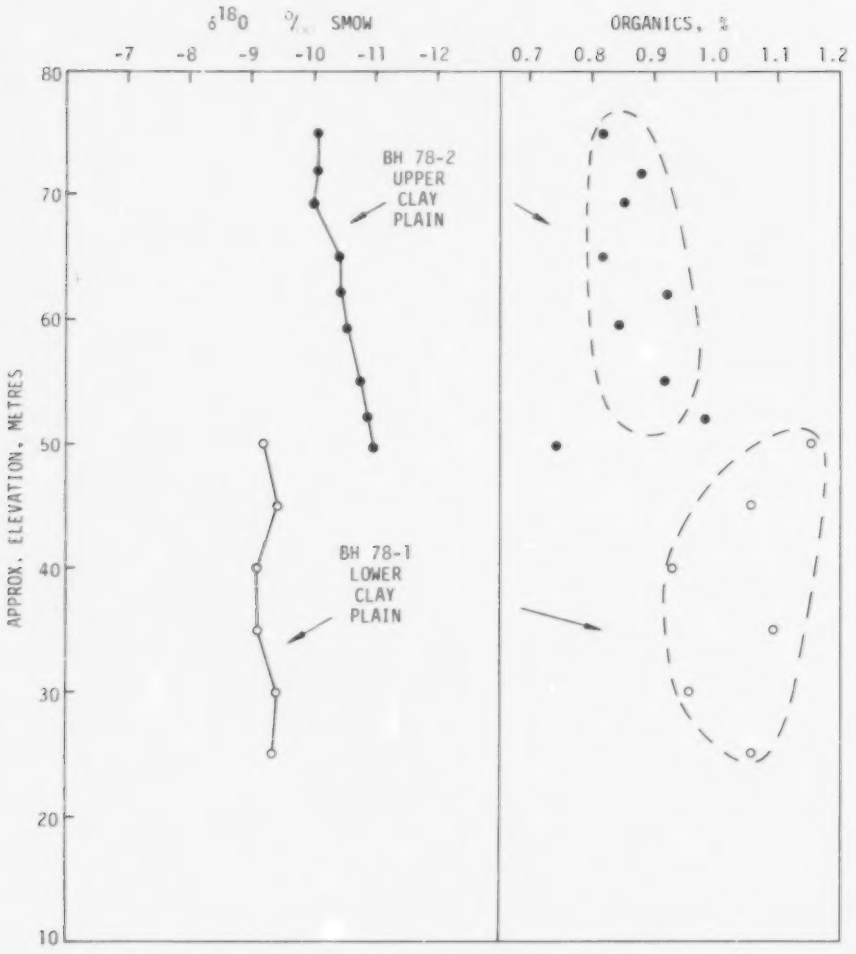

Figure 55. $\delta^{18}O$ and organic matter vs elevation, Hawkesbury area Leda clays from upper and lower clay plains.

SUMMARY

An interdisciplinary study of the geology, mineralogy, geochemistry and geotechnique of soft Champlain Sea clays at Hawkesbury, Ontario is presented in this report. The work extended from 1975 to 1980 and consisted of field studies (boreholes, vane tests, piezometer observations, soil sampling) and laboratory analyses (mineralogy, porewater cation chemistry, porewater isotopes, engineering testing).

GEOLOGY

Field mapping carried out by the Ontario Geological Survey and others is summarized in the report. The following points are of special significance to the soft clays studied.

1. Two major clay plains occur in the study area, a westerly one at ~ 50 m elevation and an easterly one at ~ 75 m elevation. A north-trending bedrock high separates the two clay basins. Significant differences in the geotechnical and chemical characteristics of the two clay deposits suggest different depositional environments.
2. The lower level clay plain is believed to have been covered by silty rhythmites and deltaic sands deposited during isostatic uplift some time after 10,500 B.P.
3. Subsequent erosion, particularly by the ancestral Ottawa River, is believed to have removed between 18 and 33 m of sediments from the lower level clay plain where extensive terrace scarps, shorelines and channel flutings have been mapped.
4. Beaches related to isostatic uplift are dated at 10,500 to 10,000 years B.P. The upper level clay plain (elevation 75 m) is estimated to have emerged 9,600 years B.P. with contained erosion channel fillings dated 9,200 years B.P. Lower level emergence (elevation 50 m) is estimated at 9,000 years B.P.
5. Erosion of the fluvial sands is believed to have taken place very soon after their deposition since the marine clays were only partly consolidated by the sands.

GEOTECHNIQUE

Both clay deposits consist of firm to very stiff grey and brown marine clay deposits capped by a 1 to 3 m thick oxidized and desiccated crust. In a few places, soft clay is found directly beneath the crust. Major differences in properties between the upper and lower level deposits are as follows:

1. The natural water content of the clays is generally close to the liquid limit (70 percent ±) yielding an average liquidity index of close to unity. In the lower level clays, the liquidity index generally decreases with depth (the usual situation) whereas in the upper level clays the liquidity index actually increases with depth.
2. The sensitivity of the lower level clays varies from about 25± at surface to about 5 at depth. The upper level clays, however, are quite different, the sensitivity reaching a maximum of about 20 near the centre of the stratum at ~ 15 m depth. These trends reflect, in part at least, the differences in liquidity index of the two clay deposits (compare Figures 56 and 57).
3. The sensitivity values noted above are quite low, probably reflecting the relatively high porefluid salt contents of greater than 1 g/L to as high as 20 g/L (Torrance 1975).
4. The plot of sensitivity versus depth for the low elevation clays (Figure 56) shows direct correlations of higher sensitivity with reduced salinity and increasing carbonate but no correlation with 'amorphous' matter. The dominant controls at this site have not yet been defined, however, with respect to the many important geochemical factors in the sensitivity equation as detailed by Quigley (1980).

5. Preconsolidation pressures measured on the clays show marked preconsolidation near top and bottom drainage boundaries of the strata, and essentially normally consolidated conditions in the central portions. This means that both sites were probably loaded by sandy fluvial sediments which were subsequently removed by erosion before 100 percent consolidation was reached. Two schemes that are compatible with the different p_c versus depth curves obtained on the upper and lower level clays (see Figures 23 and 24) are suggested in the report. On the low level clay plain it is inferred that up to 21 m of deltaic sands were removed whereas on the upper clay plain it appears that approximately 11 m of sand may have been removed by erosion. Variable erosion and interrupted consolidation make it difficult to compare preconsolidation pressures with elevation as done by Crawford (1961), for Champlain Sea clays near Ottawa.
6. Piezometer installations in the two 1978 holes established that, although there are slight gradients in both holes, the groundwater conditions are very close to hydrostatic. More importantly, the piezometers indicate that the clays are not underconsolidated relative to current *in situ* stresses (i.e. the clays are not presently consolidating and settling).

MINERALOGY

The clays exhibit a constant suite of minerals whose individual abundances seem to have been affected mostly by variations in grain size probably controlled by proximity to source sediments and the depositional mechanisms.

1. All samples consist of quartz, plagioclase feldspar, potassium feldspar, amphibole, illite/mica, chlorite, vermiculite, carbonate, and small amounts of smectite. Trace amounts of heavy minerals and amorphous constituents are also present.
2. The clay minerals chlorite and vermiculite tend to increase in relative abundance towards surface probably reflecting distal sedimentation. Correspondingly, the feldspars and quartz tend to increase at depth probably reflecting more proximal conditions. Illite/mica seem fairly uniformly distributed throughout the clay strata.
3. Scanning electron photomicrographs show a very open structure compatible with the high natural water contents.
4. Interesting framboidal pyrite cements some of the more granular layers indicating highly reducing conditions and anaerobic bacterial activity.
5. Summary plots of carbonate content (Figure 56) show an increase from about 5 percent at depth to about 8 percent near surface. Much of this increase may be due to increased planktonic activity during distal, later-phase sedimentation.

GEOCHEMISTRY

Consolidation of soft clays at upper and lower drainage boundaries, caused by the weight of the clays themselves and the weight of overlying sands, will redistribute pore fluid from the central region through an entire clay stratum. Even if overlain by freshwater clays, upward flow of salty pore fluid should render them essentially saline depending of course on many consolidation-time controls. Therefore, uniformity of pore fluid chemistry throughout a clay deposit would normally be anticipated unless it has been subjected to subsequent modification by advection and diffusion.

1. The pore fluid salinity generally increases from 1 or 2 g/L at surface to about 15 g/L at 25 m depth in the low elevation clays. The upper level clays show bow-shaped salinity curves with values of 1 or 2 g/L at surface and at 30 m depth, increasing to 4 or 5 g/L at mid layer. It is speculated that the upper level clays were deposited in a less saline sea (see Figures 56 and 57).
2. $\delta^{18}O$ values of -10 to $-11‰$ for the upper level clays compared to $-9‰$ for the lower level clays also suggest a less saline depositional environment (see Figure 48).
3. A lower average organic matter content of 0.85 percent in the upper level clays, compared to 1.1 percent in the lower level clays, also suggests a different depositional environment in the two basins (see Figure 55).
4. Final interpretation of depositional salinity awaits isotopic assessment of marine shells in the clay deposits as discussed in the text.
5. Tritium values are high (10-20 tritium units) to depths of 15 m (see Figure 48), a feature difficult to explain in view of the piezometric and flow data discussed in the report.

Although this project is now complete, the first author will be continuing with scientific studies dealing with the isotopic composition of marine shells in the clays and carbon dating of the organics. These results should establish the depositional salinities and the relative ages of the clays in the two basins. Further work will also be undertaken on some of the mathematical aspects of the preconsolidation characteristics of the clays as discussed in the report (see Quigley *et al.* 1983).

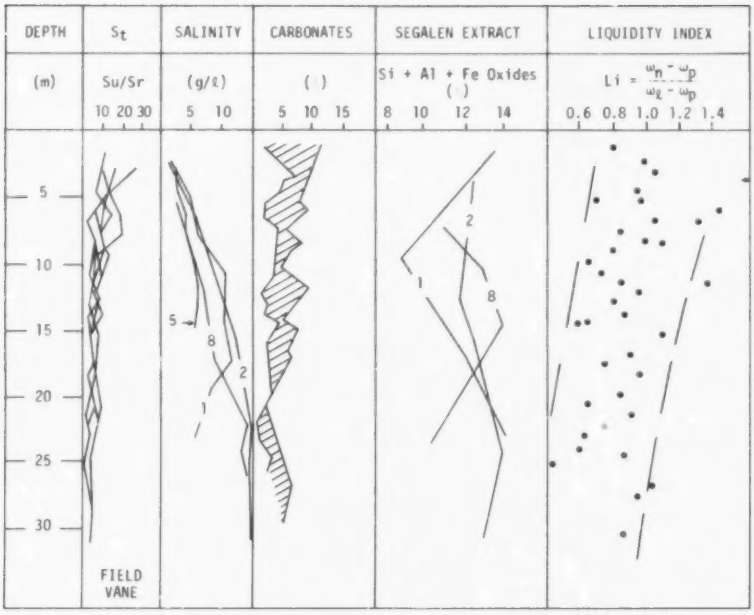

Figure 56. Sensitivity, salinity, carbonate, 'amorphous' matter and liquidity index vs depth relationships, Hawkesbury Leda clay, boreholes 75-1, 75-2, 75-5 and 75-8 (lower level clay plain).

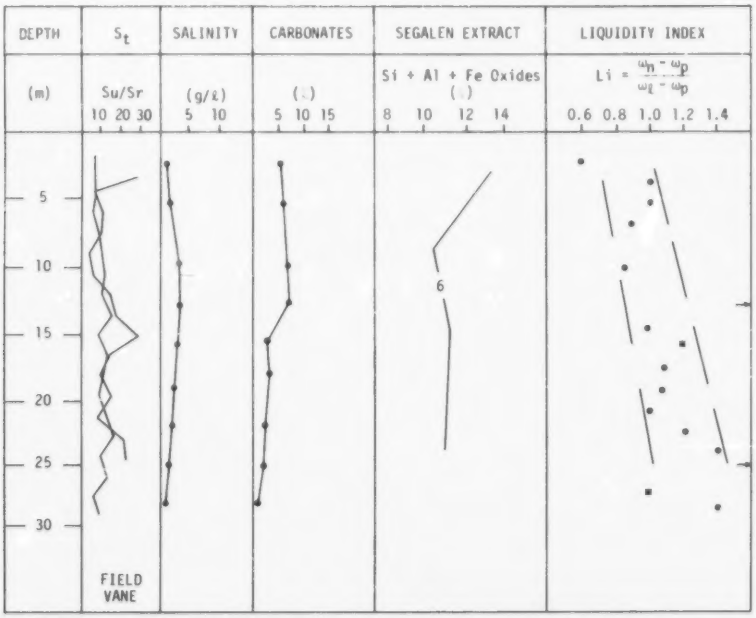

Figure 57. Sensitivity, salinity, carbonate, 'amorphous' matter and liquidity index vs depth relationships, boreholes 75-6 and 75-7 (upper level clay plain).

APPENDIX A. TESTING PROCEDURES FOR GEOTECHNICAL, GEOCHEMICAL AND MINERAL ANALYSES

The testing procedures used in all phases of the research program are briefly outlined below. Although several of the procedures and sizes are expressed in Imperial units, all plotting has been done in SI units.

GEOTECHNICAL TESTING METHODS

1. LABORATORY VANE TESTS

Undisturbed and remoulded laboratory vane strengths were obtained for selected samples from boreholes 75-3, 75-4, 75-6, 78-1 and 78-2. A vane measuring 0.5 inches in diameter and 0.5 inches in height was used to test the middle 6 inches of the 2-foot long shelby samples. It was assumed that this area of the sample would be the least disturbed. Tests were concentrated in the crustal zone where no field vane data were provided for the 1975 borings.

2. UNCONFINED COMPRESSION TESTS

Samples for boreholes 78-1 and 78-2 were tested in unconfined compression, using 2-inch diameter by 4-inch high samples and a strain rate of 1 percent per minute. See ASTM (1964) or Lambe (1951) for further details of the testing procedures. Earlier tests run on the 2-inch diameter tube samples from the 1975 boreholes have been deleted from this report.

3. CONSOLIDATION TESTS

Standard, fixed ring consolidation tests were run on six disturbed samples from borehole 75-2, at depths of 2 m, 3.5 m, 9 m, 19 m, 19.5 m and 31 m. Each sample underwent a loading sequence of 0, 1/4, 1/2, 1, 2, 4, 8, 16, 4, 1 and 0.1 tsf, with increments applied every 24 hours. See Lambe (1951) for further procedural details. A further series of tests were run on the 3-inch undisturbed tube samples from the two 1978 borings, and only the results from these latter tests are presented in the report and presented in Appendix C.

4. INDEX TESTS

The standard procedures for Atterberg limits, grain size analysis, and wet and dry unit weights are available in ASTM (1964) and Lambe (1951). Since the soils were very fine grained, hydrometer analyses only were used in the present study.

GEOCHEMICAL TESTING METHODS

The geochemical testing consisted of pH determinations, carbonate measurements, porewater analyses and organic matter analyses.

The pH was determined for samples from boreholes 75-1, 75-2, 75-5, 75-7, and 75-8 simultaneously with the general engineering index testing. It was measured by a Fisher pH meter on a soil:water slurry (ratio of 1:2). The soil:water mixture was accurately measured, then shaken and allowed to come to equilibrium overnight in an airtight bottle before being tested.

Carbonate contents were obtained on samples from boreholes 75-1, 75-2, 75-4, 75-5, 75-6, 75-7 and 75-8 using a gasometric technique and the Chittick apparatus, as described by Dreimanis (1962).

Porewater analyses were conducted on boreholes 75-1, 75-2, 75-5, 75-7 and 75-8. The porewater was obtained by squeezing a tube sample, for 6 to 8 hours, in a stainless steel cylinder under a pressure of 480 kPa (5 tsf). The liquid draining from the outlet tube was collected in a closed container and tested within 2 to 3 days. The total salinity

of the pore water, in terms of g/L NaCl equivalent, was determined by conductivity measurements. The concentrations of Ca, Mg, K, Na and Fe were measured by a Pye Unicam SP101 Atomic Absorption Spectrophotometer. Attempts were made to measure S by turbidimeter, but the volume of pore water was inadequate for this type of testing.

The organic matter determinations were carried out using the modified Walkley Black method (Allison 1965). Basically the method involves aqueous potassium dichromate oxidation of organics followed by ammonium ferrous sulphate titration to assess the amount of dichromate used.

MINERALOGICAL TESTING METHODS

1. INITIAL SAMPLE PREPARATION

Of each 100 gram, whole soil, supply sample, approximately one-half was air dried for powder patterns, carbonate determination and quartz analysis. The rest of the sample was dispersed in distilled water, using an ultrasonic probe. The soil suspension was then centrifuged to obtain a suspension of $< 2\ \mu m$ sized particles. Each sample was centrifuge fractionated three or four times to ensure collection of all the important clay sized material. The $< 2\ \mu m$ suspension was then divided into four parts and treated further as follows:

i. an aliquot of the suspension was reserved for the preparation of oriented samples, for use in X-ray identification of clay minerals;

ii. the $< 2\ \mu m$ particles in a second aliquot were concentrated into a paste by centrifuging at 10,000 rpm for 10 minutes; the sediment was used for K_2O analysis and is referred to as untreated material;

iii. a third aliquot was Mg saturated by five washings of 1 N $MgCl_2$, one of the washings lasting overnight; excess $MgCl_2$ was removed by washing with 0.001 N $MgCl_2$ and distilled water; the suspension was concentrated as in (ii) and then air dried for glycol retention analysis;

iv. the fourth aliquot was K saturated by 1 N KCl, using the procedure described in (iii); the K saturated clay sized suspension was subsequently concentrated and air dried for glycol retention analysis.

2. QUALITATIVE MINERAL IDENTIFICATION

Powder pattern samples, for identification of the non-clay minerals, were prepared by sprinkling air dried, gently crushed soil onto the surface of a freshly lacquered glass slide. Oriented samples of clay sized material were prepared by centrifuging the $< 2\ \mu m$ size clay suspension onto a porous ceramic plate creating a uniform cake of centrifuge oriented material on the surface of the plate. To Mg or K saturate the samples, 5 mL of 0.5 N $MgCl_2$ or KCl were passed through the sample, followed by 5 mL of distilled water to remove excess salts.

The mineral identifications were carried out in the Materials Science Laboratory using a General Electric XRD-5, utilizing nickel filtered, Cu$K\alpha$ radiation, a 1° beam slit, and a scan speed of 2° 2θ per minute. Powder samples were X-rayed from 32° to 2° 2θ to obtain the main non-clay mineral peaks. The oriented samples were X-rayed from 14° to 2° 2θ, in the natural (distilled water dispersed), K^+ saturated and Mg^{++} saturated states, both air dried and ethylene glycolated.

3. SEMI-QUANTITATIVE PROCEDURES

Quartz. The percentage of quartz was determined by a method of incremental additions as outlined below:

i. Approximately 50 grams of whole soil, ground to less than 200 mesh, was oven dried.

ii. Sub-samples were then taken from the oven dried soil. Oven dried quartz, less than 200 mesh, was added to the sample to make up 0, 2, 4, 6 and 8 percent by weight quartz. The final weight of soil plus ground quartz was 5 to 10 grams.

iii. The mixture was then ground by an automatic mortar and pestle for 5 hours to ensure complete mixing.

iv. In addition to a 0 percent quartz added sample, at least three other quartz percentage mixtures, below 10 percent quartz added, must be prepared for each determination.

v. The powders were then pressed into discs for X-ray diffraction analysis. A disc of 100 percent ground quartz was also prepared.

vi. The intensity of the 4.26 Å quartz peak was then measured for the soil samples and for the pure quartz powder, and the results expressed as the ratio,

($I_{4.26\ Å}$ sample) / ($I_{4.26\ Å}$ pure quartz)

vii. The intensity ratios for the 0, 2, 4, 6 and 8 percent quartz added samples were plotted versus percentage quartz added, as illustrated in Figure A-1. The percentage of quartz for the sample was determined from this plot.

At least two standard curves were prepared for each borehole.

The percentages of quartz obtained by this method for the Hawkesbury samples must be considered approximate, since the variations in intensity due to both grain size and amorphous material have been ignored.

Vermiculite. The percentage of vermiculite was determined using the difference in glycol retention between Mg and K saturated clay size material (Martin 1955). Approximately 0.2 g (accurately weighed) of K and Mg saturated clay were each saturated with glycol, and then placed under vacuum for 12 hours in an ethylene glycol saturated environment. After 12 hours, the samples were weighed, replaced under vacuum and reweighed every 4 hours until two successive readings were within 0.003 g of each other. The weight of glycol retained by the clay was determined and expressed as mg glycol per g soil. The decrease in glycol retention between the Mg and K saturated clay was attributed to the loss of surface area resulting from the collapse of the vermiculite by K to illite. The percentage of vermiculite was then calculated assuming that vermiculite has a glycol retention capacity of 150 mg/g.

Illite/Mica. The amount of illite/mica in the clay size fraction was determined from the percentage of K_2O, as measured by X-ray fluorescence. Pressed discs of air dried, ground, untreated clay size material and a pure mica standard were both analyzed for K by X-ray fluorescence in the Materials Science Laboratory, The University of Western Ontario, and the percentage of K_2O in the soil computed from the comparative peak intensities. The percentage of illite/mica in the soil was then calculated from the measured K_2O, assuming a K_2O content for the soil illite/mica. At this site, it was assumed that the illite/mica contained 10 percent K_2O. This percentage was selected because of the strength of the 10 Å mica peaks yielded by the clay fraction and also the presence of abundant mica in the silt fraction of the soils.

Carbonate. As discussed earlier, the percentage of carbonate in the soil was determined by gasometric techniques (Dreimanis 1962).

Other Minerals. The percentages of chlorite, amphibole, plagioclase feldspar and potassium feldspar were estimated by comparative peak heights, using the ratios suggested by Kenney (1967). The quartz and illite/mica peaks were used as reference peaks or internal standards since they had been quantitatively assessed by the techniques already described.

4. REMOVAL OF AMORPHOUS MATERIAL

Eighteen samples were selected for removal of amorphous material using a modification of Segalen's (1968) technique. The procedure is outlined below:

i. Weigh 0.5 g of air dried, slightly crushed soil into a plastic centrifuge bottle.

ii. Add 50 mL of 8 N HCl, and shake for 30 minutes. Centrifuge at 2000 rpm for 10 minutes.

iii. Decant the supernatant into a 100 mL flask. Add 40 mL of distilled water to the soil and shake briefly.

iv. Centrifuge at 3000 rpm for 10 minutes and decant the supernatant into the 100 mL flask. Make up to the mark with distilled water. This solution will contain dissolved Fe, Al and Si.

v. Add 50 mL of 0.5 N NaOH to the soil, shake for 30 minutes, and centrifuge at 3000 rpm for 10 minutes.

vi. Decant the supernatant into a plastic 100 mL volumetric flask and make up to the mark with distilled water. This solution contains dissolved Al and Si.

vii. Repeat procedure using alternate acid and alkaline washings until a constant concentration of Al, Si and Fe is extracted. The ion concentrations must be determined separately for each hour of treatment and each of the dissolving solutions. Resulting data are plotted as in Figure 31 or Appendix F to determine the percentage of amorphous material extracted.

viii. After the extraction procedure is completed, wash the soil with distilled water until a neutral pH is measured in the soil suspension.

ix. Immediately orient the soil suspension onto a porous ceramic plate for X-ray diffraction analysis of the treated soil.

For this investigation, the concentrations of extracted Al, Si and Fe were measured using a Pye Unicam SP101 Atomic Absorption Spectrophotometer with nitrous oxide/acetylene and air/acetylene flames, respectively.

The treated soil samples, and oriented untreated samples, were X-rayed from 32° to 2° 2θ to assess the effect of the extraction treatments on the soil mineralogy.

SCANNING ELECTRON MICROSCOPY

The samples for SEM examination were slowly air dried over several weeks and then fractured to provide fresh horizontal and vertical faces for examination. The fresh faces were cleaned of loose particles by a jet of air, and the samples then embedded in epoxy on a specimen holder. Prior to examination, the entire specimen was coated with gold-palladium by sputtering. The sputtering and electron microscopy were carried out in the research laboratories of the Dentistry Faculty, The University of Western Ontario.

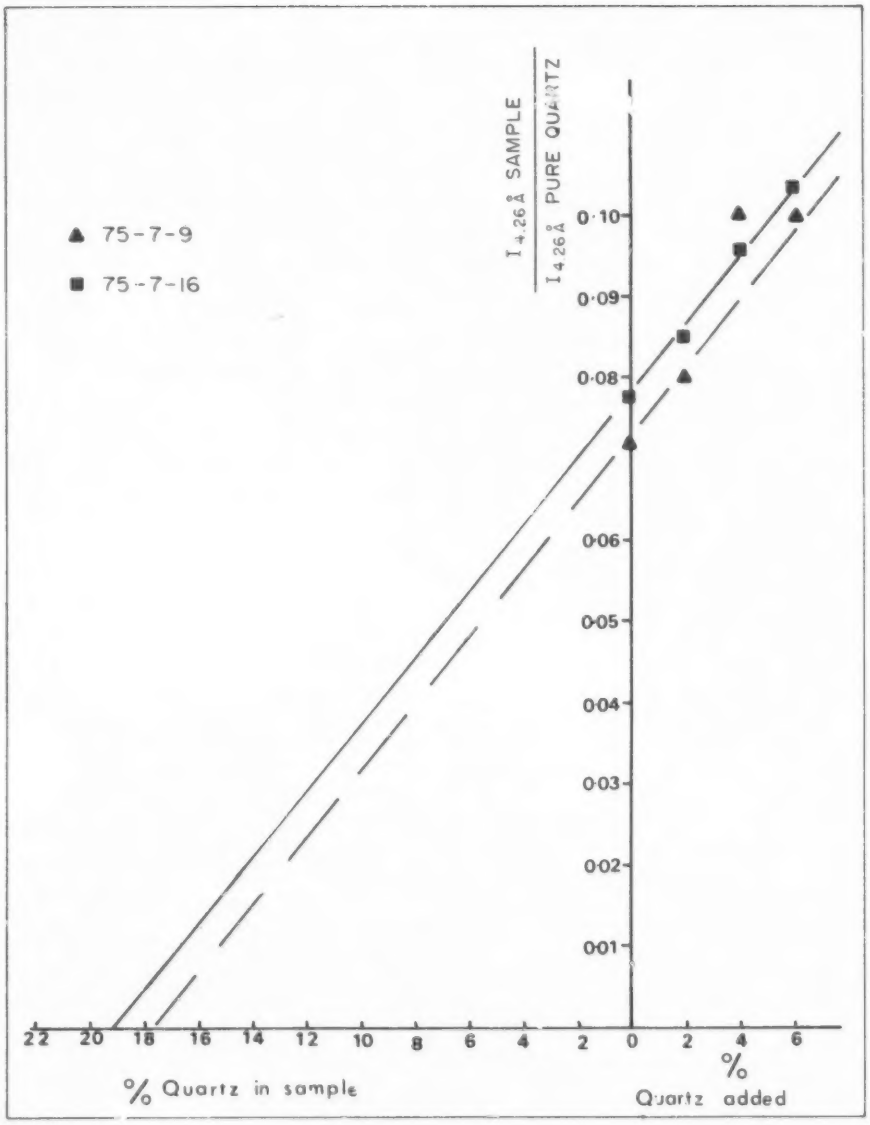

Figure A-1. Determination of abundance of quartz by method of additions.

APPENDIX B. UNCONFINED COMPRESSION TEST RESULTS

Stress-strain curves are presented for the twelve unconfined compression tests run on the 1978 samples on Figures B-1 and B-2. These strength data are also plotted versus depth on the logs on Figures 14 and 15 along with laboratory vane tests.

Stress-strain curves (obtained on disturbed 2-inch tube samples) presented in our 1976 report have been deleted.

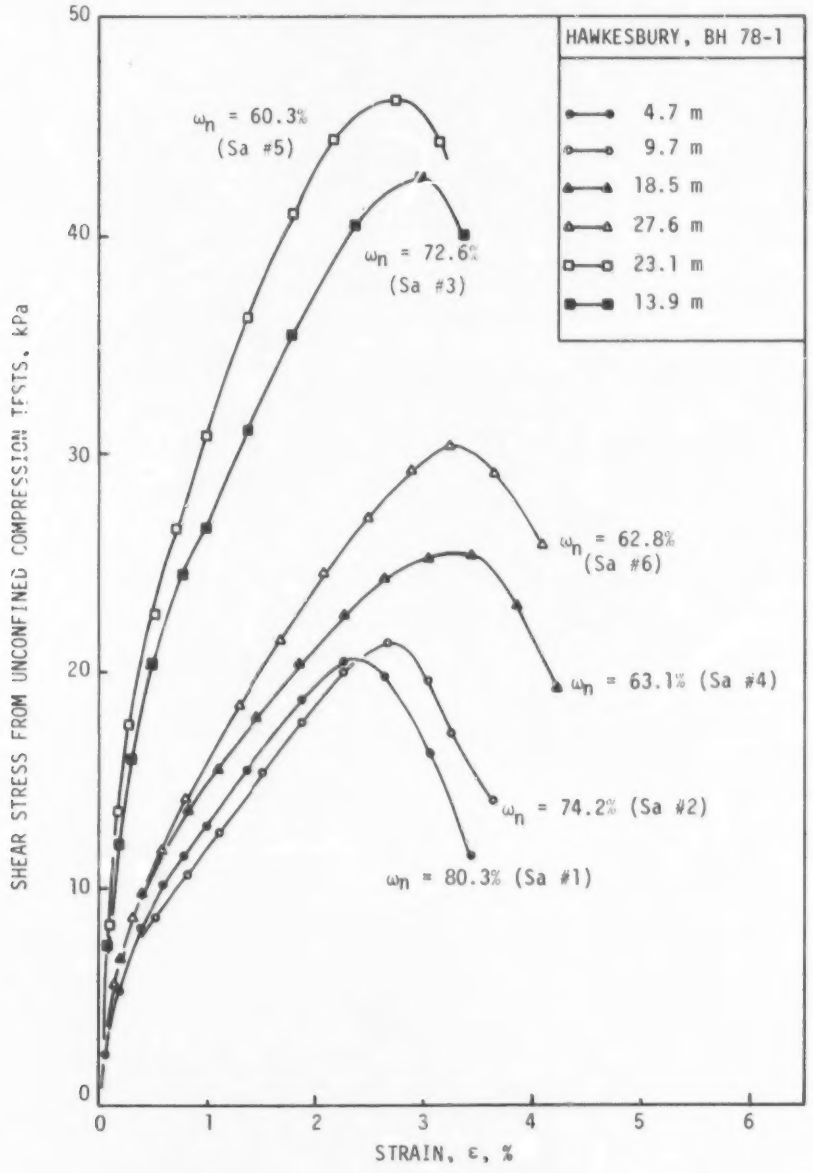

Figure B-1. Stress-strain curves for piston samples, borehole 78-1.

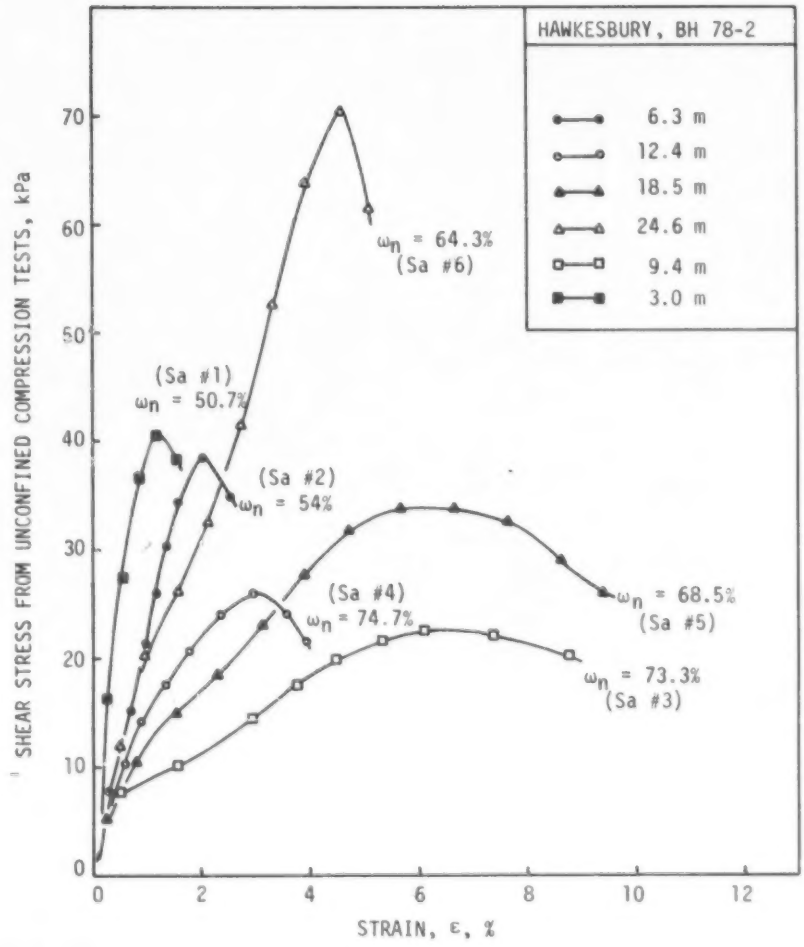

Figure B-2. Stress-strain curves for piston samples, borehole 78-2.

APPENDIX C. CONSOLIDATION TEST RESULTS

The twelve void ratio versus log pressure curves obtained on high quality 3-inch tube samples from boreholes 78-1 and 78-2 are given on Figures C-1 to C-6 inclusive. All curves illustrate the characteristic S-shape typical of Leda clay.

Values of p_o estimated from the piezometric and unit weight data are plotted along with p_c values estimated by Casagrande construction.

Table C-1 contains the results of a series of specific gravity tests used in calculation of void ratios for the consolidation plots.

TABLE C-1 SPECIFIC GRAVITY

Borehole	Sample	Depth (m)	Specific Gravity
78-1	1B	4.8	2.75
	2B	9.6	2.74
	3B	13.9	2.75
	4B	18.5	2.74
	5B	23.0	2.76
	6B	27.6	2.74
78-2	1B	3.2	2.75
	3B	9.3	2.75

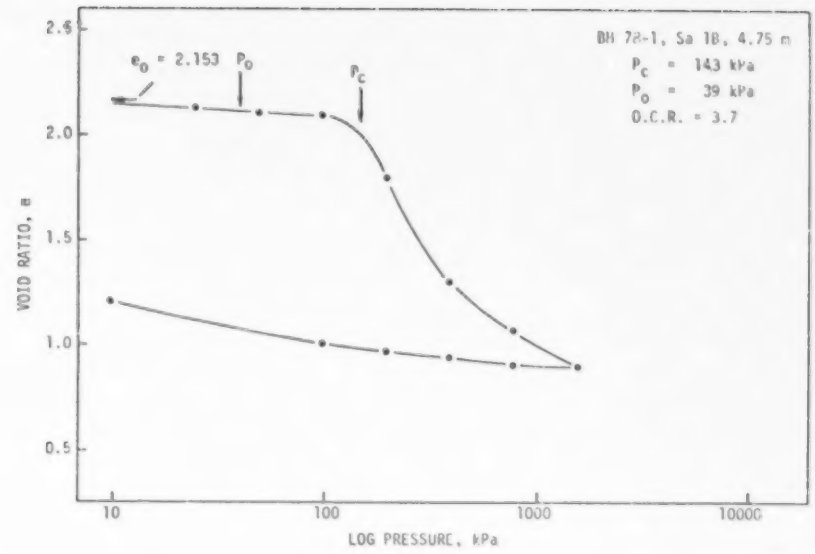

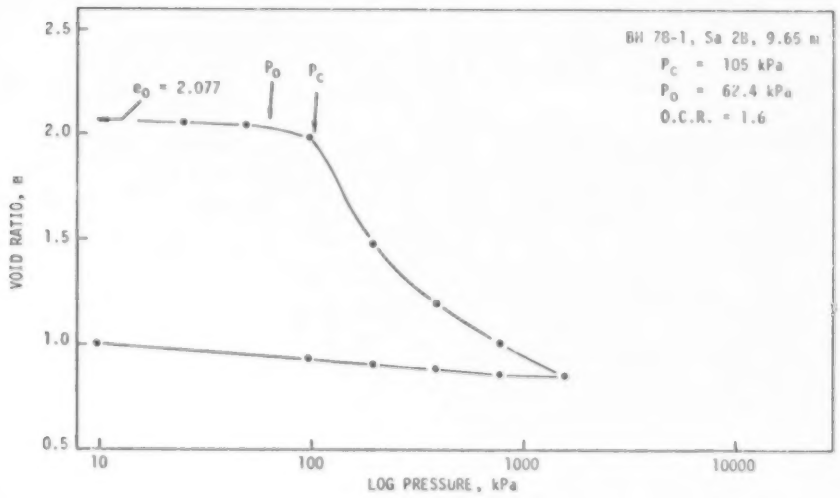

Figure C-1. Consolidation curves for borehole 78-1, 4.75 m and 9.65 m depth.

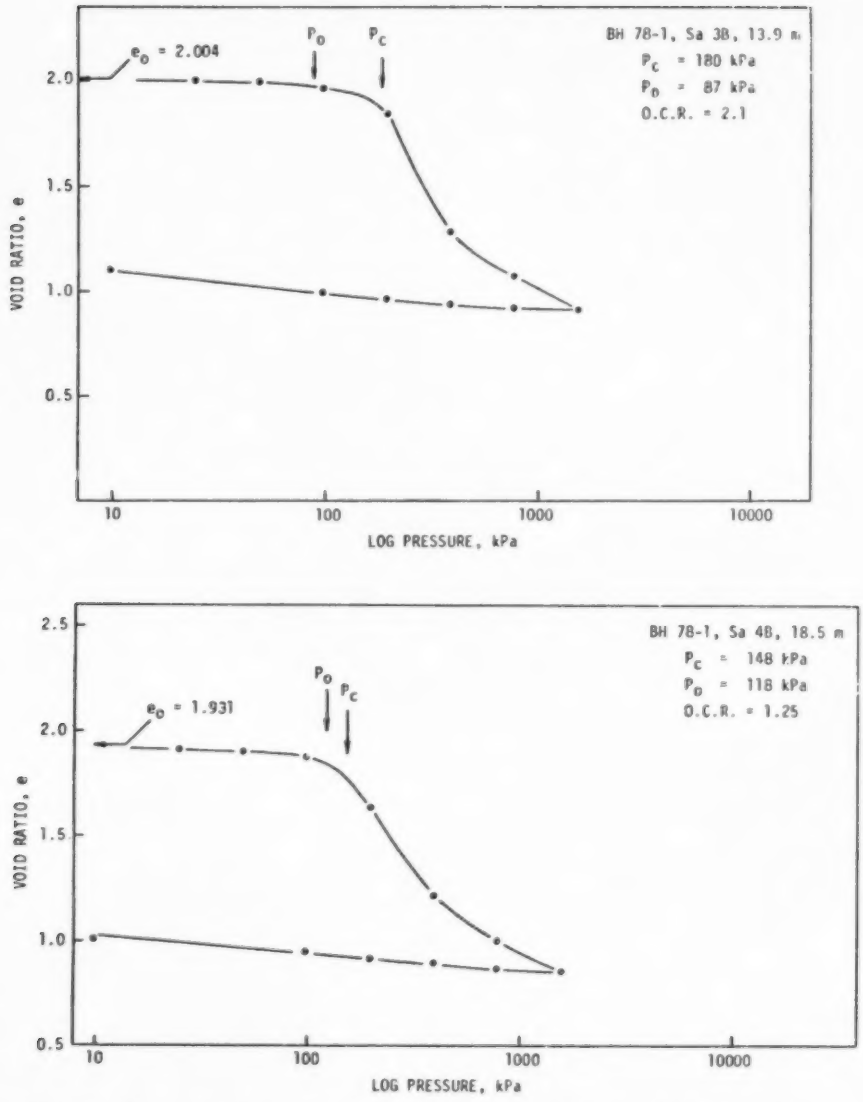

Figure C-2. Consolidation curves for borehole 78-1, 13.9 m and 18.5 m depth.

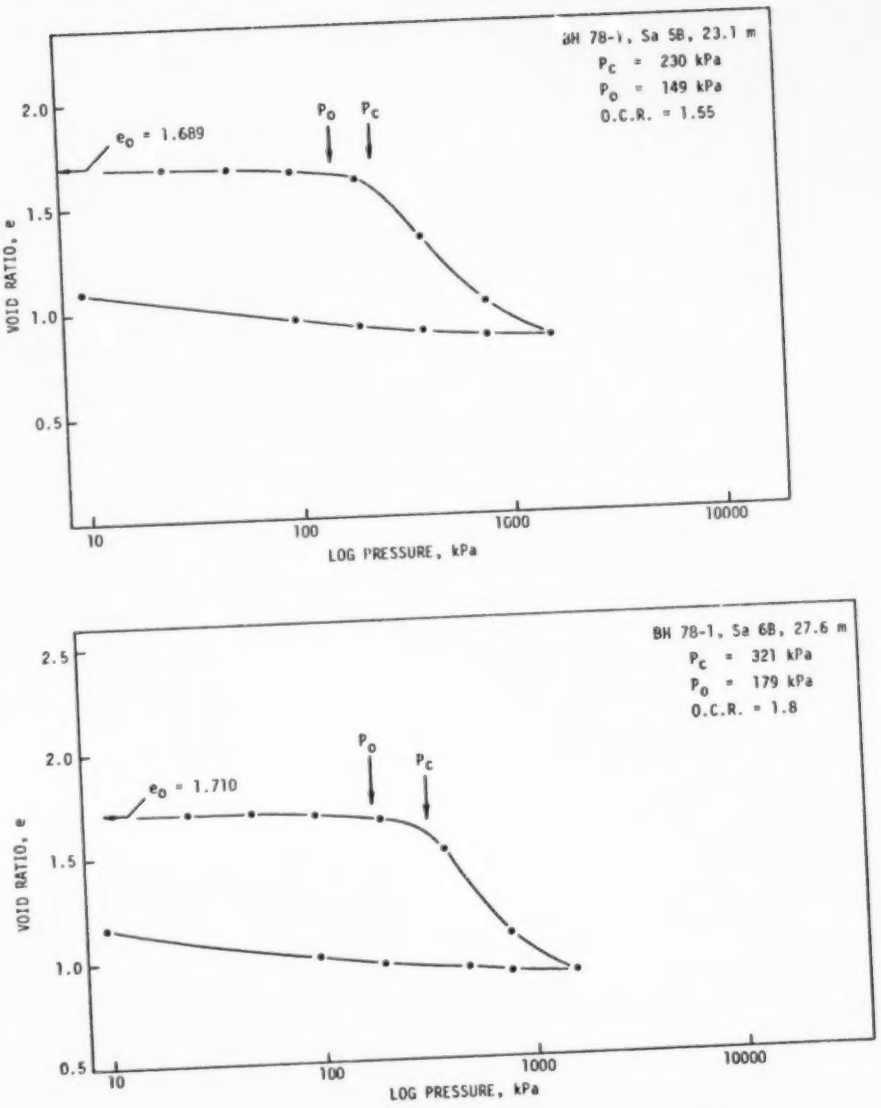

Figure C-3. Consolidation curves for borehole 78-1, 23.1 m and 27.6 m depth.

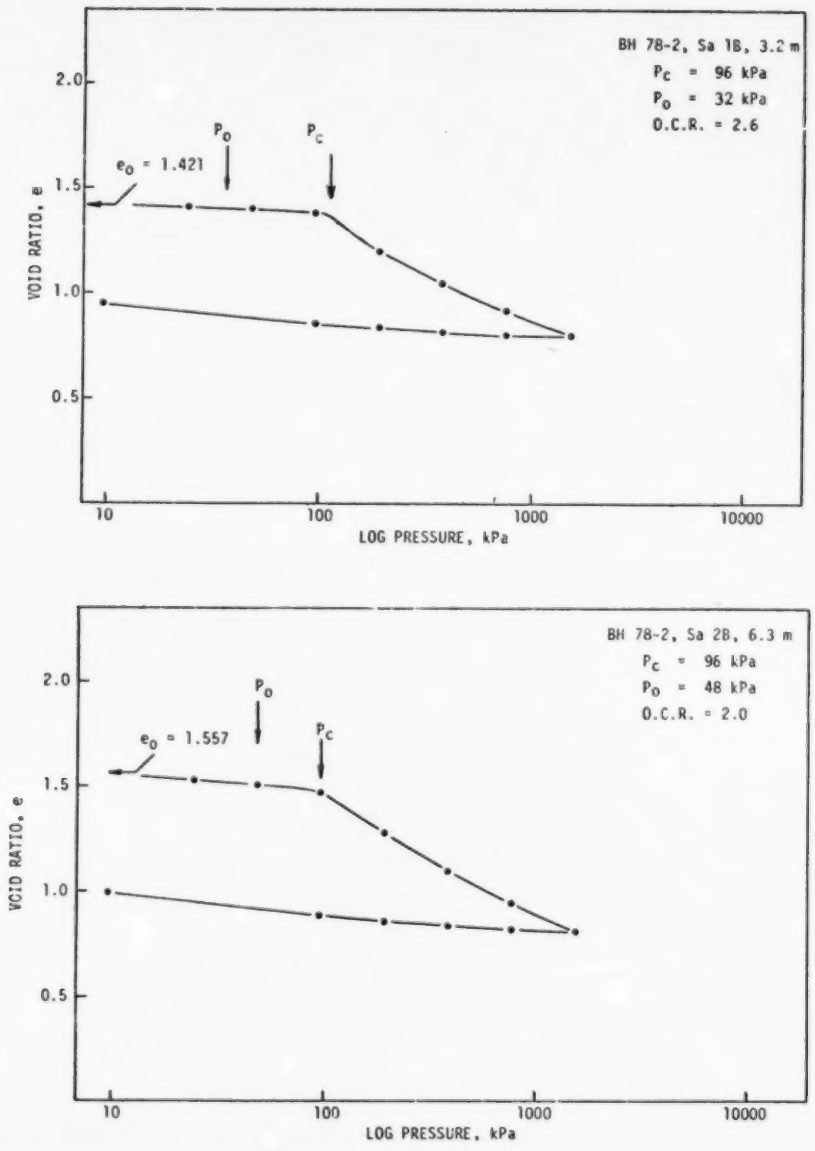

Figure C-4. Consolidation curves for borehole 78-2, 3.2 m and 6.3 m depth.

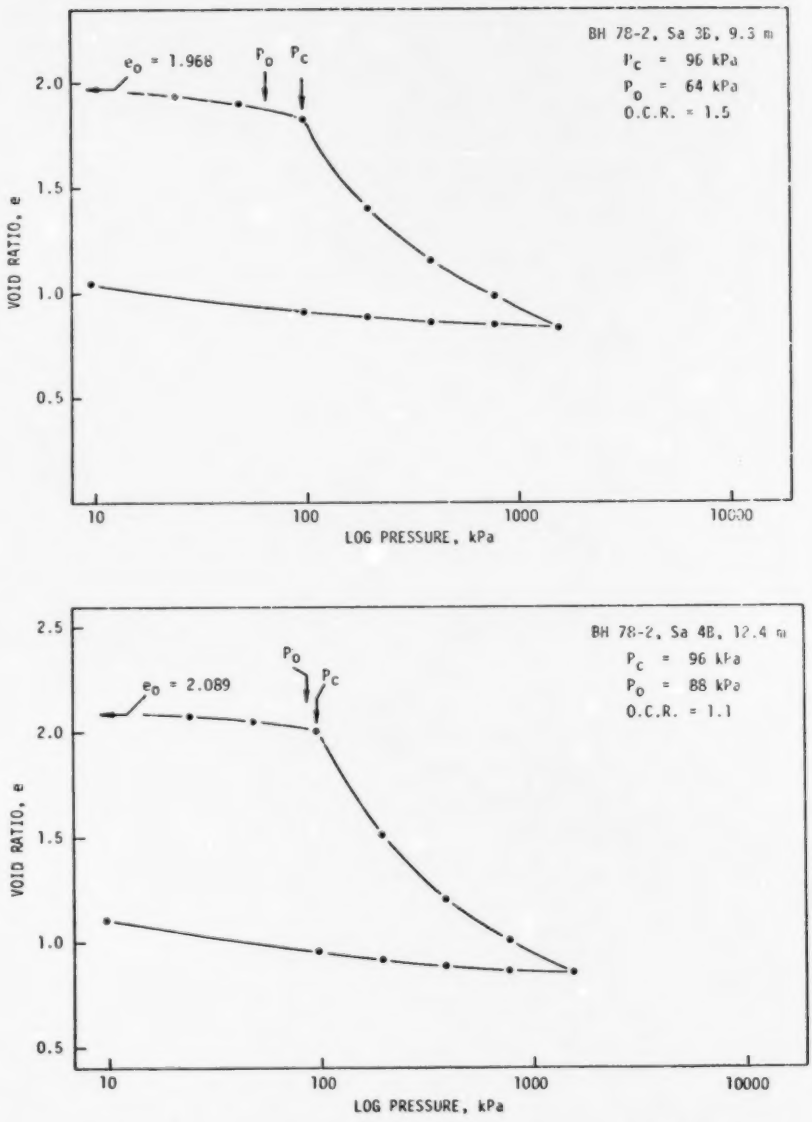

Figure C-5. Consolidation curves for borehole 78-2, 9.3 m and 12.4 m depth.

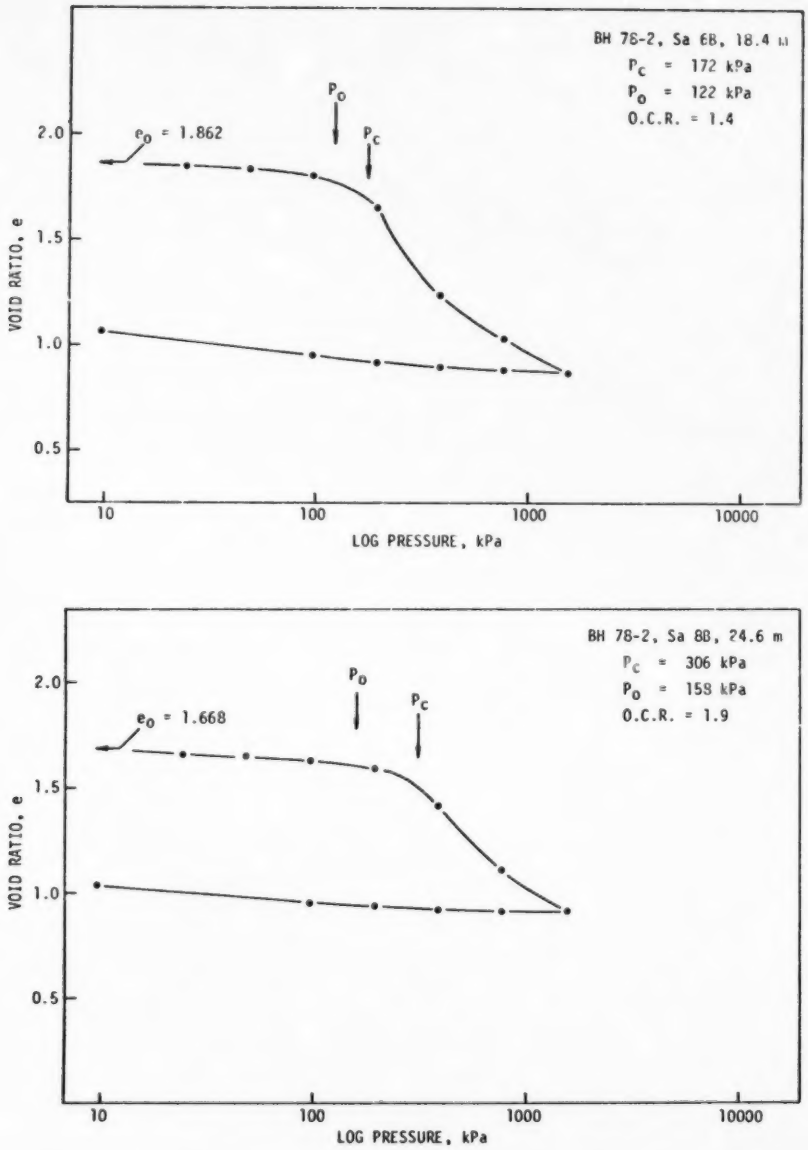

Figure C-6. Consolidation curves for borehole 78-2, 18.4 m and 24.6 m depth.

APPENDIX D. GEOTECHNICAL DATA

TABLE D-1 FIELD VANE DATA, BOREHOLE 75-1

Depth (Feet)	Cu (kPa)	Cr	S_t
18.5	47.9	6.6	7.2
23.5	55.44	5.28	10.5
28.5	50.16	7.92	6.3
33.5	52.8	15.84	3.3
43.5	77.88	11.88	6.6
48.5	76.56	10.56	7.3
53.5	80.52	13.2	6.1
58.5	99.0	13.2	7.5
63.5	79.2	18.48	4.3
68.5	116.16	11.88	9.8
73.5	137.3	23.8	5.8
78.5	147.8	34.3	4.3

*Cu = In situ undisturbed vane strength.
Cr = In situ remoulded vane strength.
S_t = Sensitivity = Cu/Cr.

TABLE D-2 FIELD VANE DATA, BOREHOLE 75-2

Depth (Feet)	Cu (kPa)	Cr	S_t
8	48.8	2.64	18.5
18	46.2	3.96	11.7
23	43.6	9.24	4.7
28	63.36	7.92	7.5
33	58.1	7.9	7.3
38	69.96	13.2	5.3
43	75.2	15.84	4.8
48	64.7	9.24	7.0
53	66.0	14.5	4.6
58	80.5	13.2	6.1
63	95.0	18.5	5.1
68	76.6	17.2	4.5
73	73.9	19.8	3.7
78	109.6	26.4	4.2
83	100.3	25.3	3.9
88	104.3	19.8	5.3
93	103.0	21.1	4.9
98	116.2	23.8	4.9
103	132.0	38.3	3.5

*Cu = In situ undisturbed vane strength.
Cr = In situ remoulded vane strength.
S_t = Sensitivity = Cu/Cr.

TABLE D-3 FIELD VANE DATA, BOREHOLE 75-3

Depth (Feet)	Cu (kPa)	Cr	S_t
8	36.86	1.32	28.0
13	44.83	2.63	17.0
18	52.67	5.27	10.0
23	52.67	5.27	10.0
28	53.98	5.27	10.0
33	59.25	6.58	9.0
38	63.2	10.53	6.0
43	71.1	9.22	7.7
48	69.78	9.22	7.6
53	79.02	10.53	7.5
60	102.7	21.07	4.9
63	110.6	18.43	6.0
71	107.96	15.80	6.8

*Cu = In situ undisturbed vane strength.
Cr = In situ remoulded vane strength.
S_t = Sensitivity = Cu/Cr.

TABLE D-4 FIELD VANE DATA, BOREHOLE 75-4

Depth (Feet)	Cu (kPa)	Cr	S_t
5	31.60	2.63	12.0
15	44.77	5.27	8.5
20	39.52	2.63	15.0
25	51.35	5.27	9.7
30	52.67	3.95	13.3
35	55.30	5.27	10.5
40	71.10	9.21	7.7
45	69.78	10.53	6.6
50	44.76	6.58	6.8
55	76.37	11.61	6.6
60	73.73	10.53	7.0
65	68.47	10.53	6.5
70	101.38	27.65	3.7
75	92.17	15.80	5.8
80	89.53	19.75	4.5
85	100.06	26.33	3.8
90	114.55	21.06	5.4
95	136.93	18.43	7.4
100	100.06	15.8	6.3

*Cu = In situ undisturbed vane strength.
Cr = In situ remoulded vane strength.
S_t = Sensitivity = Cu/Cr.

TABLE D-5 FIELD VANE DATA, BOREHOLE 75-5

Depth (Feet)	Cu (kPa)	Cr	S_t
5.5	52.8	10.6	5.0
10.5	47.5	3.96	12.0
15.5	54.1	3.96	13.7
20.5	51.5	2.6	19.5
25.5	51.4	2.6	21.0
30.5	92.4	11.9	7.8
35.5	96.4	10.6	9.1
40.5	97.7	13.2	7.4
45.5	103.0	10.6	9.8
50.5	99.0	13.2	7.5

*Cu = In situ undisturbed vane strength.
Cr = In situ remoulded vane strength.
S_t = Sensitivity = Cu/Cr.

TABLE D-6 FIELD VANE DATA, BOREHOLE 75-6

Depth (Feet)	Cu (kPa)	Cr	S_t
5.5	47.4	22.38	2.1
10.5	19.75	0	∞
15.5	34.23	5.27	6.5
20.5	35.55	3.95	9.0
25.5	31.6	3.95	8.0
30.5	42.13	13.17	3.2
35.5	39.52	7.9	5.0
40.5	36.86	2.63	14.0
45.5	46.06	2.63	17.5
50.5	35.55	1.31	27.1
55.5	48.71	2.63	18.5
60.5	59.25	6.58	9.0
65.5	76.37	5.27	14.5
70.5	72.42	10.53	6.9
75.5	84.26	3.95	21.3
80.5	57.93	2.63	22.0

*Cu = In situ undisturbed vane strength.
Cr = In situ remoulded vane strength.
S_t = Sensitivity = Cu/Cr.

TABLE D-7 FIELD VANE DATA, BOREHOLE 75-7

Depth (Feet)	Cu (kPa)	Cr	S_t
5.5	126.7	33.0	3.8
10.5	38.3	10.6	3.6
15.5	43.6	10.6	4.1
20.5	42.2	13.2	3.2
25.5	34.3	5.3	6.5
30.5	33.0	5.3	7.3
35.5	33.0	3.96	9.7
40.5	36.96	3.96	9.3
45.5	54.1	3.96	13.7
50.5	56.8	9.2	6.1
55.5	60.7	5.3	11.5
60.5	52.8	6.6	8.0
65.5	68.6	9.2	7.4
70.5	67.3	6.6	10.2
75.5	77.9	5.3	14.8
80.5	101.96	13.2	7.7
85.5	76.2	6.6	11.6
90.5	93.7	21.1	4.4
95.5	84.5	13.2	6.4

*Cu = In situ undisturbed vane strength.
Cr = In situ remoulded vane strength.
S_t = Sensitivity = Cu/Cr.

TABLE D-8 FIELD VANE DATA, BOREHOLE 75-8

Depth (Feet)	Cu (kPa)	Cr	S_t
8.5	99.0	15.8	6.25
13.5	47.5	7.9	6.0
20.5	59.2	5.3	11.3
25.5	71.3	13.2	5.4
30.5	114.8	6.6	17.4
35.5	66.0	7.9	8.3
40.5	68.6	5.3	13.0
45.5	83.2	9.2	9.0
50.5	67.3	6.6	10.2
55.5	76.6	10.6	7.3
60.5	77.9	7.9	9.8
65.5	77.9	9.2	8.4
70.5	83.2	10.6	7.9
75.5	106.9	14.5	7.4
80.5	113.5	13.2	8.6
85.5	87.1	14.5	6.0
90.5	95.0	15.8	6.0

*Cu = In situ undisturbed vane strength.
Cr = In situ remoulded vane strength.
S_t = Sensitivity = Cu/Cr.

TABLE D-9 FIELD VANE DATA, BOREHOLE 75-9

Depth (Feet)	Cu (kPa)	Cr	S_t
29.5	55.44	23.84	2.0
32	60.42	7.52	8.0
38	76.80	22.60	3.0
63	114.9	22.60	5.0
68	111.09	40.3	3.0
73	108.2	55.2	2.0
78	113.0	40.3	3.0
83	135.21	45.3	3.0
88	142.68	76.79	2.0
98	157.5	42.8	4.0
103	80.4	25.84	3.0
108	80.65	25.18	3.0
115	131.19	35.24	4.0
118	111.08	35.24	3.0
123	111.08	40.31	3.0
128	123.53	37.73	3.0
133	108.20	42.8	2.5
138	135.98	50.36	2.7
143	133.58	50.36	2.7
148	120.66	55.45	2.1
158	135.98	65.5	2.0
163	148.42	85.6	1.7
173	123.53	60.42	2.0
183	113.48	50.36	2.2
208	124.97	66.46	1.9

*Cu = In situ undisturbed vane strength.
Cr = In situ remoulded vane strength.
S_t = Sensitivity = Cu/Cr.

TABLE D-10 LABORATORY VANE DATA, BOREHOLE 75-3

Sample (No.)	Depth (Feet)	Cu (kPa)	Cr
1B	3.0	68.52	10.82
2B	5.5	45.29	9.72
3B	9.5	34.28	11.87
4B	15.5	40.55	13.12
7B	30.5	40.84	14.46
10B	45.5	52.67	6.08
12B	58.0	65.84	7.95
15B	73.4	76.41	10.00
15C	73.8	64.54	9.86

*Cu = Laboratory undisturbed vane strength
Cr = Laboratory remoulded vane strength

TABLE D-11 LABORATORY VANE DATA, BOREHOLE 75-4

Sample (No.)	Depth (Feet)	Cu (kPa)	Cr
1A	3.0	30.83	8.41
2B	8.5	25.02	6.37
3B	13.0	38.20	6.60
4B	18.0	40.84	6.85
6B	28.0	40.08	6.08
8B	38.0	50.61	6.60
12B	58.0	60.62	14.46
14B	68.0	46.87	11.87
20B	98.0	146.7	25.5

*Cu = Laboratory undisturbed vane strength
Cr = Laboratory remoulded vane strength

TABLE D-12 LABORATORY VANE DATA, BOREHOLE 75-6

Sample (No.)	Depth (Feet)	Cu (kPa)	Cr
6 – 1A	3	188.36	15.8
6 – 2B	8	21.02	7.93
6 – 3B	13	16.09	5.22
6 – 4B	18	28.97	2.63
6 – 6B	28	23.32	6.09
6 – 10B	48	25.04	4.48
6 – 14B	68	63.78	13.17
6 – 16B	78	33.42	11.87

*Cu = Laboratory undisturbed vane strength
Cr = Laboratory remoulded vane strength

TABLE D-13 INDEX TESTS, BOREHOLE 75-1

Sample	Depth (Ft.)	ω_n (%)	ω_l (%)	ω_p (%)	pH	G_s	γ_{wet} (pcf)	γ_{dry} (pcf)	$< 2\ \mu m$ (%)	$^*A_c$
1 – 2A	5.3	51.8	58.9	23.4	7.2	2.819	–	–	86	.41
1 – 4A	15.8	72.3	75.0	26.2	8.3	2.771	99.32	57.64	80	.61
1 – 6A	25.8	73.2	82.0	26.5	8.4	2.819	98.74	57.0	89	.60
1 – 8A	35.8	68.0	84.3	23.7	8.1	2.856	100.54	59.8	85	.71
1 – 10A	45.8	61.3	66.4	25.15	9.4	2.812	99.57	61.7	81	.5
1 – 12A	55.8	56.3	59.5	26.1	9.0	2.80	103.35	66.1	88	.37
1 – 14A	65.8	55.2	60.7	27.7	8.9	2.815	105.8	68.2	82	.4
1 – 16A	75.8	56.1	70.5	31.0	8.5	2.802	103.9	66.6	75	.52

$^*A_c = \frac{(\omega_l - \omega_p)}{(\% < 2\,\mu m)}$

pcf x 0.157 = kN/m^3

TABLE D-14 INDEX TESTS, BOREHOLE 75-2

Sample	Depth (Ft.)	ω_n (%)	ω_l (%)	ω_p (%)	pH	G_s	γ_{wet} (pcf)	γ_{dry} (pcf)	$< 2\ \mu m$ (%)	$^*A_c$
2 – 1A	2.8	47.7	71.1	25.0	6.6	2.839	98.68	66.8	86	.53
2 – 3A	10.4	70.12	67.6	22.0	7.7	2.813	98.38	57.83	84	.54
2 – 5A	20.3	77.01	60.5	26.8	8.1	2.840	98.92	55.9	78	.43
2 – 7A	30.3	66.6	76.3	27.9	8.35	2.822	98.68	59.44	80	.60
2 – 9A	40.3	68.55	70.0	30.3	8.6	2.783	98.80	58.44	91	.43
2 – 11A	50.3	67.55	64.8	30.7	8.4	2.788	99.17	59.19	91	.37
2 – 13A	60.3	63.57	65.1	28.4	8.4	2.715	100.41	61.39	82	.44
2 – 15A	70.3	62.6	65.7	28.9	8.5	2.801	101.32	62.31	95	.38
2 – 17A	80.3	56.47	61.0	26.5	8.3	2.75	102.98	65.82	89	.39
2 – 19A	90.3	57.37	59.2	27.0	8.7	2.759	106.26	67.52	83	.38
2 – 21A	100.3	60.83	66.0	28.0	8.4	2.758	102.17	63.52	93	.40

$^*A_c = \frac{(\omega_l - \omega_p)}{(\% < 2\,\mu m)}$

pcf x 0.157 = kN/m^3

TABLE D-15 INDEX TESTS, BOREHOLE 75-5

Sample	Depth (Ft.)	ω_n (%)	ω_l (%)	ω_p (%)	pH	G_s	γ_{wet} (pcf)	γ_{dry} (pcf)	$< 2\ \mu m$ (%)	*A_c
5 – 1A	2.8	32.5	51.7	30.9	6.8	2.85	114.03	86.08	85	.24
5 – 2A	7.8	66.8	67.6	29.7	6.7	2.79	98.89	59.29	89	.42
5 – 3A	12.8	72.0	47.5	28.2	7.4	2.83	103.21	60.00	43	.45
5 – 4A	17.8	65.6	66.9	29.3	7.5	2.82	100.59	60.76	88	.42
5 – 5A	22.8	68.7	67.4	32.2	7.6	2.82	97.59	57.86	90	.39
5 – 6A	27.8	69.6	70.55	28.8	7.9	2.82	99.80	58.85	93	.45
5 – 7A	32.8	51.6	64.2	26.0	7.2	2.76	103.47	68.23	90	.42
5 – 8A	37.8	58.9	64.7	28.65	7.6	2.79	102.62	64.58	85	.42
5 – 9A	42.8	55.2	61.9	28.65	7.4	2.90	103.50	66.69	77	.43
5 – 10A	47.8	44.64	55.2	24.65	7.7	2.82	107.62	74.4	54	.56

*$A_c = \frac{(\omega_l - \omega_p)}{(\% < 2\ \mu m)}$

pcf x 0.157 = kN/m^3

TABLE D-16 INDEX TESTS, BOREHOLE 75-7

Sample	Depth (Ft.)	ω_n (%)	ω_l (%)	ω_p (%)	pH	G_s	γ_{wet} (pcf)	γ_{dry} (pcf)	$< 2\ \mu m$ (%)	*A_c
7 – 1A	2.8	38.4	65.3	31.8	6.5	2.803	116.56	84.2	75	.44
7 – 2A	7.8	47.8	57.8	32.1	7.6	2.784	109.56	74.13	88	.29
7 – 3A	12.8	50.2	49.6	27.1	8.3	2.758	108.23	72.07	86	.26
7 – 4A	17.8	50.6	50.0	27.8	8.5	2.765	106.96	72.02	89	.24
7 – 5A	22.8	56.1	58.6	31.7	8.1	2.801	103.65	66.40	90	.29
7 – 7A	32.8	70.0	76.8	26.0	8.2	2.844	96.71	56.89	92	.55
7 – 9A	42.8	80.8	42.35	25.6	8.5	2.742	103.2	57.08	76	.21
7 – 10A	47.8	75.0	76.6	28.4	8.3	2.793	97.86	55.9	95	.50
7 – 11A	52.8	71.6	64.7	29.7	8.0	2.809	99.35	57.9	87	.40
7 – 12A	57.8	74.8	70.0	29.8	7.65	2.843	97.1	55.5	88	.45
7 – 13A	62.8	66.9	63.5	29.8	8.6	2.757	98.2	58.8	93	.36
7 – 14A	67.8	72.9	70.4	27.7	8.0	2.823	97.53	56.4	93	.45
7 – 15A	72.8	67.7	61.0	31.2	7.45	2.840	99.80	59.5	90	.33
7 – 16A	77.8	59.8	50.0	27.2	7.7	2.799	103.4	64.7	73	.31
7 – 17A	82.8	64.3	49.0	29.0	7.9	2.844	102.62	62.46	82	.24
7 – 18A	87.8	48.4	47.2	19.6	7.8	2.783	106.95	72.07	61	.46
7 – 19A	92.8	37.5	34.1	18.8	8.4		113.35	82.44	52	.29

*$A_c = \frac{(\omega_l - \omega_p)}{(\% < 2\ \mu m)}$

pcf x 0.157 = kN/m^3

TABLE D-17 INDEX TESTS, BOREHOLE 75-8

Sample	Depth (Ft.)	ω_n (%)	ω_l (%)	ω_p (%)	pH	G_s	γ_{wet} (pcf)	γ_{dry} (pcf)	$< 2\ \mu m$ (%)	*A_c
8 – 1A	17.8	49.24	60.5	24.1	7.9		103.35	69.27	87	.41
8 – 2A	22.8	61.3	53.0	26.7	7.9		101.68	63.04	75	.35
8 – 3A	27.8	62.24	59.8	27.15	8.1		104.44	64.39	70	.46
8 – 5A	37.8	69.06	56.4	21.8			93.07	55.05	87	.39
8 – 7B	48.3	46.47	59.9	27.7			106.86	72.96	72	.44
8 – 9A	57.8	54.7	61.5	31.05			103.35	66.8	91	.43
8 – 11A	67.8	52.2	63.0	31.87			102.23	67.16	87	.35
8 – 12A	72.8	64.4	76.7	30.9			99.41	60.46	85	.53
8 – 13B	78.3	56.1	75.8	28.5			101.32	64.9	91	.51
8 – 14A	82.8	52.2	78.0	32.2			101.83	66.9	93	.49
8 – 15A	87.8	62.9	62.2	29.7			93.29	57.27	76	.42

*$A_c = \frac{(\omega_l - \omega_p)}{(\% < 2\ \mu m)}$

pcf x 0.157 = kN/m³

TABLE D-18 INDEX TESTS, BOREHOLE 75-9

Sample	Depth (Ft.)	ω_n (%)	ω_l (%)	ω_p (%)	G_s	$< 2\ \mu m$ (%)	$^*A_c$
9 – 3	8	46.3	55.76	26.5	2.77	87	.3
9 – 11	36	55.74	56.4	23.0	2.81	78	.42
9 – 18	66	45.7	54.2	22.7	2.83	74	.42
9 – 56	271	52.0	68.2	30.0	2.85	84	.45

$^*A_c = \frac{(\omega_l - \omega_p)}{(\% < 2\,\mu m)}$

pcf x 0.157 = kN/m^3

TABLE D-19 ADDITIONAL GRAIN SIZE DATA FOR BOREHOLES 75-4, 5, 6 and 8

Borehole and Sample	Depth (Ft.)	% < 2 μm
75 – 4-2	8	84
4-6	28	78
4-8	38	85
4-14	68	92
4-20	98	69
75 – 5-3	13	84
75 – 6-2	8	83
6-3	13	80
6-6	28	85
6-10	48	84
6-16	78	42
75 – 8-4	33	80

APPENDIX E. GEOCHEMICAL DATA

CALCITE AND DOLOMITE

TABLE E-1 CARBONATE CONTENTS BY GASOMETRIC ANALYSIS

Sample	Total Carbonate %	Calcite %
75 – 1-2	13.0	6.0
4	10.0	4.0
6	7.0	3.0
7	7.0	4.0
8	6.0	2.0
10	10.0	3.0
12	7.0	4.0
14	5.0	3.0
16	2.0	0.6
75 – 2-1	2.0	0.6
3	4.0	2.0
5	8.0	0.2(?)
7	7.0	4.0
9	5.0	2.5
10	2.0	0.4
11	3.0	2.0
13	6.0	4.0
15	2.0	0.8
17	4.0	1.0
19	7.0	4.0
21	8.0	2.0
75 – 3-4	4.0	0.7
10	5.0	1.8
75 - 4-2	5.0	2.5
6	8.0	5.0
8	6.0	3.0
14	8.0	4.0
20	5.0	2.0
75 – 5-2	6.0	2.0
3	4.0	0.8
4	10.0	–
5-C	4.0	1.6
5-D	9.0	5.5
6	3.0	0
7	3.0	0.7
9	3.0	0.4
10	3.0	–
75 – 6-2	4.0	2.0
3	11.0	2.0
6	10.0	2.0
10	4.0	2.0
16	6.0	2.7
75 – 7-2	5.0	2.0
4	6.2	2.0
5	6.0	2.0
9	6.0	1.8
13	6.0	2.4
16	2.4	1.1
17	3.0	1.8
19	9.6	4.3
75 – 8-1	6.0	2.2
2	4.0	2.1
4	4.0	2.5
5	4.0	2.3
7	3.0	1.3
9	5.3	1.8
12	2.3	1.5
13	4.0	2.2
14	1.9	1.3
75 – 9-3	5.0	1.8
11	6.5	2.0
18	7.0	2.0
56	3.0	0.6

SALINITY AND POREWATER CATIONS

TABLE E-2 SALINITY AND POREWATER CATIONS, BOREHOLES 1, 2, 5, 7 AND 8

Sample	Total Salinity (g/L)	Porewater Cations (ppm)			
		Na	K	Ca	Mg
75 – 1-2	1.5	5850	15	50	80
4	4.75	4950	40	57.5	450
6	6.75	5850	50	61	530
8	8.75	6100	65	75	230
10	9.0	6750	68.5	72.5	290
12	10.25	6450	75	77.5	280
14	9.0	4650	62.5	89	200
16	7.0	5650	62.5	67.5	130
75 – 2-2	1.075	4500	17	45	80
5	5.5	4400	48	50	175
11	12.25	6800	91	100	400
15	15.25	9600	124	157	630
17	13.5	8600	112	105	570
21	15.5	8100	154	177	600
75 – 5-2	2.0	1500	45	30	140
3	2.9	1500	51	30	120
4	4.0	2300	52	42	140
5	4.6	2300	60	37	137
6	5.5	3250	71	47	150
7	5.8	3300	79	48	150
8	6.8	3450	98	60	180
9	7.5	4750	108	65	215
10	7.1	4200	91	55	165
75 – 7-2	1.0	780	15	26	27
4	1.55	1380	28	25	60
7	4.1	1770	45	25	90
9	4.1	2000	48	26	80
11	3.95	1825	45	20	60
13	3.25	1620	45	20	40
15	2.4	1290	40	20	26
18	1.7	930	31	14	14
19	0.75	590	26	17	10
75 – 8-1	3.0	1750	47	48	155
3	5.0	2500	50	50	155
4	6.7	3250	69	76	275
7	9.8	5400	91	72	305
9	11.0	5200	100	96	335
12	15.0	6600	125	210	600
13	14.0	5000	120	170	550
15	15.0	5085	130	200	550

ORGANIC MATTER

TABLE E-3 ORGANIC MATTER*

Borehole No.	Sample No.	Organic Matter (%)
78-1	1	1.1574
	2	1.0605
	3	0.9256
	4	1.0904
	5	0.9612
	6	1.0614
78-2	1	0.8198
	2	0.8799
	3	0.8494
	4	0.8225
	5	0.9202
	6	0.8366
	7	0.9168
	8	0.9898
	9	0.7425

*Average of two tests using Modified Walkley Black Organic Carbon method on $< 250\ \mu m$ fraction.
(Tests by Maxine Kingston, Department of Geography, The University of Western Ontario)

APPENDIX F. ANALYSES OF FLUID EXTRACTS AFTER SELECTIVE DISSOLUTION TREATMENT

(For a description of the modified Segalen extraction method used, see Appendix A)

TABLE F-1 SEGALEN 'AMORPHOUS' EXTRACTIONS

Sample	Depth (m)	Amorphous SiO_2 (%)	Amorphous Fe_2O_3 (%)	Amorphous Al_2O_3 (%)	Total Amorphous (%)
75 – 1-2	1.8				13.5
7	9.4				~9.0
12	17.1				12.0
16	23.0				~14.0
75 – 2-3	3.4				12.4
9	12.5				11.9
11	15.5				12.5
17	24.7				14.0(?)
21	30.8				13.0
75 – 6-2	2.6				13.5
6	8.7	~4.5	~3.5	~2.5	10.5
10	14.8	~5.0	~3.5	~3.0	11.5
16	23.9				11.0
75 – 8-2	7.2				11.0
4	10.2				12.7
7	14.8				14.0
13	23.9				10.5

*See Figs. F-1 to F-9 for data points and extrapolated curves used to calculate amorphous materials extracted.

All values are approximate since they are rate-time dependent.

TABLE F-2 AMORPHOUS EXTRACTIONS IN ORDER COMPLETED

Sample	Time (Hrs.)	Fe_2O_3 (%)	Al_2O_3 (%)	SiO_2 (%)	Σ (%)	Cum. Σ (%)
75 – 2-3	1	2.979	2.558	3.81	9.347	9.35
	2	.794	.759	1.99	3.543	12.89
	3	.376	.571	1.476	2.423	15.31
	4	.284	.461	.984	1.689	17.00
	5	.200	.306	.727	1.233	18.24
75 – 2-9	1	2.645	2.426	1.71	6.781	6.78
	2	.766	.703	3.743	5.212	11.99
	3	.418	.499	1.241	2.158	14.15
	4	.228	.348	.791	1.367	15.52
	5	.195	.208	.620	1.023	16.54
75 – 2-11	1	3.063	2.515	4.919	10.497	10.50
	2	.724	.706	2.139	3.569	14.07
	3	.395	.593	1.305	2.295	16.36
	4	.334	.442	.941	1.717	18.08
	5	.187	.377	.834	1.398	19.48
75 – 2-17	1	2.784	2.683	2.93	8.397	8.40
	2	1.044	.873	4.256	6.173	14.57
	3	.473	.533	1.164	5.602	20.17
	4	.228	.310	.791	1.329	21.56
	5	.187	.410	1.54(?)	2.137	23.70
75 – 2-21	1	2.868	2.513	2.63	8.011	8.01
	2	.626	.642	4.235	5.503	13.51
	3	.493	.544	1.198	2.235	15.75
	4	.334	.412	.984	1.73	17.48
	5	.237	.264	.663	1.164	18.64
75 – 8-2	1	2.645	2.059	3.286	7.99	7.99
	2	.724	.623	2.884	4.231	12.22
	3	.507	.548	1.631	2.686	14.91
	4	.339	.321	.936	1.596	16.50
	5	.200	.246	.756	1.202	17.70
75 – 8-4	1	3.062	2.362	3.061	8.485	8.48
	2	.766	.661	2.845	4.272	12.76
	3	.529	.567	1.519	2.615	15.37
	4	.312	.302	.975	1.589	16.96
	5	.186	.264	.714	1.164	18.12
75 – 8-7	1	3.118	2.418	4.149	9.685	9.68
	2	.932	.812	2.567	4.311	14.00
	3	.473	.491	1.497	2.461	16.46
	4	.284	.302	.941	1.527	17.98
	5	.167	.246	.599	1.012	19.00
75 – 8-13	1	2.784	2.191	3.294	8.269	8.27
	2	.793	.680	2.609	4.082	12.35
	3	.487	.491	1.454	2.432	14.78
	4	.278	.283	.962	1.523	16.31
	5	.181	.246	.620	1.047	17.35
75 – 6-2	1	3.173	2.346	4.406	9.925	9.92
	2	1.072	1.039	2.374	4.485	14.41
	3	.487	.498	1.454	2.439	16.85
	4	.312	.336	1.005	1.653	18.50
	5	.200	.302	.804	1.306	19.81
75 – 6-6	1	2.923	2.161	1.989	7.073	7.07
	2	.696	.567	3.016	4.279	11.35
	3	.362	.385	.941	1.688	13.04
	4	.223	.264	.919	1.406	14.45
	5	.139	.189	.620	.948	15.39

Sample	Time (Hrs.)	Fe_2O_3 (%)	Al_2O_3 (%)	SiO_2 (%)	Σ (%)	Cum.Σ (%)
75 – 6-10	1	3.118	2.252	3.23	8.6	8.60
	2	1.141	.858	2.139	4.138	12.74
	3	.557	.529	1.134	2.22	14.96
	4	.284	.302	.684	1.27	16.23
	5	.186	.264	.599	1.049	17.28
75 – 6-16	1	2.645	1.897	3.23	7.772	7.77
	2	.835	.642	1.733	3.21	10.98
	3	.401	.378	.791	1.57	12.55
	4	.186	.227	.620	1.033	13.59
	5	.145	.227	.471	.843	14.43
75 – 1-2	1	2.56	1.651	3.679	7.89	7.89
	2	1.141	.971	2.182	4.294	12.18
	3	.562	.555	1.134	2.251	14.44
	4	.273	.283	.684	1.24	15.68
	5	.248	.336	.620	1.204	16.88
75 – 1-7	1	2.283	1.334	4.278	7.895	7.90
	2	.974	.877	2.246	4.097	11.99
	3	.501	.472	.235	1.208	13.20
75 – 1-12	1	2.366	1.783	4.492	8.641	8.64
	2	1.002	.824	2.224	4.05	12.69
	3	.529	.510	1.155	2.194	14.88
	4	.292	.340	.727	1.359	16.24
	5	.223	.295	.727	1.245	17.49
75 – 1-16	1	2.923	2.105	6.310	11.338	11.34
	2	1.253	.997	2.481	4.731	16.07
	3	.570	.604	1.176	2.35	18.42
	4	.312	.321	.749	1.382	19.08
	5	.217	.283	.727	1.227	21.03

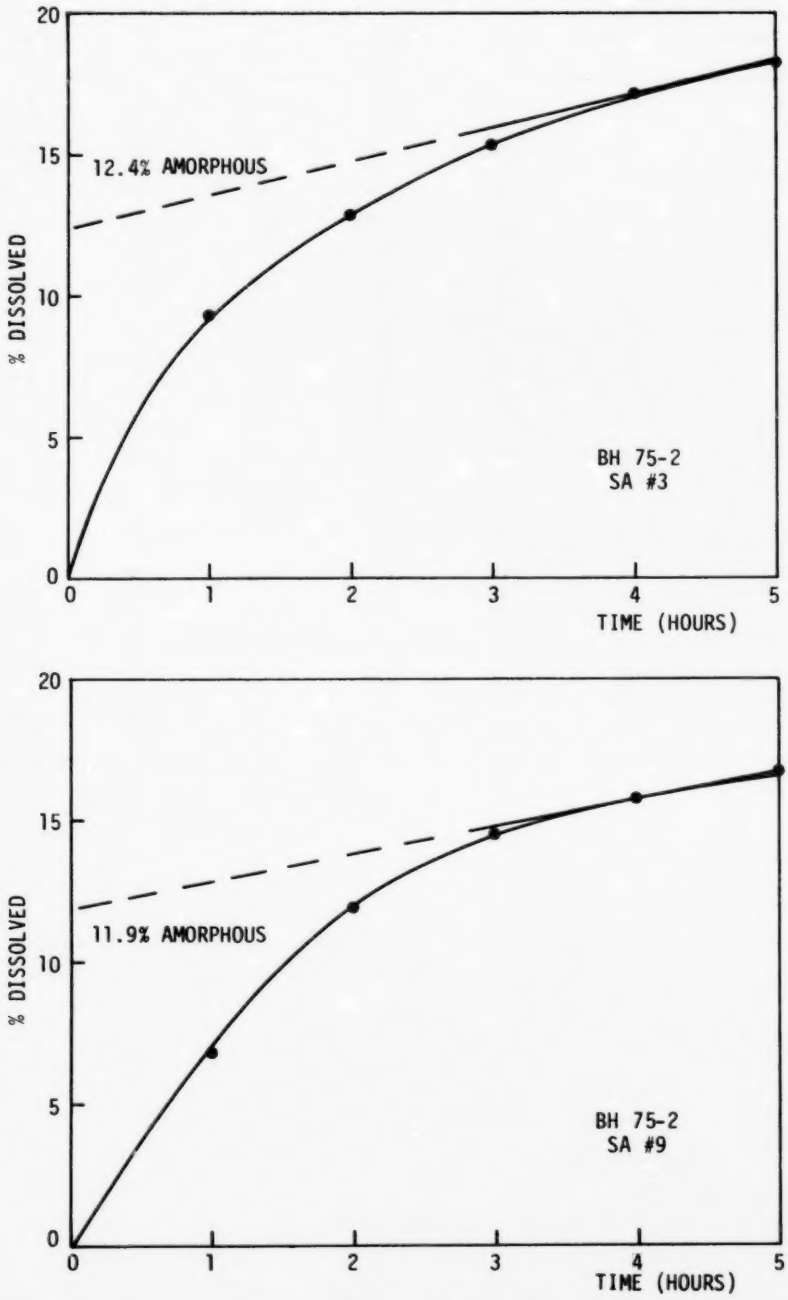

Figure F-1. Time-rate of dissolution curves for amorphous determinations, samples 75-2-3 and 75-2-9.

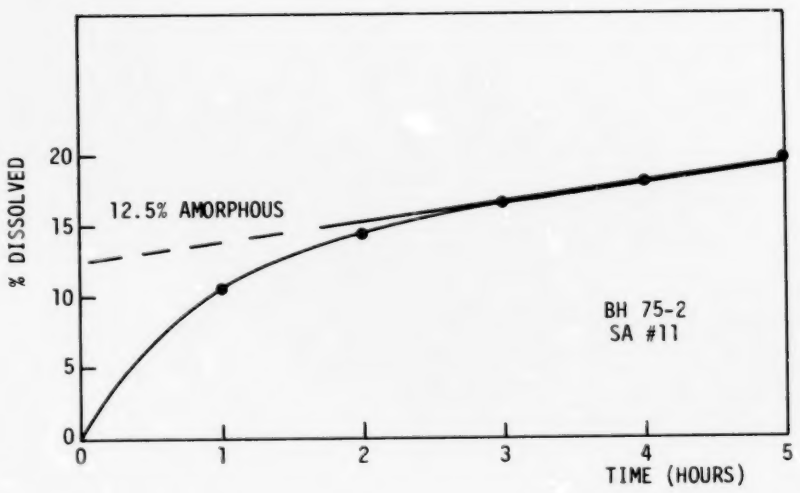

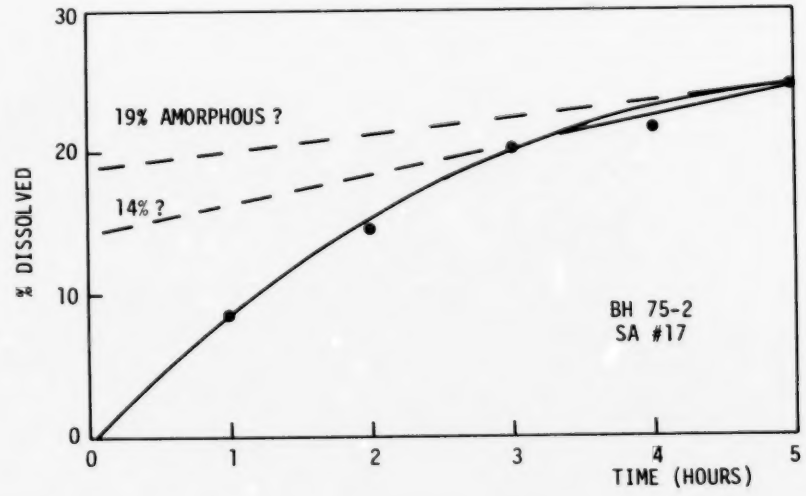

Figure F-2. Time-rate of dissolution curves for amorphous determinations, samples 75-2-11 and 75-2-17.

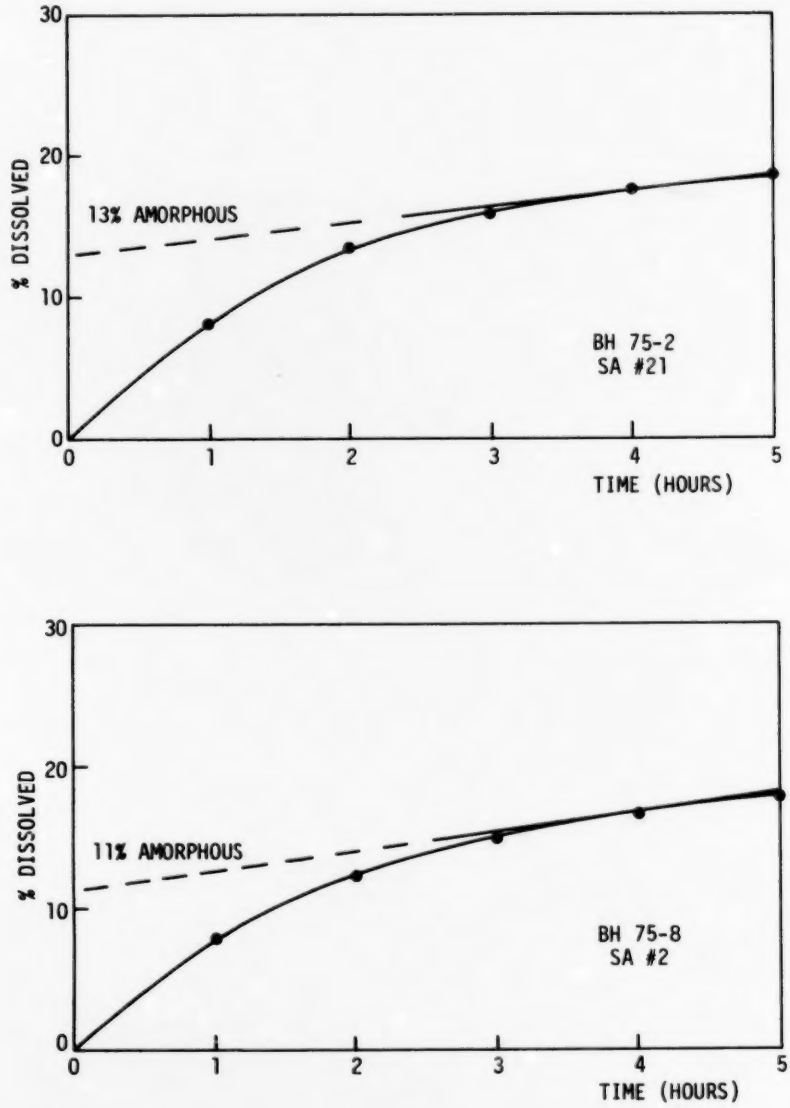

Figure F-3. Time-rate of dissolution curves for amorphous determinations, samples 75-2-21 and 75-8-2.

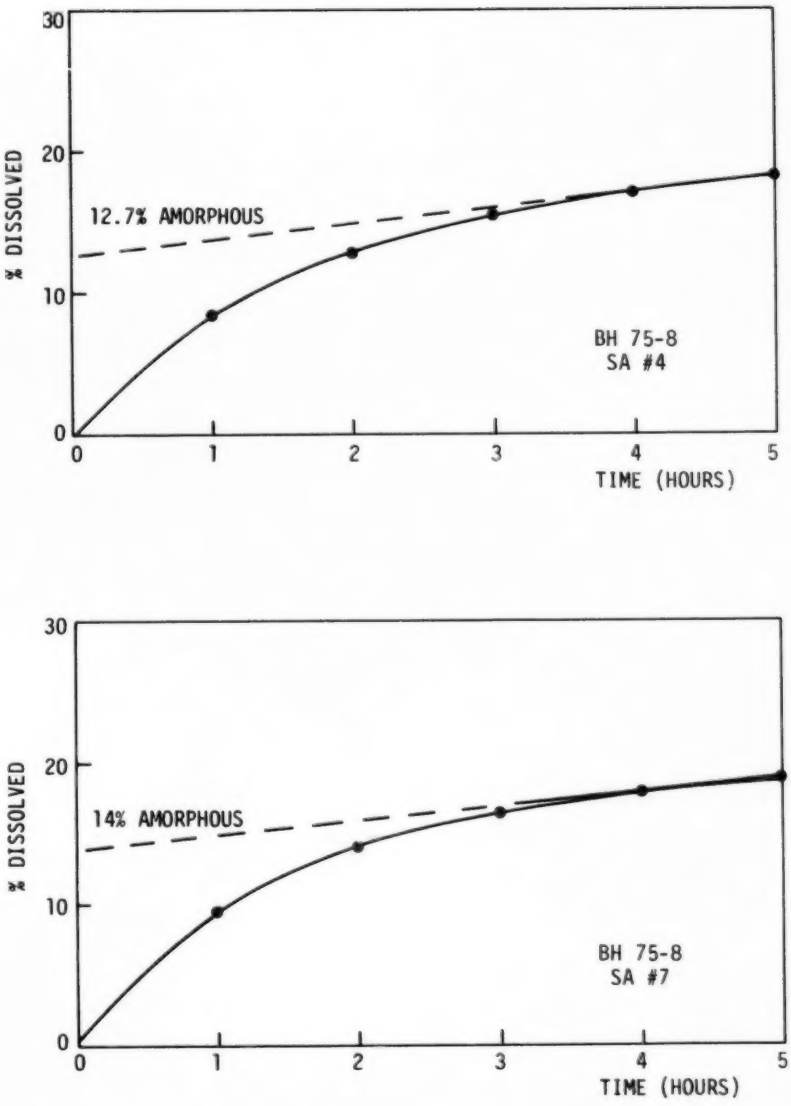

Figure F-4. Time-rate of dissolution curves for amorphous determinations, samples 75-8-4 and 75-8-7.

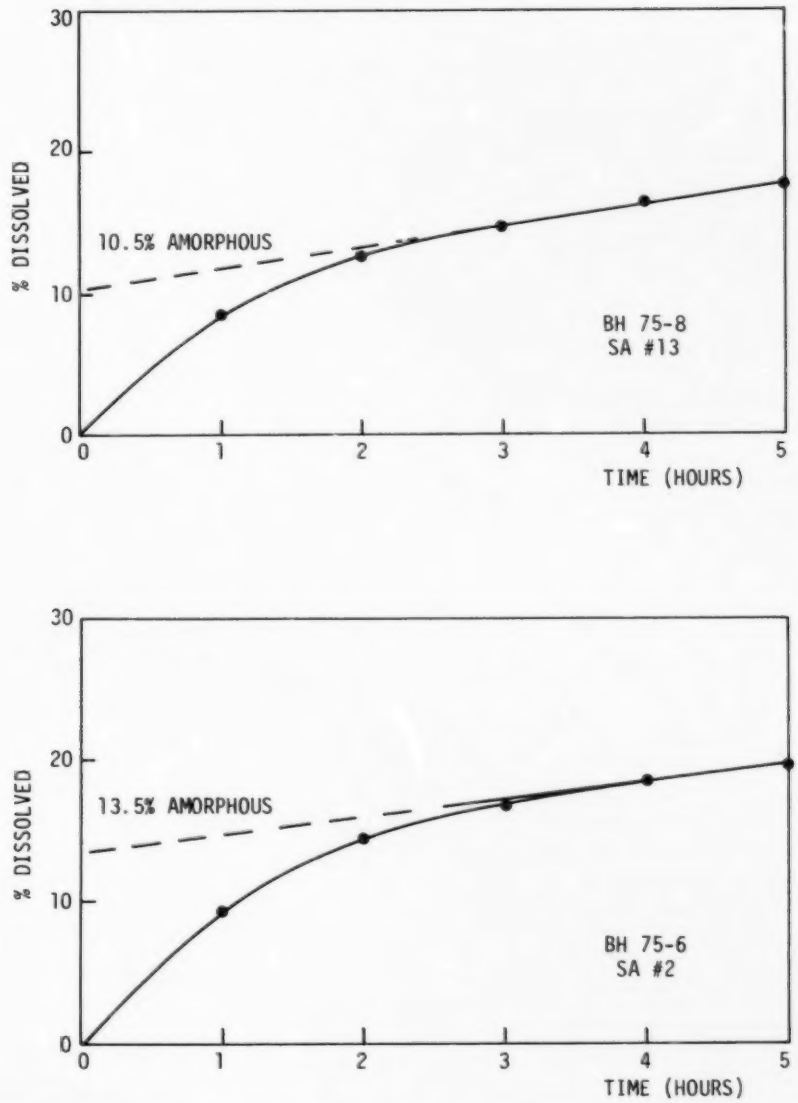

Figure F-5. Time-rate of dissolution curves for amorphous determinations, samples 75-8-13 and 75-6-2.

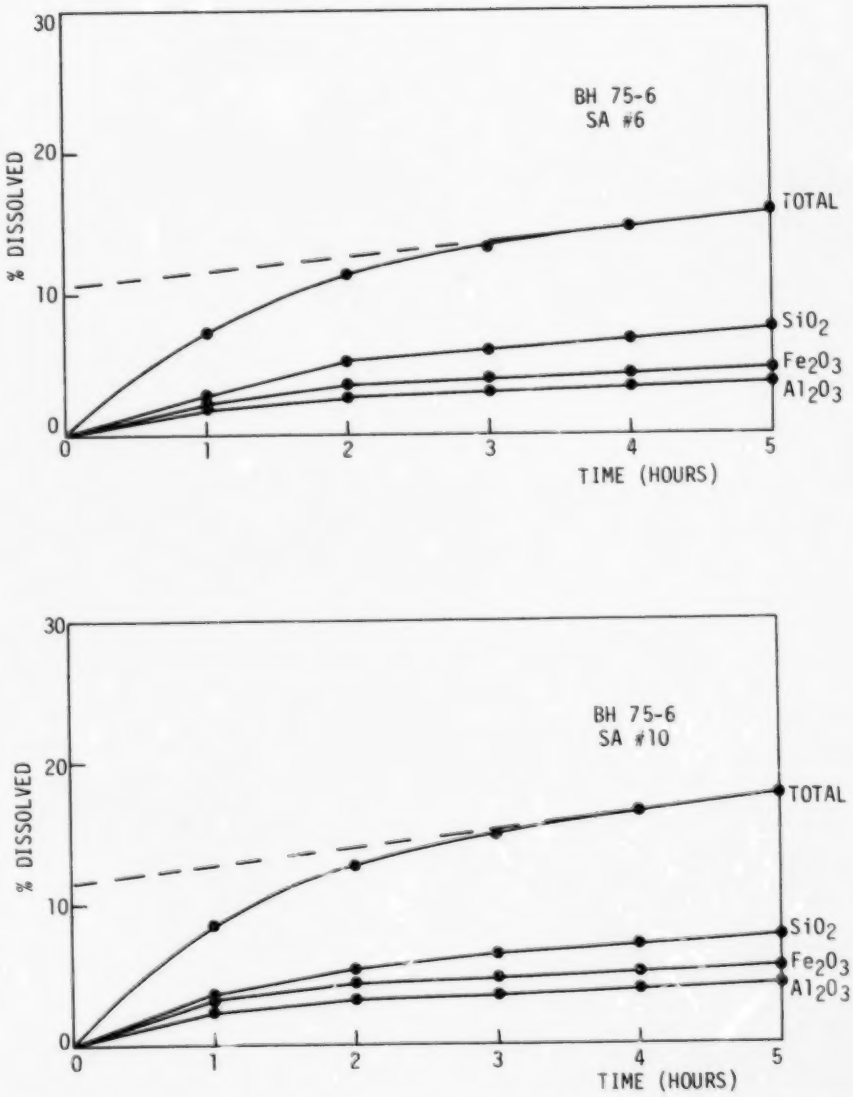

Figure F-6. Time-rate of dissolution curves for amorphous determinations, samples 75-6-6 and 75-6-10.

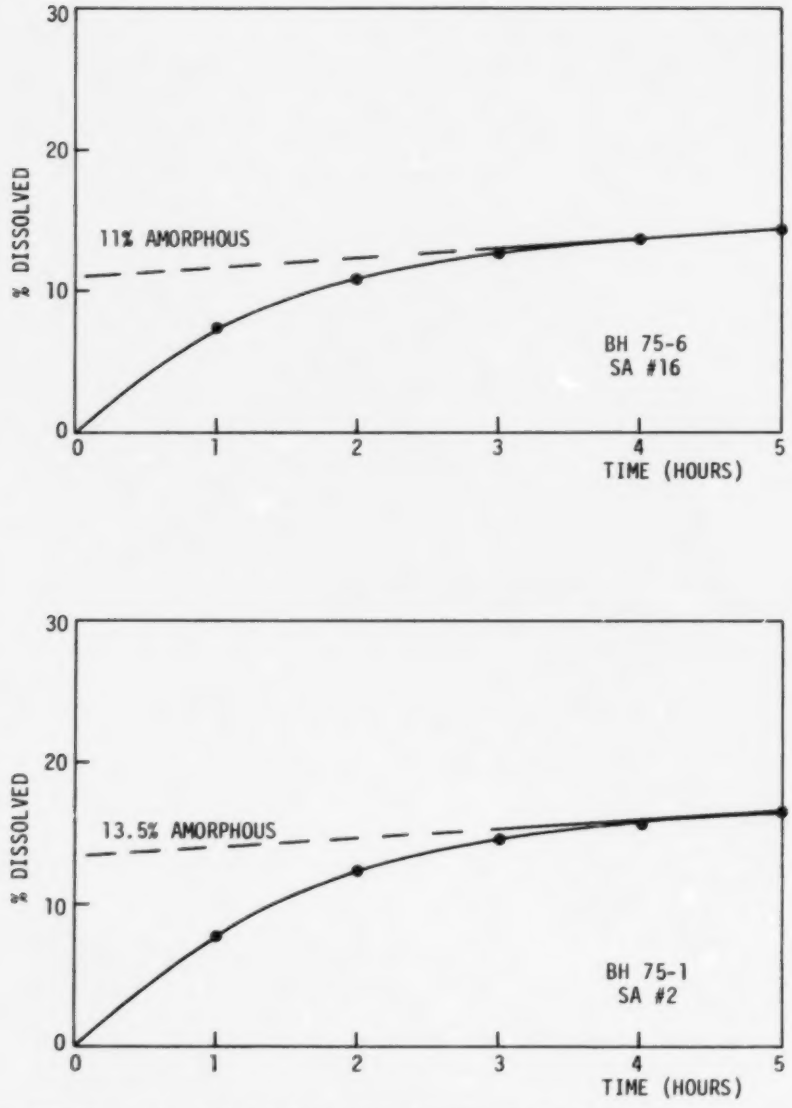

Figure F-7. Time-rate of dissolution curves for amorphous determinations, samples 75-6-16 and 75-1-2.

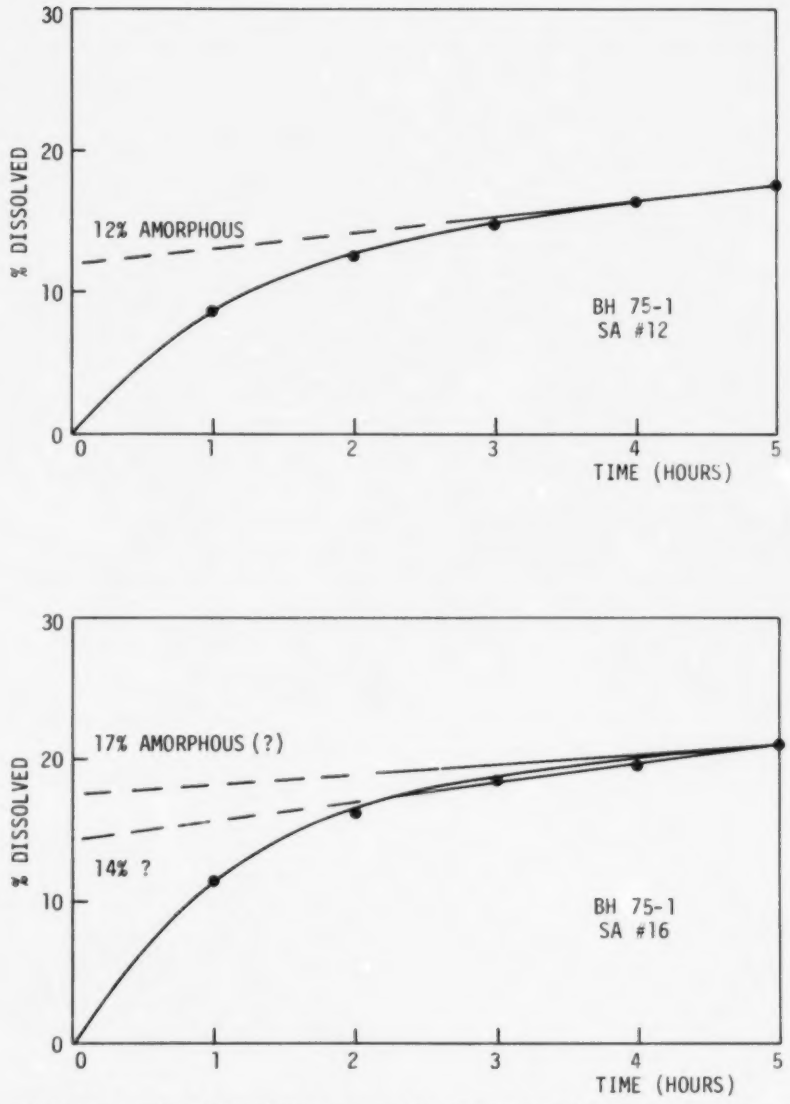

Figure F-8. Time-rate of dissolution curves for amorphous determinations, samples 75-1-12 and 75-1-16.

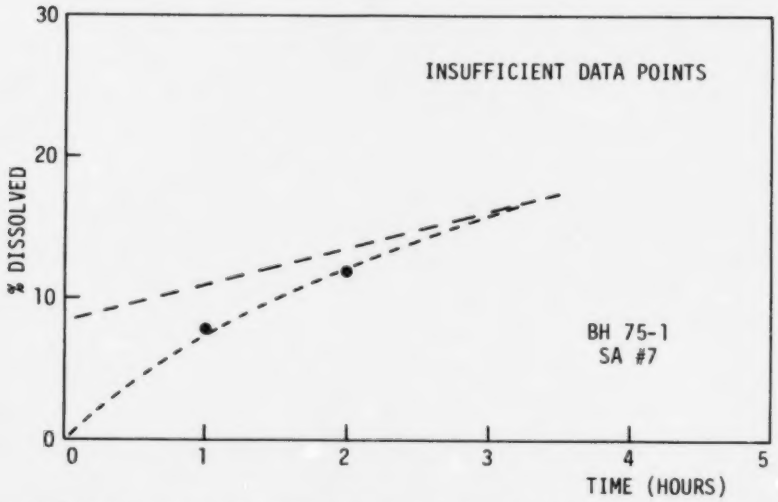

Figure F-9. Time-rate of dissolution curves for amorphous determinations, sample 75-1-7.

APPENDIX G. 1978 FIELD INVESTIGATIONS

BOREHOLE LOCATIONS

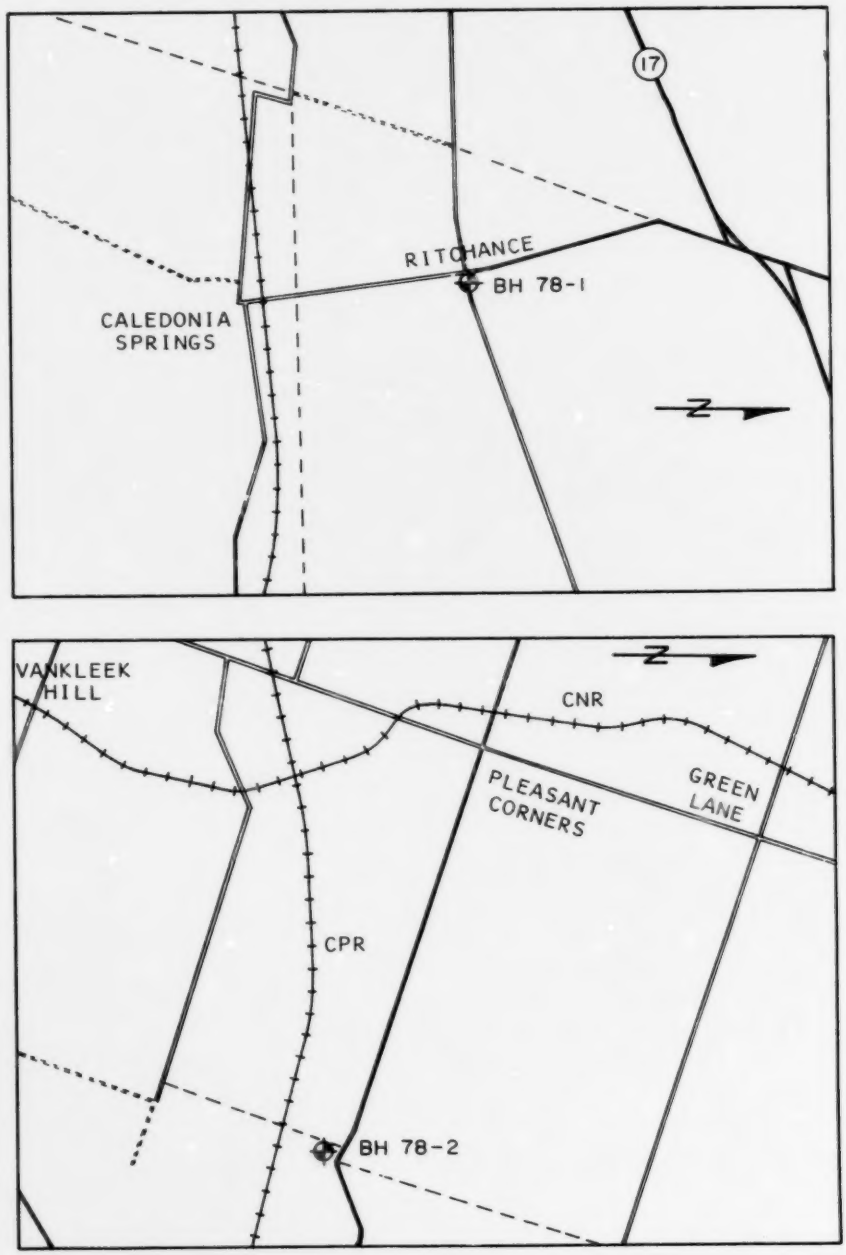

Figure G-1. Detailed site plans, borehole 78-1 (a, top) and borehole 78-2 (b, bottom). See Figure 2 for regional plan.

BOREHOLE LOGS OF SAMPLE AND PIEZOMETER LOCATIONS

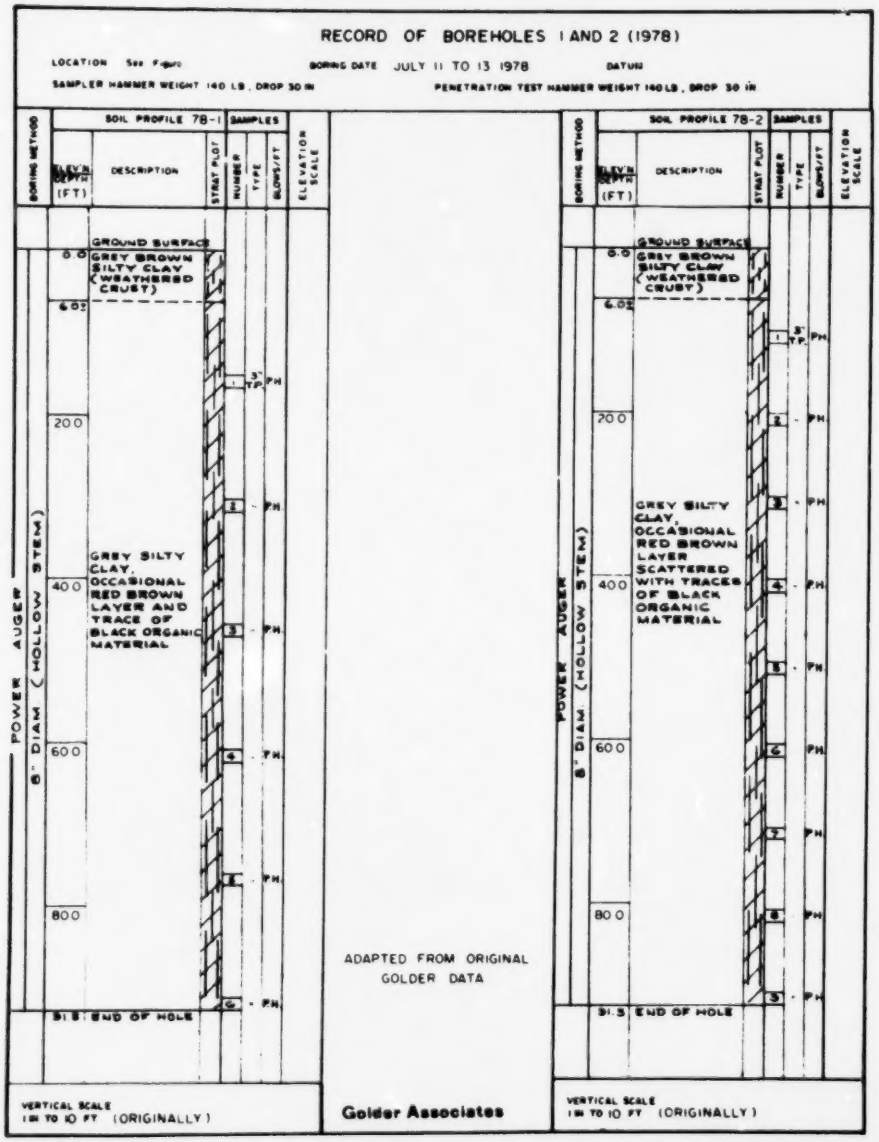

Figure G-2. Sample locations, boreholes 78-1 and 78-2, Hawkesbury project.

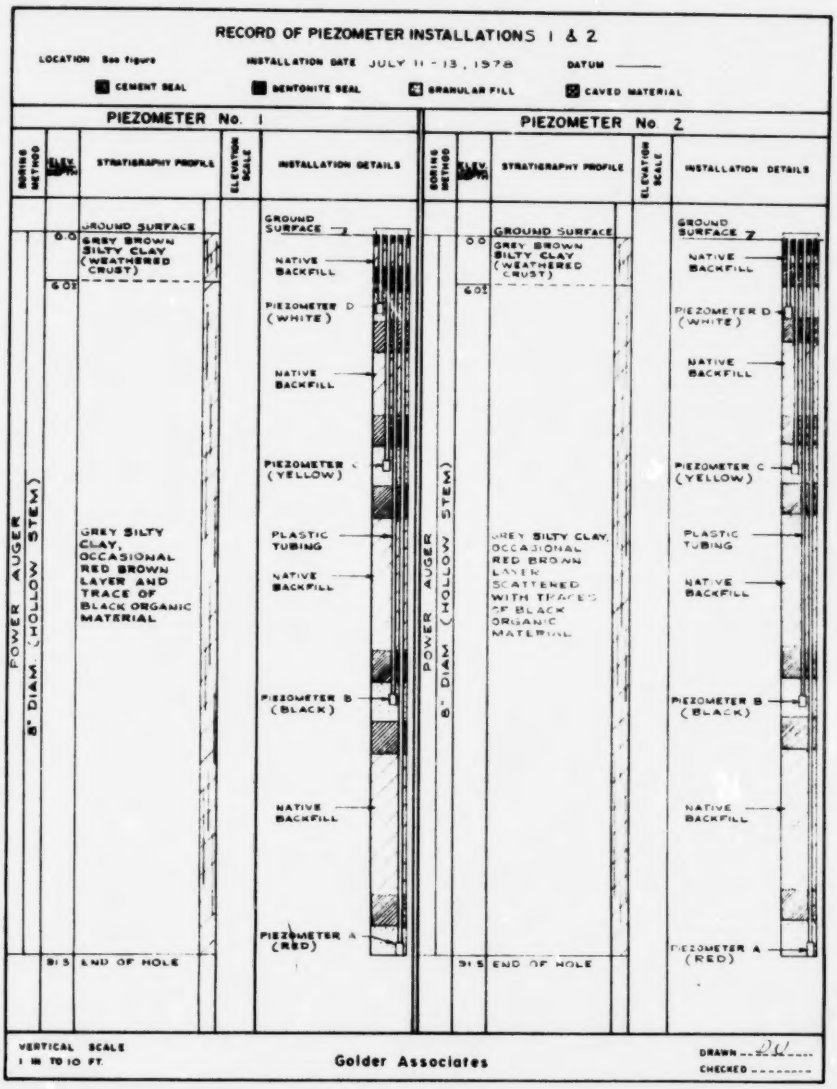

Figure G-3. Piezometer layout in boreholes 78-1 and 78-2, Hawkesbury, Ontario. (Work by Golder Associates).

RECORDS OF PIEZOMETER READINGS

TABLE G-1 RECORD OF PIEZOMETER READINGS*

Borehole No.	Piezometer Colour	Depth (m)	Date of Reading 78-7-20	78-8-17	78-10-26	78-11-23	79-5-19
78-1	Red	28	2.29	1.83	1.86	1.86	1.83
	Black	18	2.19	1.40	1.37	1.31	1.37
	Yellow	9	2.62	1.07	1.22	1.07	0.92
	White	3	1.34	1.64	1.16	0.48	0.67
78-2	Red	28	0.70	0.46	0.46	0.33	0.30
	Black	18	1.43	0.67	0.52	0.52	0.55
	Yellow	9	1.80	0.94	0.88	0.76	0.76
	White	3	1.37	1.65	1.58	0.70	0.82

*Depth to water level below surface (metres)

Original readings in feet by Golder Assoc. Ltd. (Ottawa) July 1978 to May 1979.

REFERENCES

Allison, L.E.
1965: Organic Carbon; p.1367-1378 *in* Methods of Soil Analysis, edited by C.A. Black, American Society of Agronomy Inc., Madison, Wisconsin.

ASTM
1964: Procedures for Testing Soils; American Society for Testing Materials, Special Technical Publication 194.

Craig, H.
1961: Isotopic Variations in Meteoritic Waters; Science, Vol.133, p.1702-1703.

Crawford, C.B.
1961: Engineering Studies of Leda Clay; p.200-217 *in* Soils in Canada, edited by R.F. Legget, Royal Society of Canada, Special Publication 3.

Crawford, C.B. and Eden, W.
1966: A Comparison of Laboratory Results with *in-situ* Properties of Leda Clay; Proceedings 6th International Conference Soil Mechanics Foundation Engineering, Vol.1, p.31-35.

Cronin, T.M.
1977a: Late-Wisconsin Marine Environments of the Champlain Valley (New York, Quebec); Quaternary Research, Vol.7, p.238-253.
1977b: Champlain Seas Foraminifera and Ostracoda: a Systematic SNF Paleoecological Synthesis; Geographie Physique et Quaternaire, Vol.31, p.107-122.

Dansgaard, W. and Tauber, H.
1969: Glacier Oxygen-18 Content and Pleistocene Ocean Temperatures; Science, Vol.166, p.499-502.

Dreimanis, A.
1962: Quantitative Gasometric Determination of Calcite and Dolomite using Chittick Apparatus; Journal of Sedimentary Petrology, Vol.32, p.520-529.

Eden, W.
1966: An Evaluation of the Field Vane Test in Sensitive Clay; American Society for Testing Materials, Special Technical Publication 399, p.8-17.

Elson, J.A.
1969: Late Quaternary Marine Submergence of Quebec; Revue Géographique Montréal, Vol.23, p.247-258.

Emiliani, C.
1966: Isotopic Paleotemperatures; Science, Vol.154, p.851-856.

Epstein, S. and Mayeda, T.
1953: Variation of O^{18} Content of Waters from Natural Sources; Geochimica Cosmochimica Acta, Vol.4, p.213-214.

Faure, G.
1977: Principles of Isotope Geology; John Wiley, New York.

Gwyn, Q.H.J. and Lohse, H.
1973: Quaternary Geology of the Alexandria Area, Southern Ontario; Ontario Division of Mines, Preliminary Map P.906.

Gwyn, Q.H.J. and Thibault, J.
1973a: Quaternary Geology of the Hawkesbury Lachute Area, Southern Ontario; Ontario Division of Mines, Preliminary Map P.1010.
1973b: Drift Thickness of the Hawkesbury Lachute Area, Southern Ontario; Ontario Division of Mines, Preliminary Map P.909.

Haynes, J.
1975: Mineralogy and Bonding of Leda Clay at four Sites; M.E.Sc. thesis, University of Western Ontario, 165p.

Haynes, J.E. and Quigley, R.M.
1976: Mineralogy and Physico-Chemistry of Leda Clay from Deep Boreholes, Hawkesbury, Ontario; Report to Ontario Ministry of Natural Resources, August 16, 1976, 131p.
1978: Framboids in Champlain Sea Sediments; Canadian Journal of Earth Sciences, Vol.15, p.464-465.

Hillaire-Marcel, C.M.
1979: Les Mers Post-Glaciaires du Québec: Quelques Aspects; Published Doctorat d'Etat thesis, Université Pierre et Marie Curie, Paris, France, 2 volumes.

Kenney, T.C.
1967: The Influence of Mineral Composition on the Residual Strength of Natural Soils; Proceedings Oslo Geotechnical Conference, Vol.1, p.123-129.

Lambe, T.W.
1951: Soil Testing for Engineers; Wiley and Sons Ltd., Toronto.

Lawrence, J.R and Taylor, H.P., Jr.
1972: Hydrogen and Oxygen Isotope Systematics in Weathering Profiles; Geochimica Cosmochimica Acta, Vol.36, p.1377-1393.

Martin, R.T.
1955: Ethylene Glycol Retention by Clays; Proceedings Soil Science Society of America, Vol.19, p.160-164.

McKyes, E., Sethi, A. and Yong, R.
1974: Amorphous Coatings on Particles of Sensitive Clay Soils; Clays and Clay Minerals, Vol.22, p.427-434.

Quigley, R.M.
1980: Geology, Mineralogy and Geochemistry of Canadian Soft Soils: a Geotechnical Perspective; Canadian Geotechnical Journal, Vol.17, p.261-285.

Quigley, R.M. and Bohdanowicz, A.
1979: Supplementary Research, Piezometric Water Conditions, Preconsolidation and Isotope Analyses on Leda Clay from Deep Boreholes, Hawkesbury, Ontario; Report to Ontario Ministry of Natural Resources, July 24, 1979, 40p.

Quigley, R.M., Gwyn, Q.H.J., White, O.L., Rowe, R.K., Haynes, J.E., and Bohdanowicz, A.
1983: Leda Clay from Deep Boreholes at Hawkesbury, Ontario, Part I: Geology and Geotechnique; Canadian Geotechnical Journal, Vol.20, p.288-298.

Segalen, P.
1968: Note sur une Methode de Determination des Mineraux Amorphes dans certains Sols Hydroxydes Tropicaux; Cahier ORSTOM, série Pedalogie, Vol.6, p.105-126.

Shackleton, J.N. and Opdyke, N.
1973: Oxygen Isotope and Paleomagnetic Stratigraphy of Equatorial Pacific Core v-28-238: Oxygen Isotope Temperatures and Ice Volumes on a 10^5 Year and 10^6 Year Scale; Quaternary Research, Vol.3, p.39-55.

Torrance, J.K.
1975: On the Role of Chemistry in the Development and Behaviour of the Sensitive Marine Clays of Canada and Scandinavia; Canadian Geotechnical Journal, Vol.12, p.326-335.

Yong, R.N., Sethi, A.J. and La Rochelle, P.
1979: Significance of Amorphous Material Relative to Sensitivity in some Champlain Clays; Canadian Geotechnical Journal,Vol.16, p.511-520.

Wagner, F.J.E.
1970: Faunas of the Pleistocene Champlain Sea; Geological Survey of Canada, Bulletin 181, 104p.

INDEX

Activity. 13
  Borehole 75-1. 17,95
  Borehole 75-2. 18,95
  Borehole 75-3. 19
  Borehole 75-4. 20
  Borehole 75-5. 21,96
  Borehole 75-6. 22
  Borehole 75-7. 23,97
  Borehole 75-8. 24,98
  Borehole 75-9. 25,99
  Definition. x
Alfred. 7,8,9
Alfred Bog. 4,8
Alluvium, older
  Map. 5
Amorphous matter. 12,45
  Depth, vs
    Borehole 75-1. 44,74,103
    Borehole 75-2. 44,74,103
    Borehole 75-4. 74
    Borehole 75-6. 44,74,103
    Borehole 75-7. 74
    Borehole 75-8. 44,74,103
  Elevation, vs
    Borehole 75-1, 2, 6 & 8. 44
  Extraction
    Borehole 75-1. 105
    Borehole 75-2. 104
    Borehole 75-6. 104-105
    Borehole 75-8. 104
  Mineralogy. 35-36
  Removal procedure. 78
  Time-rate of dissolution
    Borehole 75-1. 112-114
    Borehole 75-2. 106-108
    Borehole 75-6. 42,110-112
    Borehole 75-8. 108-110
  see also Segalen selective dissolution
Amphibole
  Semiquantitative mineralogy
    Borehole 75-1, 2, 4, 5, 6, 7 & 8. 46-47
Arctic waters
  Salinity vs Oxygen18. 68
Atterberg limit. 13
  Borehole 75-1. 17
  Borehole 75-2. 18
  Borehole 75-3. 19
  Borehole 75-4. 20
  Borehole 75-5. 21
  Borehole 75-6. 22
  Borehole 75-7. 23
  Borehole 75-8. 24
  Borehole 75-9. 25
  see also Liquid limit, Plastic limit, Water (moisture) content
Beaches, ancestral. 8
  Geochronology. 9,71
Bog deposits. 8
  Map. 5
Borehole
  Location maps. 6,115
Borehole 75-1
  Amorphous/Segalen matter. 44,74,103,105
    Time-rate of dissolution. . 112-114
  Geochemical data
    Carbonate. 58,74,100
    Cation. 58,101
    Salinity. 17,58,74,101
  Geotechnical/Index data
    Activity. 17,95
    Atterberg limits. 17,95
    Clay size particles (<2μm). 17,95
    Dry unit weight. 95
    Liquidity index. 74
    pH. 17,95
    Sensitivity/Field vane/Laboratory vane. 17,74,89
    Shear strength. 17
    Specific gravity. 95
    Wet unit weight. 17,95
  Scanning electron photomicrographs. 55
  Semi-quantitative mineralogy. . . . 46
Borehole 75-2
  Amorphous/Segalen matter. 44,74,103,104
    Time-rate of dissolution. . 106-108
  Geochemical data
    Carbonate. 58,74,100
    Cations. 58,101
    Salinity. 18,58,74,101
  Geotechnical/Index data
    Activity. 18,95
    Atterberg limits. 18,95
    Clay size particles (<2μm). 18,95
    Dry unit weight. 95
    Liquidity index. 74
    pH. 18,95
    Sensitivity/Field vane/Laboratory vane. 18,74,89
    Shear strength. 18

Specific gravity. 95
Wet unit weight. 18,95
Powder pattern. 40
Scanning electron photomicrograph. . . . 49,50,51,54
Semi-quantitative mineralogy. . . . 46
X-ray diffraction. 36-37
Borehole 75-3
Geochemical data
Carbonate. 100
Geotechnical/Index data
Activity. 19
Atterberg limits. 19
Clay size particles (<2μm). . . . 19
Sensitivity/Field vane/Laboratory vane. 19,90,93
Shear strength. 19
Borehole 75-4
Geochemical data
Carbonate. 100
Geotechnical/Index data
Clay size particles (<2μm). 20,99
Sensitivity/Field vane/Laboratory vane. 20,90,94
Shear strength. 20
Semi-quantitative mineralogy. . . . 46
Borehole 75-5
Geochemical data
Amorphous/Segalen matter. . . 74
Carbonate. 59,74,100
Cations. 59,101
Salinity. 59,74,101
Geotechnical/Index data
Activity. 21,96
Atterberg limits. 21,96
Clay size particles (<2μm). 21,96,99
Dry unit weight. 96
pH. 21,96
Liquidity index. 74
Salinity. 21
Sensitivity/Field vane/Laboratory vane. 21,74,91
Shear strength. 21
Specific gravity. 96
Wet unit weight. 21,96
Semi-quantitative mineralogy. . . . 46
X-ray diffraction. 39
Borehole 75-6
Amorphous/Segalen matter. 44,74,103,104-105
Time-rate of dissolution 42,110-112
Geochemical data
Carbonate. 74,100
Salinity. 74
Geotechnical/Index data
Clay size particles (<2μm). 22,99
Liquidity index. 74
Sensitivity/Field vane/Laboratory vane. 22,74,91,94
Shear strength. 22
Scanning electron photomicrograph. 52
Semi-quantitative mineralogy. . . . 46
Borehole 75-7
Amorphous/Segalen matter. 74
Geochemical data
Carbonate. 59,74,100
Cation. 59,101
Salinity. 23,59,74,101
Geotechnical/Index data
Activity. 23,97
Atterberg limits. 23,97
Clay size particles (<2μm). 23,97
Dry unit weight. 97
Liquidity index. 74
pH. 23,97
Sensitivity/Field vane/Laboratory vane. 23,74,92
Shear strength. 23
Specific gravity. 97
Wet unit weight. 23,97
Quartz. 79
Scanning electron photomicrograph. 53
Semi-quantitative mineralogy. . . . 47
X-ray diffraction. 38
Borehole 75-8
Amorphous/Segalen matter. 44,74,103,104
Time-rate of dissolution. . 108-110
Geochemical data
Carbonate. 60,74,100
Cations. 60,101
Salinity. 24,60,74,101
Geotechnical/Index data
Activity. 24,98
Atterberg limits. 24,98
Clay size particles (<2μm). 24,98,99
Dry unit weight. 98
Liquidity index. 74
pH. 24,98

Sensitivity/Field vane/Laboratory vane. 24,74,92
Shear strength. 24
Specific gravity. 98
Wet unit weight. 24,98
Semi-quantitative mineralogy. . . . 47
Borehole 75-9
Geochemical data
Carbonate. 100
Geotechnical/Index data
Activity. 25,99
Atterberg limits. 25,99
Clay size particles (<2μm). 25,99
Sensitivity/Field vane. 25,93
Shear strength. 25
Specific gravity. 99
Borehole 78-1
Consolidation curves. 83-85
Consolidation test. 30
Deuterium. 64
Geotechnical profile. 26,29
Location map. 115
Log. 116
Organic matter. 102
Organics vs elevation. 70
Oxygen-18. 64
Oxygen-18 vs deuterium. 69
Oxygen-18 vs elevation. 70
Oxygen-18 vs salinity. 66
Piezometer. 31,32,117,118
Specific gravity. 82
Stress-depth & post depositional erosion. 32
Stress-strain curves (unconfined compression). 80
Tritium. 64
Borehole 78-2
Consolidation curves. 86-88
Consolidation test. 30
Deuterium. 64
Geotechnical profile. 26,29
Location map. 115
Log. 116
Organic matter. 102
Organics vs elevation. 70
Oxygen-18. 64
Oxygen-18 vs deuterium. 69
Oxygen-18 vs elevation. 70
Oxygen-18 vs salinity. 66
Piezometer. 31,32,117,118
Specific gravity. 82
Stress-depth & post-depositional erosion. 33
Stress-strain curves (unconfined compression). 81
Tritium. 64
Calcite
Borehole 75-1, 2, 3, 4, 5, 6, 7, 8 & 9. 100
Carbonate. 11,56,71,72
Borehole 75-1. 46,58,74,100
Borehole 75-2. 46,58,74,100
Borehole 75-3. 100
Borehole 75-4. 46,100
Borehole 75-5. 46,59,74,100
Borehole 75-6. 46,74,100
Borehole 75-7. 47,59,74,100
Borehole 75-8. 47,60,100
Borehole 75-9. 100
Testing methods 75,77
Cations, porewater. 56
Borehole 75-1. 58,101
Borehole 75-2. 58,101
Borehole 75-5. 59,101
Borehole 75-7. 59,101
Borehole 75-8. 60,101
Cementation. 35,36,45,72
Photo. 55
Inclusion. 53
Layer. 54
Champlain Sea
Deposits. 7,13
Elevation. 7
Oxygen-18. 67,68
Salinity. 68
Chlorite. 45,72
Borehole 75-1, 4, 5, 6, 7 & 8. . . 46-47
Chlorite, Fe
Deposit below crust. 34
Clay, marine. 7
Fluting, erosional. 8
Geotechnique. 13
see also Champlain Sea
Clay mineralogy
Oxidized crust. 34
X-ray diffraction pattern. 36
Deposit below crust. 34-35
X-ray diffraction pattern. . . 37-39
Clay, non
Mineralogy. 35,40-41
Clay size particles, % <2μm
Borehole 75-1. 17,95
Borehole 75-2. 18,95

Borehole 75-3. 19
Borehole 75-4. 20
Borehole 75-5. 21,96
Borehole 75-6. 22
Borehole 75-7. 23,97
Borehole 75-8. 24,98
Borehole 75-9. 25,99
Mineralogical testing methods. . . 76
Clay plains
Elevation
Oxygen-18. 70
Organics. 70
Geology. 71
Geotechnique. 71-72
Geochemistry. 73
Lower
Sensitivity, salinity, carbonate, amorphous matter & liquidity index vs depth. . 74
Upper
Sensitivity, salinity, carbonate, amorphous matter & liquidity index vs depth. . 74
Compression, unconfined
Test methods. 75
Test results. 80-81
Borehole 78-1. 80
Borehole 78-2. 81
see also Stress-strain curves
Consistency
Definition. x
Consolidation. 10,11,27,28,30
Test methods. 75
Test results. 8288
Specific gravity
Borehole 78-1 & 78-2. 82
Consolidation curves
Borehole 78-1. 83
Crust
Mineralogy. 34
X-ray diffraction pattern
Borehole 75-2. 36
pH. 56
Crust, deposit below
Mineralogy. 34-35
X-ray diffraction pattern
Borehole 75-2. 37
Borehole 75-5. 39
Borehole 75-7. 38
Deltaic deposits. 8
Map. 5
Distal. 7
Erosion. 8
Desiccation, crust. 13
Deuterium, ^2H
Meteoritic water. 65
Oxygen-18, relationship with Hawkesbury Leda clay. 69
Porewater isotopes. 61-64
Borehole 78-1. 64
Borehole 78-2. 64
Dissolution rates
Borehole 75-6. 42
Dolomite
Borehole 75-1 to 75-9. 100
Dry unit weight
Borehole 75-1. 95
Borehole 75-2. 95
Borehole 75-5. 96
Borehole 75-7. 97
Borehole 75-8. 98
Erosion. 28,71
Fluvial. 89
Post-depositional
Borehole 78-1. 32
Borehole 78-2. 33
Escarpment
Earth flow. 5
Fabric. 45
Fauna
see Organic matter
Feldspar. 45,72
Feldspar, plagioclase
Borehole 75-1, 2, 4, 5, 6, 7 & 8. 46-47
Feldspar, potassium
Borehole 75-1, 2, 4, 5, 6, 7 & 8. 46-47
Field Investigations. 10
Field vane data
Borehole 75-1. 89
Borehole 75-2. 89
Borehole 75-3. 90
Borehole 75-4. 90
Borehole 75-5. 91
Borehole 75-6. 91
Borehole 75-7. 92
Borehole 75-8. 92
Borehole 75-9. 93
Borehole 78-1. 29
Borehole 78-2. 29
see also Laboratory vane data, Sensitivity
Flow, time for (Darcy). 28

Fluting
Curvilinear. 8
Fluvial deposits. 8
Fluvial erosion
see Erosion, fluvial
Fort Covington Till
Map. 5
Fossils
see Organic matter
Fournier. 7,8,9
Fractures
Fabric. 45
Framboid. 45,72
Definition. xi
Photo. 53
Geochemical studies. 11,56-60
Calcite & Dolomite data (Carbonate)
Borehole 75-1 to 75-9. 100
Cations, porewater
Borehole 75-1, 2, 5, 7 & 8. . . . 101
Organic matter
Borehole 78-1 & 2. 102
Salinity data
Borehole 75-1, 2, 5, 7 & 8. . . . 101
Summary. 72-73
Testing methods. 75-76
Geochronology. 9
Geology
Summary. 71
see also Quaternary geology
Geotechnical studies
Borehole 75-1. 17
Borehole 75-2. 18
Borehole 75-3. 19
Borehole 75-4. 20
Borehole 75-5. 21
Borehole 75-6. 22
Borehole 75-7. 23
Borehole 75-8. 24
Borehole 75-9. 25
Field vane data
Borehole 75-1. 89
Borehole 75-2. 89
Borehole 75-3. 90
Borehole 75-4. 90
Borehole 75-5. 91
Borehole 75-6. 91
Borehole 75-7. 92
Borehole 75-8. 92
Borehole 75-9. 93
Grain size data
Borehole 75-4, 5, 6 & 8. 99
Index tests
Borehole 75-1. 95
Borehole 75-2. 95
Borehole 75-5. 96
Borehole 75-7. 97
Borehole 75-8. 98
Borehole 75-9. 99
Laboratory vane data
Borehole 75-3. 93
Borehole 75-4. 94
Borehole 75-6. 94
Summary. 11,13-33,71-72
Testing methods
Laboratory vane. 75
Unconfined compression. 75
Consolidation. 75
Index. 75
Glacial meltwater
Porewater isotopes. 62,63
Salinity vs Oxygen-18. 66,68
Grain size data
see Clay size particles, $< 2\mu m$
Groundwater
see Piezometric investigations
Hydrogen Isotope Studies. 12
see also Deuterium
Illite
Deposit below crust. 34
Illite/mica. 72
Borehole 75-1, 2, 4, 5, 6, 7 & 8. 46-47
Testing methods. 77
Inclusions. 45
Cemented
Photo. 53
Index tests. 13
Borehole 75-1. 95
Borehole 75-2. 95
Borehole 75-5. 96
Borehole 75-7. 97
Borehole 75-8. 98
Borehole 75-9. 99
Testing methods. 75
see also Activity, Clay particles, Dry unit weight, Liquid limit, pH, Plastic limit, Specific gravity, Water content, Wet & Geotechnical Profile
Isostasy. 8
Isotopes, porewater. 61-70
Laboratory Investigations. 11-12

Laboratory vane data
Borehole 75-3. 93
Borehole 75-4. 94
Borehole 75-6. 94
Testing methods. 75
see also Field vane data, Sensitivity
Landslide debris
Map. 5
Lefaivre. 7
Liquid limit. 71
Borehole 75-1. 95
Borehole 75-2. 95
Borehole 75-5. 96
Borehole 75-7. 97
Borehole 75-8. 98
Borehole 75-9. 99
Definition. x
see also Atterberg limits
Liquidity index. 13,14,71
Borehole 75-1, 2, 5, 6, 7 & 8. 74
Definition. x
L'Orignal. 7,9
Little Rideau Creek. 7,9
McCrimmon. 7
Magnesium
Deposit below crust. 34
Marine deposits. 7
Deepwater
Map. 5
Meander, ancestral
Ottawa River. 4,8
Meteoritic water
Deuterium & Oxygen-18
Contour map of United States. 65
Mica
Deposit below crust. 34
see also Illite/mica
Microscopy, scanning electron. 45
Photo
Borehole 75-1. 55
Borehole 75-2. 49,50,51,54
Borehole 75-6. 52
Borehole 75-7. 53
Testing methods. 78
Mineral, nonclay
Semi-quantitative mineralogy
Borehole 75-1, 2, 4, 5, 6, 7 & 8. 46-47
Mineralogical studies. 11-12
Qualitative. 34-44
Scanning electron microscopy. . . 45
Semi-qualitative. 45-48
Photos. 49-55
Summary. 72
Testing methods
Initial sample preparation. . . . 76
Qualitative. 76
Removal of Amorphous matter. 78
Semi-qualitative. 77-78,79
Moisture content. 13
Borehole 78-1. 26
Borehole 78-2. 26
see also Atterberg Limits
Ordovician, Lower and Middle
Map. 5
Organic matter. 11,57
Borehole 78-1. 26,102
Borehole 78-2. 26,102
Elevation, relationship with Upper and Lower clay plain. 70,73
Oxygen-18 vs depth. 67
Porewater isotopes. 63,64
Testing methods. 76
Ottawa River
Ancestral. 4,8
Overconsolidation ratio
Borehole 78-1 & 78-2. 30
Definition. xi
see also Consolidation
Oxygen-18. 12
Arctic waters. 68
Champlain Sea. 67,68
Definition. xi
Deuterium, relationship with Hawkesbury Leda clay. 69
Elevation, relationship with Upper & Lower clay plains. 70,73
Fossil groups & depth. 67
Meteoritic water. 65
Porewater. 61-64
Borehole 78-1. 64,66
Borehole 78-2. 64,66
Precipitation. 65
Salinity, relationship with. 66
PDB
Definition. xi
Permeability. 27
pH. 56
Testing methods. 75
Borehole 75-1. 17,95
Borehole 75-2. 18,95
Borehole 75-3. 19
Borehole 75-4. 20

Borehole 75-5. 21,96
Borehole 75-6. 22
Borehole 75-7. 23,97
Borehole 75-8. 24,98
Borehole 75-9. 25
Photo, scanning electron micrograph
Borehole 75-1. 55
Borehole 75-2. 49,50,51,54
Borehole 75-6. 52
Borehole 75-7. 53
Piezometric investigations. . . . 10,27,72
Borehole 78-1 & 78-2. . 31,32,117,118
Plantagenet. 7,8,9
Plastic limit. 13
Borehole 75-1. 95
Borehole 75-2. 95
Borehole 75-5. 96
Borehole 75-7. 97
Borehole 75-8. 98
Borehole 75-9. 99
Definition. x
see also Atterberg limits
Porewater analyses
Testing methods. 75-76
Porewater isotopes
see Isotopes, porewater
Porosity. 28
Portlandia arctica. 7
Powder pattern
Borehole 75-2. 40,43
Borehole 75-6. 41
Testing methods. 76
Precipitation
Oxygen-18
Contour map of world. 65
Pressure, preconsolidation
Borehole 78-1 & 78-2. 27,28,29
Definition. x
Upper & Lower clay plain. 72
see also Consolidation
Proulx. 7
Pyrite. 45,72
Photo. 54
Quartz. 45,72
Abundance
Borehole 75-7. 79
Borehole 75-1, 4, 5, 6, 7 & 8. . . 46-47
Testing methods. 77
Quaternary geology. 79
Deltaic & fluvial deposits. 8
Fluvial erosion. 89
Geochronology. 9
Map. 5
Marine deposits. 7
see also Geology
Riceville. 7,8,9
Ritchance. 9
Routhier. 7,8,9
Rythmites. 7,8
Map. 5
Salinity, porewater. 11,28,56,57
Borehole 75-1. 17,58,74,101
Borehole 75-2. 18,58,74,101
Borehole 75-3. 19
Borehole 75-4. 20
Borehole 75-5. 21,59,74,101
Borehole 75-6. 22,74
Borehole 75-7. 23,59,74,101
Borehole 75-8. 24,60,74,101
Borehole 75-9. 25
Borehole 78-1. 26
Borehole 78-2. 26
Definition. x
Isotopes. 62,63,71,73
Oxygen-18
Arctic waters. 68
Borehole 78-1. 66
Borehole 78-2. 66
Champlain Sea. 68
Sand
Deltaic. 8
Fluvial. 8
Marine. 7
Scanning Electron Microscopy. 12
See page 27-28
Segalen selective dissolution 35,103-114
see also Amorphous matter
Sensitivity. 14,71
Borehole 75-1. 17,74,89
Borehole 75-2. 18,74,89
Borehole 75-3. 19,90
Borehole 75-4. 20,90
Borehole 75-5. 21,74,91
Borehole 75-6. 22,74,91
Borehole 75-7. 23,74,92
Borehole 75-8. 24,74,92
Borehole 75-9. 25,93
Definition. x
see also Field & Laboratory
vane data
Shear Strength
Borehole 75-1. 17

Borehole 75-2. 18
Borehole 75-3. 19
Borehole 75-4. 20
Borehole 75-5. 21
Borehole 75-6. 22
Borehole 75-7. 23
Borehole 75-8. 24
Borehole 75-9. 25
Borehole 78-1. 26,29
Borehole 78-2. 26,29
Champlain Sea Clays. 13,14-26
Field vane. 14
Remoulded vane. 14,57
Stratigraphic crosssection. . . . 15,16
Unconfined compression. 14
Shells
Geochronology. 9
Silt. 13
Fluvial. 8
Marine. 7
Smectite
Oxidized crust. 34
SMOW
Definition. xi
"Soft Zone". 14
Champlain Sea Clays. 13
Soil Classification. 13
Soil Fabric. 12
Soil Samples. 10
Specific gravity
Borehole 75-1. 95
Borehole 75-2. 95
Borehole 75-5. 96
Borehole 75-7. 97
Borehole 75-8. 98
Borehole 75-9. 99
Borehole 78-1 82
Borehole 78-2. 82
Stratigraphic Crosssection
East-West. 15
North-South. 16
Strength Testing, in situ. 10
Stress, in situ effective
Borehole 78-1 & 78-2. 29
Definition. x
Stress-depth relationships
Borehole 78-1. 32
Borehole 78-2. 33
Stress-strain curves. 14
Borehole 78-1. 80
Borehole 78-2. 81
see also Compression, unconfined
Terrace-scarps. 5,8-9
Topography. 4
Tritium
Porewater. 61-62,73
Borehole 78-1. 64
Borehole 78-2. 64
Vankleek Hill. 7,8
Vermiculite. 45,72
Borehole 75-1, 2, 4, 5, 6, 7 & 8. 46-47
Crust. 34
Testing methods. 77
Void ratio
Borehole 78-1 & 78-2. 30
Water conditions
Borehole 78-1 & 78-2. 27
Water content. 13
Borehole 75-1. 95
Borehole 75-2. 95
Borehole 75-5. 96
Borehole 75-7. 97
Borehole 75-8. 98
Borehole 75-9. 99
Definition. x
see also Atterberg limits
Wet unit weights. 13
Borehole 75-1. 17,95
Borehole 75-2. 18,95
Borehole 75-3. 19
Borehole 75-4. 20
Borehole 75-5. 21,96
Borehole 75-6. 22
Borehole 75-7. 23,97
Borehole 75-8. 24,98
Borehole 75-9. 25
Wood
Geochronology. 9
X-ray diffraction
Borehole 75-2-1. 36
Borehole 75-2-11. 37
Borehole 75-2-13. 37
Borehole 75-7-13. 38
Borehole 75-7-19. 38
Borehole 75-5-7. 39